Integrated Geophysical Characterization for Building Foundation at Kilinto, Akaki Kality Sub-City, Addis Ababa, Central Ethiopia

Belete Getahun

A Thesis Submitted to

School of Earth sciences of Addis Ababa University

Presented for Partial Fulfillment of the Requirements for the Degree of Masters of Sciences in Geophysics (Applied Geophysics)

ADDIS ABABA UNIVERSITY

COLLEGE OF NATURAL AND COMPUTATIONAL SCIENCES

ADDIS ABABA, ETHIOPIA

June, 2018

Integrated Geophysical Characterization for Building Foundation at Kilinto, Akaki Kality Sub-City, Addis Ababa, Central Ethiopia

Belete Getahun

A Thesis Submitted to

School of Earth sciences of Addis Ababa University

Presented for Partial Fulfillment of the Requirements for the Degree of

Masters of Sciences in Geophysics (Applied Geophysics)

ADDIS ABABA UNIVERSITY

COLLEGE OF NATURAL AND COMPUTATIONAL SCIENCES

ADDIS ABABA, ETHIOPIA

June, 2018

Addis Ababa University

School of Graduate Studies

Declaration of originality

This is to certify that the thesis prepared by **Belete Getahun**, entitled: Integrated Geophysical Characterization for Building Foundation at Kilinto, Akaki Kality Sub-City, Addis Ababa, Central Ethiopia and submitted for the partial fulfillment for the Degree of Master of Science in Geophysics (Applied Geophysics) complies with the regulations of the University and meets the accepted standards with respect to originality and quality.

Belete Getahun	_____	_____
Name of the candidate	Signature	Date

Approved by the Examining Committee:

Dr. Getnet Mewa	_____	_____
Advisor	Signature	Date
Prof. Tilahun Mammo	_____	_____
Examiner	Signature	Date
Dr. Tarun K. Raghuvanshi	_____	_____
Examiner	Signature	Date

_____

School Chairman or Graduate Committee Coordinator

June, 2018

Addis Ababa, Ethiopia

ABSTRACT

An integrated geophysical investigation was carried out at a site nearby Addis Ababa Science and Technology University, Kilinto, Akaki, just in front of the Tulu-Dimtu condominiums, Southeastern Addis Ababa, Ethiopia. The principal objective of this research is to map the subsurface geology and elucidate its suitability for the construction of multistory residential and commercial complexes through employing electrical resistivity and seismic refraction techniques. Nine Vertical Electrical Sounding points distributed along five profiles, two dipole-dipole lines and three seismic refraction spreads were conducted to characterize the foundation materials within the study site. Qualitative and quantitative interpretations of the collected data were made by integrating with borehole log data available from nearby areas. The results have revealed that the subsurface geology is consisted of three to four distinct units that reflect different physical properties (resistivity and velocity). The upper most layers consist of black cotton soil (clay and silty clay) have shown very low resistivities (3-11 Ω-m) and low average P-wave velocity (< 350 m/s). The thickness of this layer varies from 3.5 to 7 m. Underlying this unit there is a relatively intermediate resistive (9- 24 Ω-m) and intermediate p-wave velocity (a maximum of 1070 m/s) attributed to decomposed rock with comparatively enhanced thickness. The third and bottom layer associated with weathered and fractured basalt is characterized by relatively high resistivity (25 to 115 Ω-m). The depth to the surface of this unit reaches about 40 m. These properties suggest that the third layer can adequately serve as a competent foundation material that can resist any imposed load from multistory engineering structures. Generally, the study result indicates that the entire study area is characterized by very low resistivity and low compressional wave velocity that is less than 115Ω-m and 1070 m/s respectively. Therefore, development of engineering structures in this vicinity requires proper measures, including proper drainages, compaction, stabilization, removing and backfilling by another well graded material that enable, in order to make the structures stand the impacts of natural geo-hazard event.

Key words; building foundation, p-wave velocity, resistivity

ACKNOWLEDGMENT

Above all, I would like to thank almighty god for keeping my health and being with me, not only for this study but also throughout my life.

Firstly, My heart felt thank goes to my advisor Dr. Getnet Mewa for his fatherly approach, constructive comments, encouragement, guidance and reviewing the thesis and providing all the relevant information's for the finalization of this thesis work. I haven't words to express his support and fatherly advice not only the subject matter but also for my future career.

Secondly, I would like to thank Addis Ababa University Institute of Geophysics, Space Science and Astronomy (IGSSA) admistrators for allowing me to use all the geophysical instruments and vehicle for the fieldwork.

Next, I would like to thank Addis Ababa University School of earth sciences Administrator's.

Special thanks go to Prof. Tilahun Mammo, Prof. Tigistu Haile and Dr. Abera Alemu for their fruitful and supportive discussions on various theoretical aspects of the geophysical methods.

I would like to thank Dr. Genet Tamiru for introducing and assisting in seismic refraction data processing. I will never forget her motherly approach and unlimited support throughout my life. I am thankful to IGSSA staff members especially, Mr. Befekadu and Mr. Tatek for their incredible support and assistance in the field data collection.

I would like to thank all my classmates (MSc. Graduate class of this year of geophysics stream students), Duressa, Getachew, Shewangizaw, Tariku and Tulu for their incredible support and assistance in the field data collection as well as in geophysical data processing. Special thank also goes to my best friends Gashaw and Gedefaw for their help in the field data collection. I will never forget their support throughout my life.

Great appreciation goes to Addis Ababa Water Sewerage Authority, Ethiopian Construction Design and Supervision Works Corporation, and Geological survey of Ethiopia for providing me the necessary reports and borehole log data.

Lastly, but not least I am thankful to NMC realstate project and other private land owners for the permission to enter and collect relevant data.

CONTENTS

List of Figures

List of Tables

LIST OF ACRONYM

BRA	Bed Rock Acceleration
CDSC	Construction Design Share Company
ECDSWC	Ethiopian Construction Design and Supervision Enterprise
GPS	Global positioning System
MER	Main Ethiopian Rift
NE	Northeast
NW	Northwest
P	Primary
PLC	Private Limited Company
S	Secondary
SARIS	Sintrax Automated Resistivity Imaging System
SE	Southeast
SW	Southwest
UTM	Universal Transverse Mercator
VES	Vertical Electrical sounding
WWDSE	Water Works Design and Supervision Enterprise
YTVL	Yerer Tuluwellel Volcanic Lineaments
1D	One Dimensional
2D	Two Dimensional
3D	Three Dimensional

CHAPTER ONE

1. INTRODUCTION

1.1 Background

Human being has developed the art of proper designing, accessing and constructing buildings and other civil engineering structures through time to complement the basic needs and future purposes with consideration of competency of earth materials over which structures are to be erected (Lateef and Adegoke, 2016). All engineering structures constructed on the Earth surface directly or indirectly associated with the ground surface and have their own substructure, foundations that are supported by the soils and rocks (Bell, 2007; Lateef and Adegke, 2016). As a result, their long term performance and environmental sustainability are primarily controlled by the nature of the underlying geological features where the structures are founded. As a geological context, underlying lithology contrast, presence of groundwater, fractures, near surface cavities and seismic activity govern its sustainability. The causes of risks in civil engineering discipline results essentially from concealed near-surface structures, such as cavities and/or inhomogeneity in the foundation of earth materials (Soupois *et al.*, 2007).

According to (Bell, 2007) site investigation is the first requirement for the successful economic design of engineering structures and earthworks. However, constructions founded over the ground without or with insufficient site investigations may face problems at the time of development as well as completed stages. For instance, structures erected on expansive soil with insufficient bearing capacity may result to settlement, collapse and cracking on the components of structures.

The principal concern of any site investigation is to evaluate its suitability for the intended purpose. As such, it encompasses exploring the ground conditions at and below the surface (Bell, 2007). Essentially, this is achieved by exploring of the near surface geological situations through geotechnical and geophysical investigations (Soupois *et al.*, 2007). To obtain a complete picture of the site subsurface condition detail sampling and measurement is needed. Incase this might be done via drilling, trenching, pitting or indirect means. However, for a wide area with thick overburden to the bedrock and diversified geological situation (with variation in

lithology and structure) it is practically impossible to address the whole target through direct geotechnical investigation due to limited information up to a certain depth and they are costive. Yet, geophysical methods can addresses/resolves the subsurface target with a reasonable cost and safe to the surrounding environment. It saves the unnecessary cost, time and environmental disruption arises from boring, drilling, pitting and trenching activities. In most situations, integration of geophysical investigation and geotechnical investigation highly improve the long term performance of buildings and other constructions in civil engineering. Geophysics helps to provide solutions for determining subsurface properties and developing a reasonable model of the subsurface structure. It also provides useful information regarding the early detection of potentially dangerous subsurface conditions (Soupois *et al*., 2007). Two geophysical methods, namely electrical resistivity and shallow seismic refraction are very popular in site investigations (Emmanuel *et al*., 2016). Both of the methods use artificial sources which is effective for shallow ground investigation.

The existence of diversified geological, tectonic, climatic and geomorphological situations are the prominent natural events appear in Ethiopia this further makes the country prone to different geohazards like landslide, earthquake, ground collapse, sinking and the like. Specifically, in Addis Ababa, the geology is covered by different volcanic rocks, the city is near to main Ethiopian rift, the existence of Filwuha fault at the middle of the city by itself and the existence of thick black cotton soil in the majority areas of the city may aggravate to the occurrence of geological interruption which eventually leads infrastructural devastation, property loss and loss of live.

From time to time urbanization is booming in Addis Ababa. Hence, currently massive constructions undertaken by private and government owners are undergoing throughout the city to suite different purposes. Among them massive residential house constructions are undergoing to solve housing problem and modernize the city. However, most of the constructions are carried out with limited geotechnical investigations that incorporate scarce borehole data with insufficient depth to adequately understand the subsurface. Therefore, in city like Addis Ababa, where a radical change manifested by rapid population growth, infrastructural development, industrialization and modern urbanization, attention has to be given for proper site investigation

using integrated methods before designing and constructing of such multistory engineering structures. With such considerations, the present work was conducted to characterize multistory building foundation site at Kilinto site, located nearby the Addis Ababa Science and Technology University, Akaki Subcity, Addis Ababa, Ethiopia.

1.2 Site description

1.2.1 Location and accessibility

The study area is situated in the central highlands of Ethiopia which is far from a few kilo meters away from the western margin of the Main Ethiopian Rift (MER). The site is specifically located at Kilinto, nearby Addis Ababa Science and Technology University, Akaki Kality sub-city, Addis Ababa. It is approximately bounded by 479600 to 480100 m Easting and 981000 to 981150 m Northing UTM coordinates. It has good accessibility in all seasons and can be easily accessed through Piazza- Arat Kilo - Megenagna - Goro –Tulu Dimtu asphalt route.

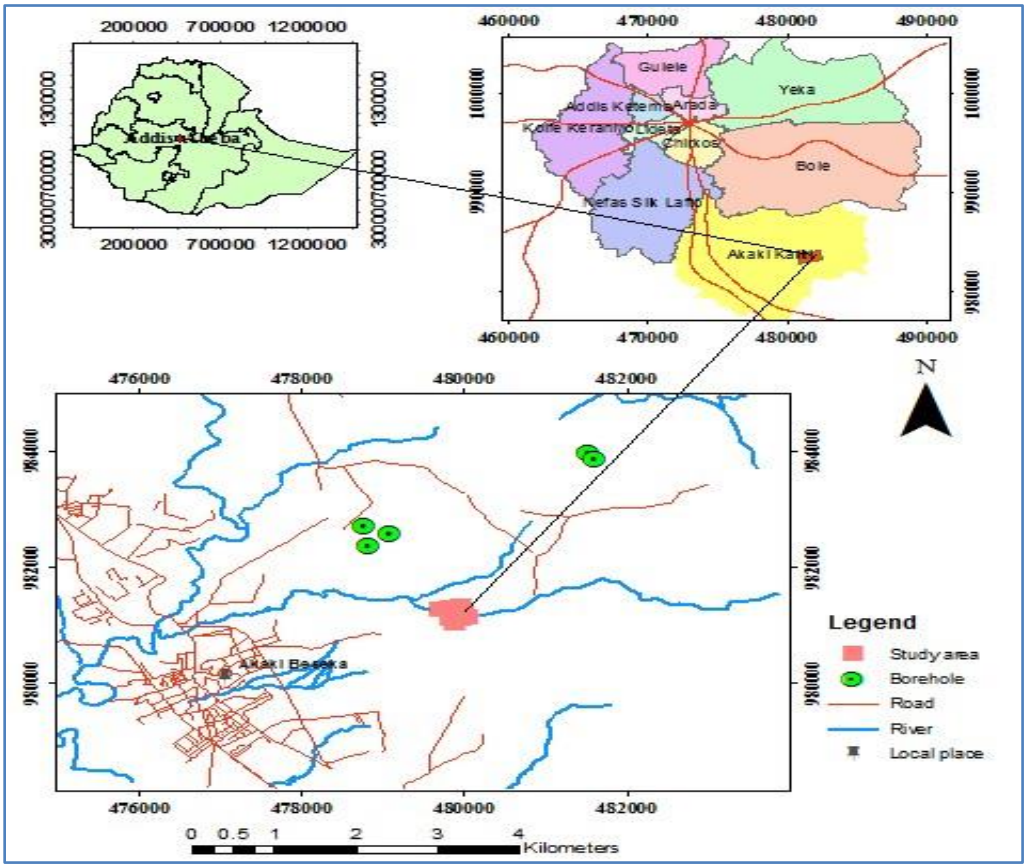

Figure 1.1: Location map of the study area

1.2.2 Physiography and drainage

The general geomorphic feature of the Addis Ababa city declines from NE towards SW and it has 2015 and 3050 m minimum and maximum elevation above mean sea level respectively. It is surrounded by Furi Mountain from the left, Entoto Mountain Ridge from the north and Wechecha Mountain from right. The drainage of Addis Ababa show dendritic pattern and it consists of intermittent and permanent rivers (Figure 1.3). Regionally, it is found within the Upper Awash Basin of the Akaki River catchment. In the northern border of the site, small stream runs NE to SW. The topography of the specific studied site is nearly flat as shown in Figure 1.2. The maximum and minimum elevations reach 2143 and 2149m above mean sea level respectively.

Figure 1.2: Partial view of the study site

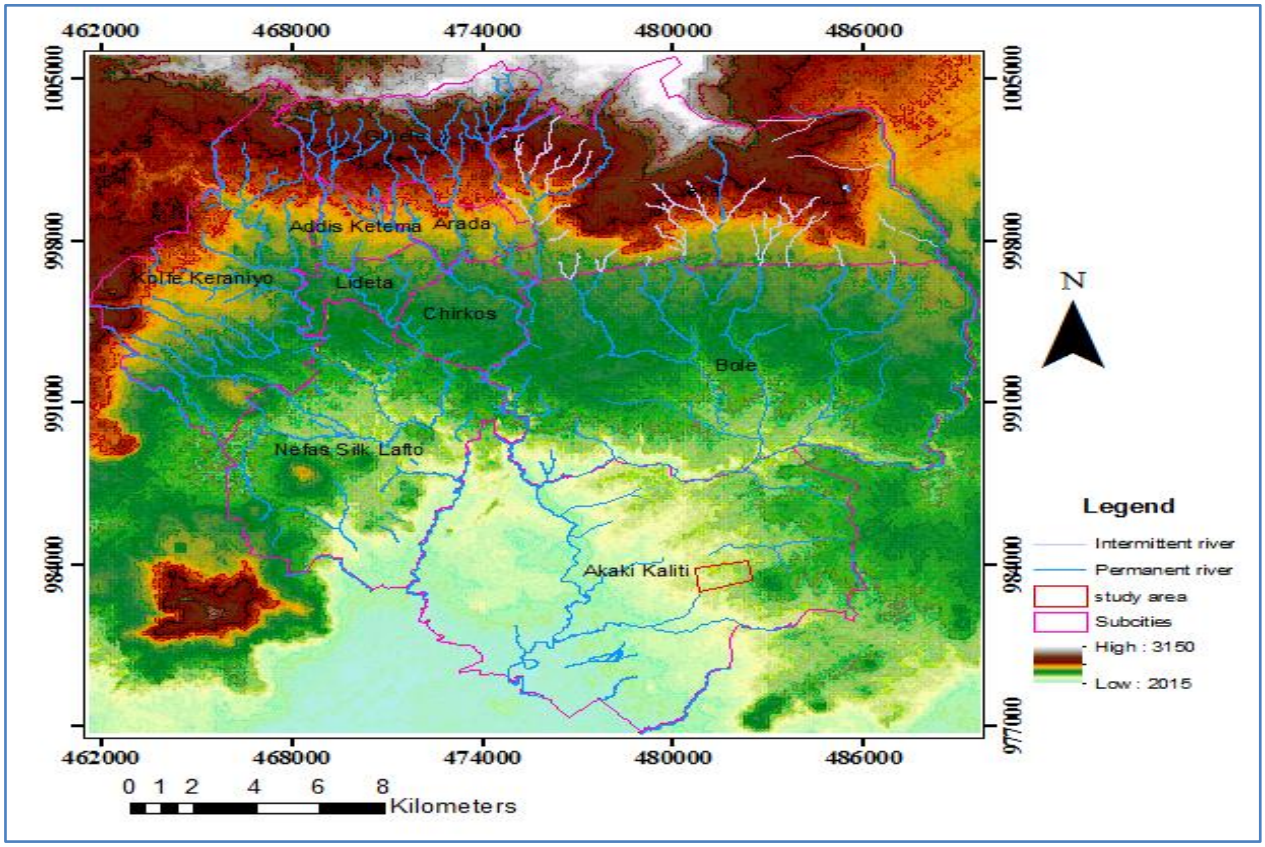

Figure 1.3: Drainage map of Addis Ababa

1.2.3 Climate

According to Cwb koppen and Geiger classification system, the climate of Addis Ababa is categorized as warm with an average annual temperature of 16.3 °C and a temperatures variation of 3.2°C annually (Available at https://en.climate-data.org/location/532/). The dry season extends from October to May, while from June to September it is wet, with intermittent rainfall in the rest of the months as shown (Table 1.1). The summer seasons are much rainier than the winter. The average precipitation in the city is 1143mm. The difference in precipitation between the driest month and the wettest month is estimated nearly 255mm.

Table 1.1: Annual temperature and precipitation of Addis Ababa city

Particulars	Jan	Feb	March	April	May	June	July	Aug	Sep	Oct	Nov	Dec
Average temperature (°C)	15.4	16.6	17.9	17.9	18	17	15.9	15.8	16.2	15.7	14.8	14.9
Minimum temperature (°C)	7.4	8.7	10.5	11.1	10.8	10.6	11.1	11	10.7	8.7	6.7	7
Maximum temperature (°C)	23.5	24.5	25.4	24.8	25.2	23.4	20.7	20.7	21.7	22.7	23	22.9
Precipitation (mm)	17	39	66	86	84	118	256	263	161	34	8	11

Available at https://en.climate-data.org/location/532/)

1.3 Problem statement

Failures of engineering structures are often associated with lack of knowledge and experience of builders about the physical characteristics of the underlying geologic features that determine the overall competency of foundation materials. Moreover, inadequate planning and undermining the need of conducting detail investigations employing appropriate techniques cause structural problems that result in damage of buildings with visible fracture and cracks on the walls, sinking and total collapse that finally lead to loss of lives and properties (lateef and Adegoke, 2016).

To construct safe and sustainable multistory building for any purpose, investigation of near surface lithologies, tectonic structures, hard rock morphologies, seismicity and groundwater condition beneath the site and its immediate surrounding are very essential. Therefore, in this study, limited geotechnical data, generated using samples collected from limited shallow boreholes (with depth less than 15m) as well as test pits are used. Nevertheless, for detail analyses the availability of such limited data points with large sampling separations may not be sufficient and hardly represent the whole area of interest in case if the subsurface conditions between the sampling points show variation in composition, structure, degrees of weathering, and other near surface characteristics. Therefore, for better understanding of the subsurface geological environment and infer the suitability / influence of the Earth materials as stability foundation for civil engineering structures integrated geophysical investigations consisted of shallow seismic refraction and electrical resistivity methods were employed in this study. These methods, which have no impact on the natural environment, are the most suitable techniques used to address similar geotechnical problems.

1.4 Research objectives

1.4.1 General objective

The principal objective of this research is to map subsurface geology in the area located at the south eastern part of Addis Ababa city (Akaki Kality Subcity), Central Ethiopia) and elucidate its suitability for the construction of multistory residential and commercial complexes through application of integrated geophysical techniques.

1.4.2 Specific objectives

- Delineate the underlying lithological units, particularly the competent bed rock that serve as solid foundation for building construction
- Determine depth and thickness of each layer and infer their probable effects on the sustainability of the civil engineering structures
- Map any structural discontinuities within the site that might pose impacts on safety of buildings foundations
- Determine any water bearing formation beneath the site (if it exists at shallow depth) and depth to groundwater table

1.5 Significance of the study

The results of this research may help to understand the foundation conditions of the present site with regard to its suitability for building foundation. This means civil engineers may find key inputs to develop engineering designs and also mitigations plans for anticipated problems that might happen anytime in the future.

Moreover, the result of this research provides valuable input for geologist- geophysicist researchers, city planners and other decision makers, which require relevant geotechnical information.

1.6 Thesis structure

This thesis is organized in to six chapters, where Chapter one is introduction part, which deals with the general background, site description, objectives, problem statement and methodology followed; Chapter two discusses the general geology, hydrogeology and seismicity of the study area; Chapter three covers the basic theoretical aspect of the geophysical techniques, particularly electrical resistivity and seismic refraction methods that are applied in this research. Chapter four describes field data acquisition, processing and presentation of the study, whereas Chapter five presents the result, discussion and interpretation of the data collected in this project. The final part, Chapter six, provides the main conclusion drawn from this research.

1.7 Methodology

A systematic methodology was followed within in the given time and resource to achieve the objectives stated in section 1.4. . Accordingly, both secondary and primary data have been used. Considering the site condition, i.e., geological and geo-morphological characteristics, including site accessibility, in this research integrated engineering geophysical methods, namely seismic refraction and electrical resistivity surveying, were implemented along selected profiles in order to portrait the near surface earth features beneath the target site. The geological and geophysical data have been prepared and modeled using AutoCAD, ArcGIS, WinResist, IPI2WIN, RES2DINV, Prosys–II, SeisImager/2D and Surfer software.

The overall methodology followed in this research is presented in the flow chart displayed in Figure 1.4. It is evident from this chart that this thesis work was conducted in three stages, classified as desk study, field work, and post-field data processing, presentation, interpretation and analyses. More description about each stage is given below.

1.7 .1 Desk study

This stage covers the activities done before starting the actual fieldwork, in which secondary data related to the study has been collected from different sources, including from archives of federal and regional government offices, internet and others. The real activities performed during this stage can be summarized as follows:

- Collection of geological , hydro-geological and geotechnical, including borehole, data from government organizations and internet
- Review of both published and unpublished previous works related to the subject matter
- Preliminary site visit, and preparation of field survey design
- Checking the functionality of survey instruments and other ancillaries

1.7.2 Fieldwork

Acquisition of primary data has been the main purpose of this stage and therefore, relevant geophysical, to some extent geological, data representing the research area its immediate surroundings were collected during this stage. Works progressed in this stage are listed as follows:

- Collection of nine vertical electrical resistivity sounding data using schlumberger configuration with maximum current electrode spacing of 220 m (AB/2=220m) using both IRIS and SARIS resistivity measuring instruments. The spacing between each successive sounding stations ranges from 80-200m.
- Collection of 2D imaging data with the help of high voltage source IRIS instrument along two profiles by employing dipole- dipole configuration with maximum unit electrode spacing of 30m.
- By utilizing 48channel *Dolang Seismograph* refraction seismic data was collected along three profiles using two 24 and one 12-channels. For all spreads the spacing between each successive geophones (receivers) were maintained to be 5m.

1.7.3 Data analysis and presentation

The primary electrical resistivity and seismic refraction field data were filtered and converted to appropriate formats, which then were processed using different geophysical software, such as *ArcGIS, WinResist, IPI2WIN, RES2DINV, PROSYS–II, SeisImager/2D, AutoCAD* and *Surfer.* Subsequently, geophysical contour maps, sections and profiles were prepared and the correlation between geophysical and geological data was made. Finally, maps and profile sections are

interpreted to represent the corresponding geological information which leads to the discussion and conclusion about the result of the study.

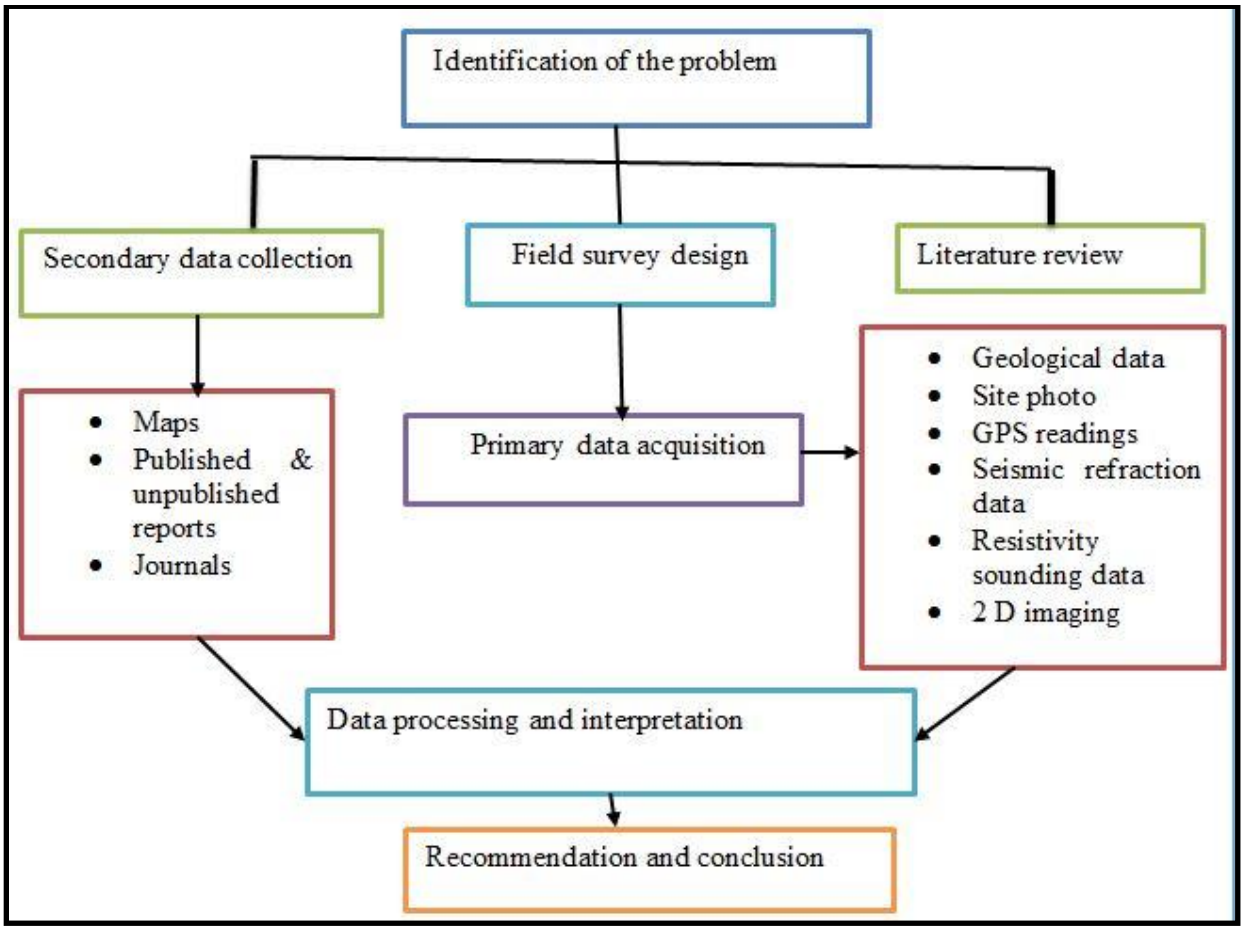

Figure 1.4: General methodology followed to achieve this thesis work

1.8 Previous Works

A number of geological, engineering geological, geotechnical and geophysical works have been conducted in Addis Ababa city and its surroundings in view to different perspective. Some of the related works which, are used as an input for this study are reviewed in the following manner.

a) Assiged Getahun (2007) studied the geology of Addis Ababa city classified into volcanic rocks of Intoto trachyte, Intoto mixed rocks, Foota basalt, Cheleka basalt, Repi basalt (trachyte basalt and basalt), lower ignimbrite, Wechecha-Furi-Year trachyte

and trachyte basalt, Wechecha-Furi-Yere ignimbrite, Quaternary olivine basalt, Quaternary Scoria, Tertiary sediment and Lake sediment.

b) Kebede and Taddessse (1990) studied engineering geology mapping of Addis Ababa area. Accordingly in the area are trachyte and rhyolite, ignimbrite tuff, trachyte basalt and basalt of different ages was mapped.

c) Construction Design Share Company (2011) conducted direct geotechnical investigation at Addis Ababa science and Technology University which is a few meters to the studied area. Accordingly, the drilled borehole is 10 m and the encountered lithologies are dark clay soil, completely decomposed rock and weathered basalt.

d) Hilemariam Syuim (2011) conducted integrated geophysical and direct geotechnical investigation at Addis Ababa Science and Technology University site which is near by the present study site.

e) Best consulting PLC (2014) conducted geotechnical investigation at Koye and Feche condominium sites which is nearby the present study area. Accordingly, 24 boreholes 10m for four story and 15m for seven story buildings were drilled. In their result clay soil and completely weathered rock cover the area in depth.

f) Ethiopian Construction Design and Supervision Works Corporation (2014) conducted geotechnical investigation at Koye and Feche massive housing projects. Accordingly more than 100 boreholes are drilled and their result in majority of boreholes indicates the top soil (black cotton and siltyclay soil) reaches more than the drilled depth. However, in some boreholes completely decomposed rock and weathered basalt rock are encountered beneath the clay soil cover.

1.9 Limitations of the study

Maximum effort has been made to effectively carry out this thesis work through the allocated time and financial resources. Well planned and proper field survey has been carried out in different seasons to acquire reliable geological information about the vertical and horizontal stratification of construction site. However, some situations render the field survey as well as the final interpretation of this study. Some of the major limitations encountered are stated as follows:

a) The presence of relatively thick black cotton soil cover with low degree of compaction have significant effect on the propagation of seismic signals deep in to the ground and thereby limits the depth of investigation.

b) As the study area is located nearby the Addis – Adama express way and new residential houses construction site, there is too much noise from heavy traffic flows, construction machineries, carts, animals and human beings. Generally, these situations have made the field work tedious, time consuming, particularly the seismic refraction survey and unable to collect more data. The presence of power line, metallic objects, highways and buildings in and around the study area have hindered the application of other geophysical surveys, like magnetic.

c) Absence of well-documented lithological log data within this specific site has made difficult a refined detail geophysical data interpretation.

CHAPTER TWO

2 OVERVIEW OF THE GEOLOGY, HYDROGEOLOGY AND SEISMICITY OF THE STUDY AREA

2.1 Regional Geology

The Ethiopian landmass is covered by three major geological terrains, i.e., the Proterozoic crystalline basement rocks, Late-Paleozoic-Mesozoic sedimentary rocks and Cenozoic volcanic rocks. Among those, the Cenozoic volcanic rocks and quaternary sediments cover the majority of the country's landmass (Solomon Gerra, 2002).

Addis Ababa is situated at the junction of the Ethiopian plateau and the Main Ethiopian Rift System, and its geology is composed of an amalgamation of both the plateau and rift related volcanic sequences with different composition and age (Haile Selasie Girmay and Getaneh Assefa, 1989). Different researchers have studied the geology of Addis Ababa city and adjacent areas. Assiged Getahun (2007) mapped the geology of Addis Ababa and classified the volcanic rocks into Intoto trachyte, Intoto mixed rocks, Foota basalt, Cheleka basalt, Repi basalt (trachyte basalt and basalt), lower ignimbrite, Wechecha-Furi-Year trachyte and trachyte basalt, Wechecha-Furi-Yere ignimbrite, Quaternary olivine basalt, Quaternary scoria, Tertiary sediments and Lake sediments. While conducting the engineering geological mapping of Addis Ababa area, Kebede Tsehayu and Taddessse Hilemariam (1990) have delineated that trachyte and rhyolite, ignimbrite tuff, trachyte basalt and basalt of different age.

2.1.1 The stratigraphic sequence

The work of Haileselassie Girmay and Getaneh Assefa (1989) presents the stratigraphic sequence of Addis Ababa and its adjoining places. Its stratigraphy consists of Miocene - Pleistocene volcanic successions. Accordingly, from oldest to youngest Alaji rhyolites and basalts, Intoto silicic, Addis Ababa basalts, Nazareth group and Bofa basalts constitute the lithostratigraphic succession of Addis Ababa.

2.1.1.1 Alaji Basalt

The outcrop of this volcanic rock is exposed in the Entoto Mountain from the end of Oligocene until middle Miocene (Zanettin and Justin, 1974). This series is represented by Alaji rhyolites and Alaji Basalts and underlain by tuffs and ignimbrites. These basalts, with grey and glassy welded tuff intercalation, show highly variable texture that ranges from highly pophyric to aphyric. Its distribution extends from the crest of Entoto ridge (bordering the northern parts of Addis Ababa) towards the north (Haileselassie Girmay and Getaneh Assefa, 1989).

2.1.1.2 Entoto Silicic

The Entoto Silicic volcanic are unconformably overlain by Addis Ababa basalt on the foothill of Entoto and underlain by Alaji basalt. These units are composed of early Miocene rhyolite and trachyte with minor amount of welded tuff and obsidian. Silicic volcanic unit could denote localized terminal episodes to massive Oligocene fissure basalt activity in the Addis Ababa region (Morton *et al.*, 1979). The thickness of the flow becomes maximum on the top of Entoto ridge and thin at the eastern part of Addis Ababa (Haile Selassie Girmay and Getaneh Assefa, 1989).

2.1.1.3 Addis Ababa Basalt

This unit mainly exposed in the central part of the city. It is underlain by the Entoto silicic and overlain by Lower welded Tuff of the Nazareth group. The maximum thickness exceeding 130 meters and the outcrop was exposed at ketchene stream. Olivine porphyritic basalts outcrop in the central part of the town that includes Mercato, Teklehaymanote and Sidist Kilo. The distribution of plagioclase porphyritic basalt is almost the same as that of the olivine porphyritic basalt. It outcrops in an area, which includes Sidist Kilo, General Winget School and French Embassy. The Lower Welded Tuff overlies both types of basalt nearby the Building College, the Kolfe Police School, the Kokobe Tseba School and YecaMariam Church (Haile Selassie Girmay and Getaneh Assefa, 1989).

2.1.1.4 Nazaret Group

The lithological units identified in this group are Lower Welded Tuff, Aphanitic basalt and Upper Welded Tuff. They are underlain by Addis Ababa basalt and overlain by Bofa basalts .These welded tuff outcrops as small discontinuous body at Filwoha, western parts of Addis Ababa and Sululta areas. It is glassy with abundant fiamme and has columnar joints. It is overlain by the Aphanitic basalt and underlain by the olivine and plagioclase porphyritic basalt. Aphanitic Basalt covers the southern part of the town, especially the areas of Bole International Airport and Lideta Airfield.

The rock shows vertical curved columnar jointing together with sub-horizontal sheet jointing. The basalt is overlain by pumeacoues pyroclastic falls and the pyroclastic falls. It consists of labradorite, augite, rarely olivine and magnetite. The crystals of plagioclase show marked flow alignments. Upper Welded Tuff outcrops all over the southern part of the town; including Bole, Nefas Silk and Railway station; nevertheless it is also present in the central and northern parts of the town. It is grey colored, vertically and horizontally jointed and composed of sandine, orthoclase, quartz, pumice and unidentified volcanic fragments. The welded tuff is underlain by Aphanitic basalts and overlain by young olivine basalts.

2.1.1.5 Bofa Basalts

These basalts comprised of olivine porphyritic basalt, scoria, vesicular and scoriaceous basalt and trachyte-basalt lava flows. They extend in to the south from Akaki River and have a thickness of about 10 meters (Anteneh Girma, 1994). They appear to have a maximum thickness of 20 - 40m over the Akaki well field, and get thinner, even absent in other places.

2.1.1.6 Alluvial and Residual Deposits

These deposits consisted of quaternary to recent alluvial and residual deposits. Those deposits are mainly found in some localities along small and Big Akaki Rivers, especially south and southwest of the capital city. A thick alluvial deposit occurs in the area between Akaki town and Abba Samuel Lake. Some deposits occur along the Kebena River, north-west of Bole area. Soils, which are developed in-situ by the decomposition of rocks, are located in the central, southeast, northeast, and Gullele and Kolfe areas. The thickness of these deposits varies between 5 and 50m.

2.2 Tectonic setting

The geology of Addis Ababa is the result of the intersection of two major tectonic lineaments and Cenozoic to Quaternary volcanism. The two tectonic features are the Yerer-Tullu Welele Volcanic Lineament (YTVL) and the western margin of the Main Ethiopian Rift (MER).The YTVL is an East–West running fault and volcanic zone. The intersection between YTVL and MER created the Addis Ababa embayment, where the rift becomes wider and the step faults defining the rift are subdued (Abebe *et al*., 1998).

The Addis Ababa area is highly tectonized and complex due to its location with proximity to the margin of the Main Ethiopian Rift (Assegid Getahun, 2007). Accordingly, the main diastrophic structures encountered are lineaments and faults, whereas the non-diastrophic structures are bedding and volcanic layering.

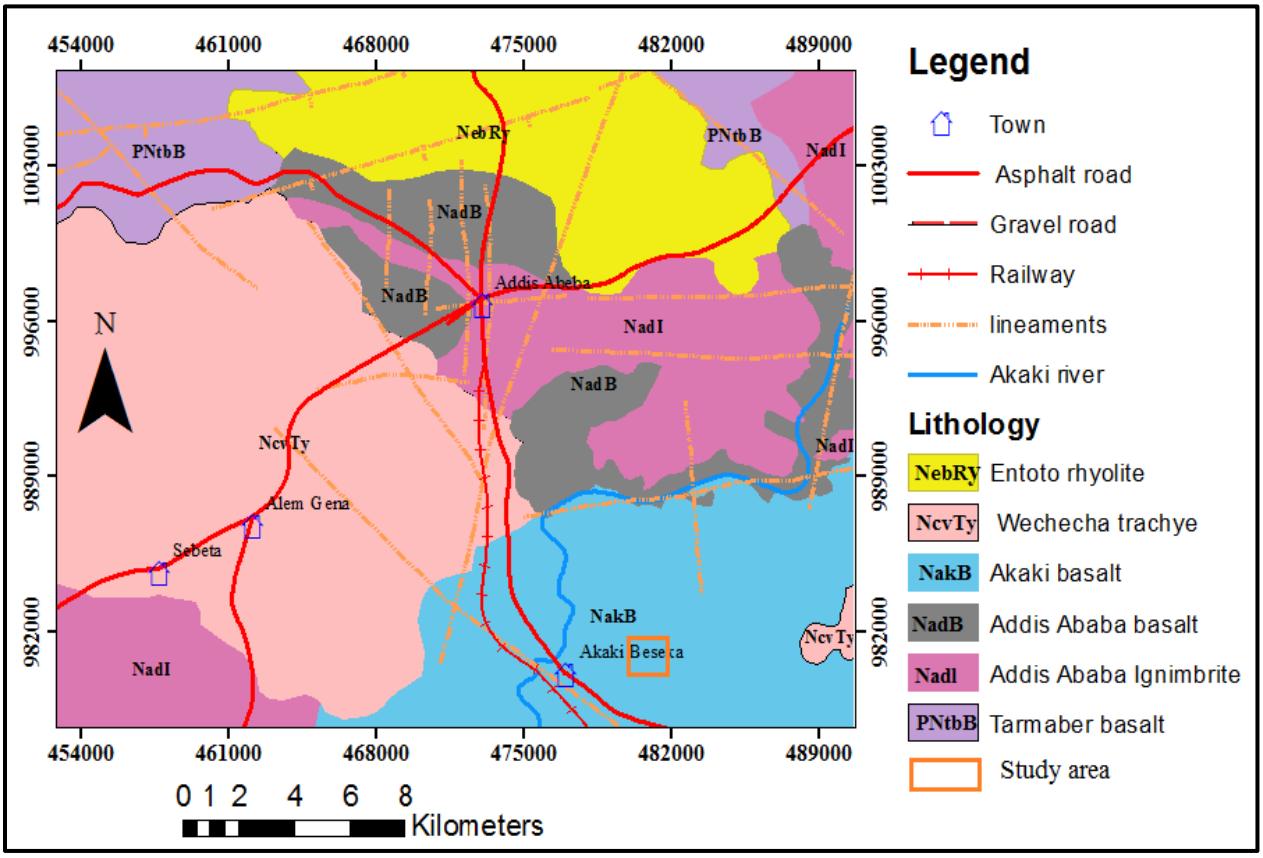

Figure 2.1: Geological map of Addis Ababa (modified from WWDSE, 2008)

Different geomorphic features align mostly in NE-SW direction, which is parallel to the rift structures or rift margin. Most of the faults mainly trend in NE-SW direction. These faults, which cut the entire section, are mainly normal faults. Joints and fractures are observed in rocks. The sizes of these structures vary from few centimeters to several meters in length (Assegid Getahun, 2007).

2.3 Site geology

From surface exposure and borehole log data the study area consists of exposure of black cotton soil, siltyclay soil and completely decomposed rock and highly to moderately weathered basalt.

2.3.1 Soil

The occurrence and distribution of soils within a specific locality is controlled by topography, geology and climate. Soils in the study area could be the result of physical, chemical and biological decomposition of the surrounding volcanic rocks. The nature of soils is an important parameter in the development of civil engineering structures which directly poses social, environmental and economic impacts. Their effect is more pronounced for shallow foundation structures due to their proximity to surface. From visual observation, nearby borehole and ongoing construction sites, the top layer is represented by black cotton soil with strongly expansive behavior that shows desiccation cracks and variable moisture content (Figure 2.2). Rough estimations show that the thickness of the top soil reaches a minimum of 2.5 m.

Figure 2.2: Photo taken from the site, where the black cotton soil showing visible cracks (red dotted lines).

Based on the ECDSWE (2014) and CDSC (2011)) report, the black cotton soil (dark clay), silty clay soils, completely decomposed rock and weathered basalt are encountered up to 15m depth. Sampled lithological log sections are presented in Appendix 2.

2.4 Hydrogeology

The occurrence, movement and storage of groundwater at particular place depend upon the surrounding geological setup, climatic conditions and surface morphology. In this case, porosity and permeability of the volcanic rocks and recent sediments distributed within this specific area determine the hydro-geological characteristics. The possible mechanism for rocks to acquire porosity and permeability is associated with the formation primary porosity and post-rock formation processes, such as weathering and fracturing.

Different volcanic rocks, unconsolidated sediments and black cotton clay soils cover the study area and its surroundings. The expected aquifer type in such geological condition is mainly volcanic aquifer. The groundwater in the study area related with the nature of the surrounding lithology, structure and topographic features. The means of recharge mechanism is streams and seasonal rainfall.

2.5 Seismicity

Crustal extension and associated volcanic phenomena sign a warning for the occurrence of earthquake events. The Main Ethiopian Rift System and the Afar Depression are parts of the great East African Rift System, where numerous seismic activities take place indicating tectonically dynamic nature of this region. As such the study area is located at the western margin of the main Ethiopian Rift seismic activity should be considered.

According to the report compiled by World Bank Group (2015), Addis Ababa is urbanizing and growing at a rapid pace. However, the city faces potential shocks and stresses that could hinder it from achieving its development goals. These include urban flooding, earthquakes and rapid urbanization. The city lays in the seismically active region it could experience moderate seismic risk (Messele Haile, 2012). It is located only 75-100 kilometers away from the western margin of the Main Ethiopian Rift Valley, which is a hotbed of tremors and active volcanoes. In addition

to Addis Ababa, some major cities in Ethiopia are very near to the major fault lines, like the Wonji fault, Nazret fault, Addis-Ambo-Ghedo fault, and Filowha fault lines along which numerous earthquakes of varying magnitude have been registered in the past (Samuel Kindie, 2002).

The presence of the Filwoha hot springs at the heart of Addis Ababa city itself is a good example of nature's reminder that the city lies on fault zone that slowly builds strains. It is the release of these strains accumulated over the years that cause the phenomenon of earthquake (Samuel Kindie, 2002).

In one century of its existence Addis Ababa has witnessed a number of earthquakes. Some of the recorded occurrences are listed in table 2.1.

Table 2.1: previously occurred earthquakes in Addis Ababa (Laikemariam Asfaw, 1985 as cited in Messele Haile, 2012).

Year	Earthquake magnitude	Epicenter distance from Addis Ababa	Location
1906	6.8	100km	South of Addis Ababa
1961	6.6	200 km	Karakore
July 1997	4.0	22 km	Southwest of Addis Ababa
1977 and 1984	Small	Far but felt in high rise buildings	-

Based on the Ethiopian Building Code Standard (1995), the country is divided in to five seismic zones, namely Zone 0, 1, 2, 3 and 4 (Figure 2.3). Accordingly, the study area lies under zone 2, where a moderate seismic risk is expected. The seismic zonation shown in Figure 2.3 is related to bed rock acceleration (BRA) and the study area fall under Zone 2 with the corresponding BRA of 0.05 (Table 2.2).

Table 2.2: Ethiopian seismic zone and their equivalent bed rock acceleration

Zone	4	3	2	1
Bed rock acceleration(α_0)	0.1	0.07	0.05	0.03

Generally, the existence of hot springs and the proximity of the city to the Central Main Ethiopian Rift are clear indications of the dynamic nature of the region, and therefore, attention should be given for the development of proper designs and constructions of civil engineering infrastructures in the city.

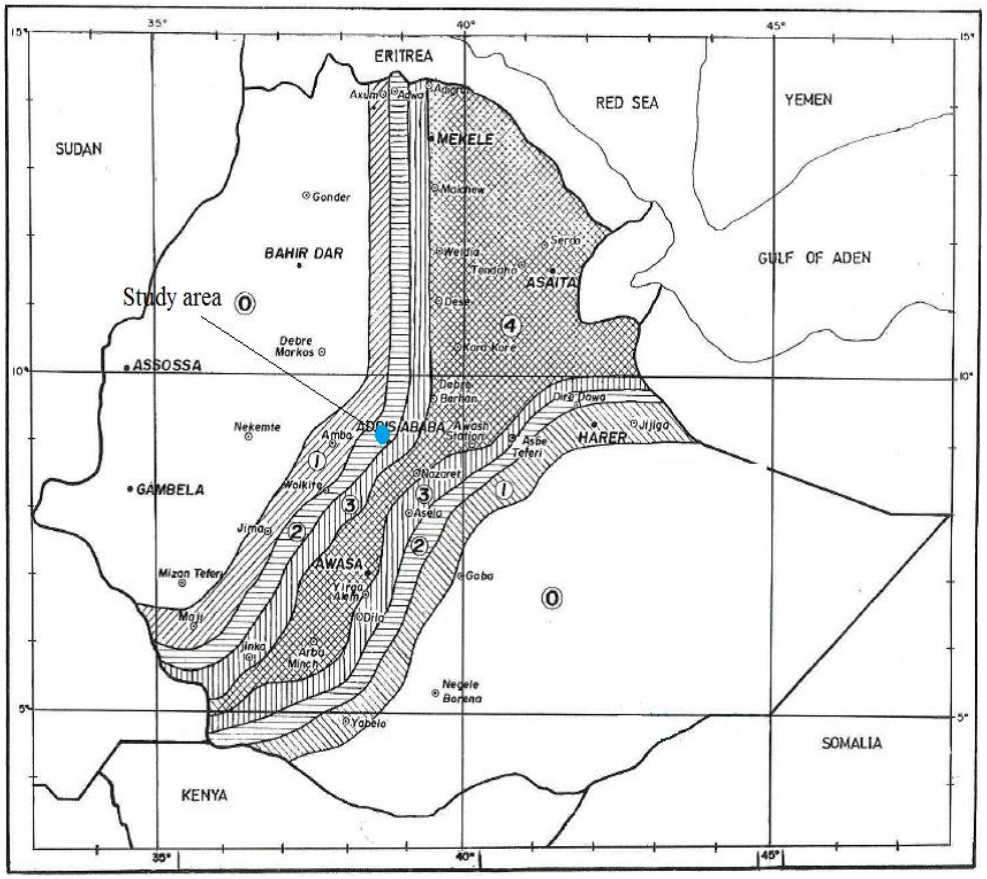

Figure 2.3: Seismic hazard map of Ethiopia (Ethiopian Building Code Standards, 1995)

CHAPTER THREE

3 THEORETICAL BACKGROUND OF THE METHODS EMPLOYED

3.1 Preamble

In general, exploration geophysics utilizes various geophysical methods to detect subsurface geological features through indirect means by taking various physical measurements at surface, on air or within a borehole. It provides for collecting geological and hydro-geological information in cost effective and efficient manner. Now a days, these techniques can be utilized to determine the hydro-stratigraphic framework, depth to bedrock, location of subsurface cavities, fractures, location of abandoned wells and the like. Geophysical surveying results are more effective when they are integrated with a drilling activity or known geological condition.

Utilizing integrated geophysical method is more preferable than a single one because it can provide to better refine conceptual model, minimize ambiguities and it allows against one method failing providing useful data. The selection and effectiveness of a particular geophysical technique depends on objective of the investigation, site geology, site access and the experience of the personnel to the particular investigation. When the investigation is performed in a systematic way and utilized in early stage of site characterization process, the methods can also provide valuable information about the subsurface information and they can be used later in the investigation to confirm and improve site characterization.

In this study, electrical resistivity and seismic refraction methods are only presented. Both methods can provide extensive spatial data about the subsurface. However, each method has their own merit and demerit and may not be applicable in every situation. Site-specific geology, site access, and the presences manmade features affect the geophysical measurement and determine the success of those particular geophysical methods. Therefore, it is advisable to conduct integrated survey in case one fails or if there is a need to fill in data gaps in another one. Brief theoretical detail of the methods employed in this study presented in next sections.

3.2 Electrical resistivity method

3.2.1 Basic theory and principles

The resistivity method is based on the fact that any subsurface variation in resistivity alters the pattern of current flow in the ground and therefore changes the distribution of electric potential at the surface. Since the electrical resistivity of such factors as superficial deposits and bedrock differ from each other, the resistivity method may be used in their detection and to give their approximate thicknesses, relative positions and depths (Bell, 2007).

Electrical resistivity is based on the contrast in electrical resistivity of different rocks and soils within the earth. The primary application of electrical resistivity surveying method is to determine the subsurface resistivity variation by taking measurements on the ground surface. The true resistivity of the subsurface formation can be estimated from the measured apparent resistivity. The estimated ground resistivity valve is corresponds with various geological parameters such as the mineral and fluid content, porosity and degree of water saturation in the rock. This surveying technique has been utilized for hydro-geological, mining, environmental and geotechnical investigations (Loke, 2001).

To relate the resistivity valve into geological information, prior knowledge of typical resistivity values for different types of subsurface materials and the geology of the site is important. Igneous and metamorphic rocks have higher resistivity values than the corresponding sedimentary rocks. The degree of fracturing, porosity and the percentage of the fractures filled with ground water determine the resistivity variation of subsurface. Generally, sedimentary rocks are more porous and have higher water content than other group of rocks has lower resistivity values. Moisturized soils and fresh groundwater have also lower resistivity values. Clayey soils have a lower resistivity value than sandy soils at normal condition.

However, different class of rocks and soils may have similar range of resistivity values (see Table 3.1). This is because the resistivity of a specific rock or soil material depends on the porosity, the degree of water saturation and the concentration of dissolved salts. Resistivity values show larger significant range compared to other physical quantities mapped by other

geophysical methods. The resistivity valve of rocks and soils for a specific site can vary by several ranges of magnitude (Loke, 2001).

Table 3.1: Resistivity valve of common earth materials (Loke, 2001)

Common earth materials	Resistivity (Ω.m)
Slate	6×10^{2}-4×10^{7}
Marble	10^{2}-2.5×10^{8}
Quartzite	10^{2}-2×10^{8}
Granite	5×10^{3}-10^{6}
Basalt	10^{3}-10^{6}
Sandstone	8-4×10^{3}
Shale	20-2×10^{3}
Limestone	50-4×10^{2}
Clay	1-100
Alluvium	10-800
Groundwater(fresh)	10-100
Sea water	0.2

3.2.2 Field procedures

In the electrical resistivity surveying work, an electric current is introduced into the ground by means of two current electrodes (C1 & C2) and the potential difference between two potential electrodes(p1 & p2) is measured as shown in Figure 3.3. Direct measurement of the potential drop or apparent resistance in Ohms is preferable than the observed current and voltage. Finally, the apparent resistance value is converted to apparent resistivity by use of a geometric factor that depends on the particular electrode configuration used in the particular survey (Bell, 2007).

Two common procedures are well known in resistivity surveying work. The particular procedure to be used depends on whether one is interested in resistivity variations with depth or with lateral

extent as well as in both directions. In order to acquire data different electrode configurations are available. The selection depends on the study objectives and site access conditions.

3.2.2.1 Vertical Electrical Sounding (VES)

This procedure is 1D surveying applied for detection of subsurface resistivity variations in depth. It uses a fixed center with an increasing spreads symmetrically. The procedure is especially utilized to study the vertical resistivity variations.

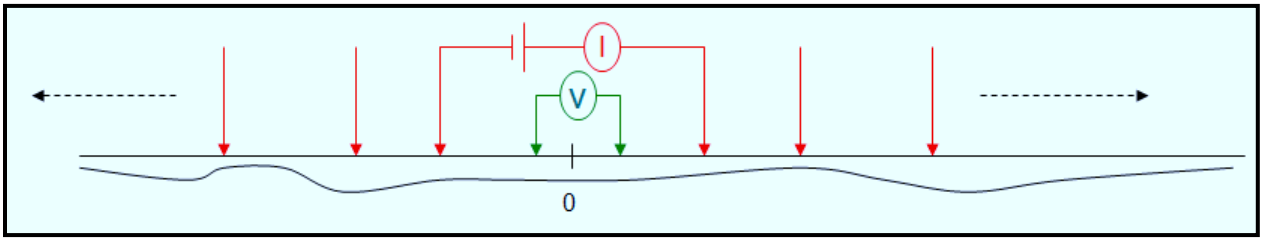

Figure 3.1: Vertical electrical sounding survey layouts

3.2.2.2 Horizontal profiling

1D profiling survey is mainly applied for investigation of the subsurface lateral lithological and/or structural variations. In contrary to the resistivity sounding, the electrodes are fixed in length but systematically displace along the survey line (Figure 3.2).

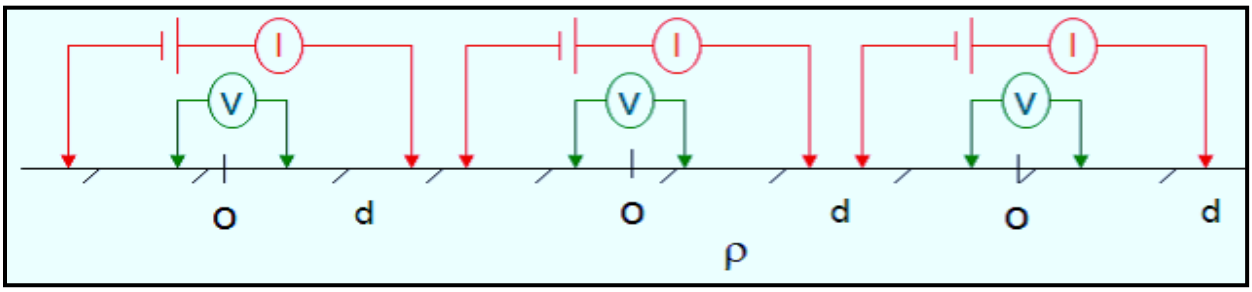

Figure 3.2: Layout of the resistivity profiling

3.2.2.3 2D Imaging

The greatest drawback of the VES survey is that it only considers vertical variation in the subsurface resistivity and to fill this gap, a two-dimensional (2-D) model is introduced. 2-D model show resistivity change in the vertical direction as well as in the horizontal direction along

the survey line. It is more accurate and reliable model of the subsurface. In this case, it is assumed that resistivity is constant in the direction that is perpendicular to the survey line. Nowadays, 2-D surveys are the most practical and cost effective means of obtaining accurate results of the subsurface resistivity contrast compared to 3D survey. 1-D resistivity sounding surveys usually involve limited readings, while 2-D imaging surveys involve about hundreds to thousands of measurements. In many geological conditions, the use of 2-D electrical imaging surveys can provide useful results that are complementary to the information obtained by other geophysical surveys (Loke, 1999).

Many electrode configurations are available in resistivity surveying work to carry out the above justified procedures and the general array layout is shown in figure 3.3. However, in practice the Wenner, Schlumberger and dipole-dipole arrays are commonly used. The selection of the particular configurations is depending on the objective and specific problem formulated to ground investigation interest vertical drilling or horizontal profiling as well as both.

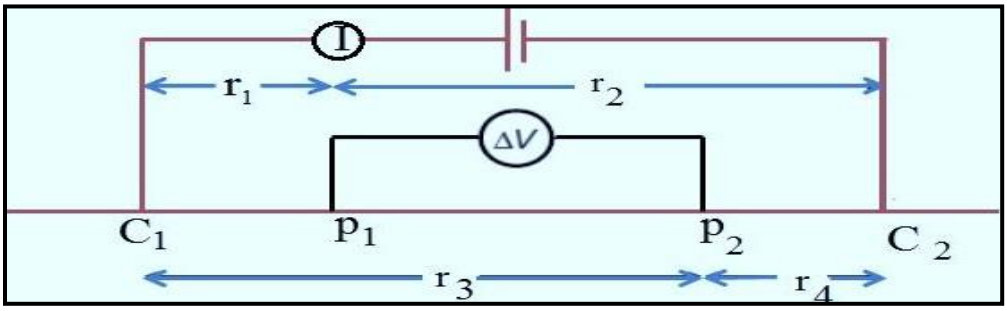

Figure 3.3: Layout of the general electrode configuration

From the general array layout one can find the apparent resistivity of the subsurface mathematically as follows:

$$\Delta V = V_{P1} - V_{P2} = \frac{I\rho}{2\pi}\left[\frac{1}{r_1} - \frac{1}{r_2} + \frac{1}{r_3} + \frac{1}{r_4}\right] \qquad 3.1$$

a) Wenner array

In this layout the current and potential electrodes are uniformly spaced in a line shown in figure 3.4. For depth exploration using the Wenner array, the electrodes are expanded about a fixed

center, increasing the spacing an in steps. For lateral extent variation, the spacing remains constant (a) and all four electrodes are moved along the line and shifted to another profile.

In the case of Wenner array, r_1=a, r_2=2a, r_3=2a and r_4= a

Substitute within the general array equation (3.1) the potential looks like

$$\Delta V = V_{P1} - V_{P2} = \frac{I\rho}{2\pi}\left[\frac{1}{a} - \frac{1}{2a} - \frac{1}{2a} + \frac{1}{a}\right]$$

After simplification it becomes $\Delta V = V_{P1} - V_{P2} = \frac{I\rho}{2\pi}\left[\frac{1}{a}\right]$

$$\rho_a = \pi\left[(2a)\left(\frac{\Delta V}{I}\right)\right] \qquad 3.2$$

Where 2πa is a geometric factor

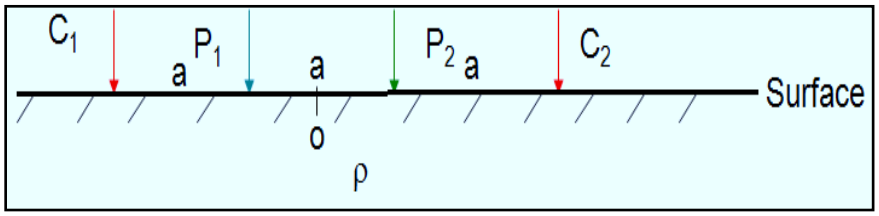

Figure 3.4: Layout of the Wenner configuration (C1p2=p1p2=p2C2=a)

b) Schlumberger array

In this configuration, the electrodes are symmetrically placed about a point at the center of the array (O) as depicted in Figure 3.5. We use this array commonly to study the resistivity variation in depth.

$$\Delta V = V_{P1} - V_{P2} = \frac{I\rho}{2\pi}\left[\frac{1}{r_1} - \frac{1}{r_2} - \frac{1}{r_3} + \frac{1}{r_4}\right]$$ For this array, r_1=s-b, r_2=s+b, r_3=s+b, r_4=s-b

$$\Delta V = V_{P1} - V_{P2} = \frac{I\rho}{2\pi}\left[\left(\frac{1}{s-b} - \frac{1}{s+b}\right) - \left(\frac{1}{s+b} - \frac{1}{s+b}\right)\right]$$

After a certain mathematical simplification it becomes the apparent resistivity becomes

$$\rho_a = \pi\left[\left(\frac{s^2-b^2}{2b}\right)\left(\frac{\Delta V}{I}\right)\right] \qquad 3.3$$

The expression $\pi\left[\frac{s^2-b^2}{2b}\right]$ is a geometric factor for this array

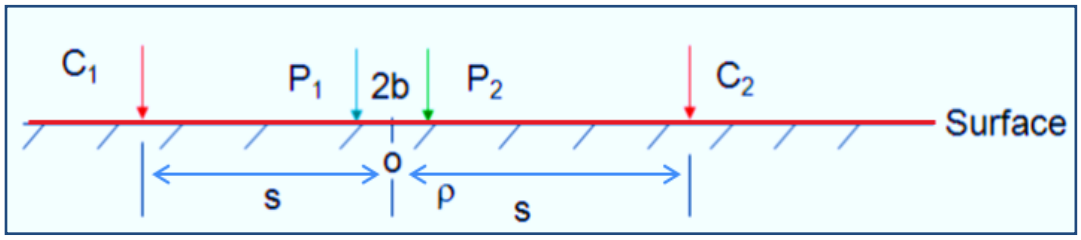

Figure 3.5: Layout of the Schlumberger array (C1C2≥5P1P2)

c) Dipole- Dipole array

For this array type, the distance between the current dipole and the potential dipole is increased in discreet steps in order to increase the depth of penetration. Dipole-dipole array includes six different configurations but for the present study axial array were utilized and the general layout is presented in Figure 3.6.

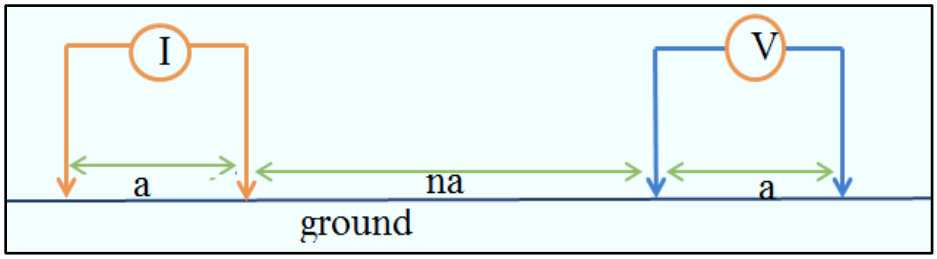

Figure 3.6: Dipole -dipole configuration setup (Note that C1C2=p1p2=a & n is the dipole number)

3.2.3 Data processing and presentation

Prior to quantitative and qualitative interpretation of electrical resistivity raw data, it has to be filtered, processed and presented in form of profiles, sections and contour maps. For this purpose there a number of electrical resistivity inversion software enabling to translate the measured apparent resistivity values in to true resistivity and thickness of the subsurface source bodies.

The working principle of behind this software's is primarily based on different assumptions, geometric models and mathematical models.

3.2.4 Data interpretation

Non-uniqueness and ambiguities in interpretation are the common problems in the inversion of resistivity and other geophysical data. For a unique measured raw data, set of models may fit to the same calculated apparent resistivity values. To minimize the range of possible models, normally assumptions are made about the nature of the subsurface and incorporated into the inversion subroutine (Loke, 2001). For the same reason, of integrated techniques and prior knowledge about the subsurface geology are utilized to lessen problems encountered during quantitative and qualitative data interpretations and refine the most probable model. There are a number of both direct and indirect resistivity data interpretation techniques available in the field of geophysics. Currently, computer based direct interpretation tools, like *winResist*, *IPI2WIN* and *2DRESINV* software is widely used.

3.3 Seismic Refraction Method

3.3.1 Basic theory and principles

In seismic surveying, seismic waves are created by a controlled source and propagate through the subsurface (Figure 3. 7). Some waves will return to the surface after refraction or reflection at geological boundaries within the subsurface as shown in figure 3.8. Instruments distributed along the surface detect the ground motion caused by these returning waves and hence measure the arrival times of the waves at different ranges from the source. These travel times may be converted into depth values and, hence, the distribution of subsurface geological interfaces may be systematically mapped. In this study, the focus is refracted seismic waves solely and taking other waves as a noise.

Seismic refraction method is based on the propagation seismic waves on different geological materials which leads contrast in velocity and the seismic wave refracts when it crosses contact between the underlying soils and rocks. For engineering geophysical site characterization, an artificial impulse is generated by using a heavy hammer source at ground surface (Redpath, 1985).

On the local scale, refraction surveys are widely used in foundation studies on construction sites to derive estimates of depth to bed rock underlying unconsolidated materials. The use of the plus–minus method or the generalized reciprocal method provides to study irregular rock head geometries in detail and thus reduces the need for test drilling with its associated high costs.

The theory of refraction seismic method is based on the combinations of Snell`s laws, Fermat's principle and Huygens's principle. Consequences of Snell`s law for the refracted wave in two layer medias with velocity v_1 and v_2 is expressed as:

a) When the velocity of the first layer and the second layer are the same ($v_1 = v_2$), the waves go straight and there is no refraction (constant velocity).

b) When $v_2 > v_1$, the wave is refracted away from the normal and there is a possibility to measure the refracted wave at the surface. In this case seismic refraction will work.

c) When $v_2 < v_1$, the wave is refracted towards the normal and there is a no possibility to measure the refracted wave at the surface.

Hence, the seismic refraction method faces problems in the case of inverted layer and blind zone (i.e. in case of velocity inversion, when there is a low velocity layer beneath a higher velocity layer and thin layer).

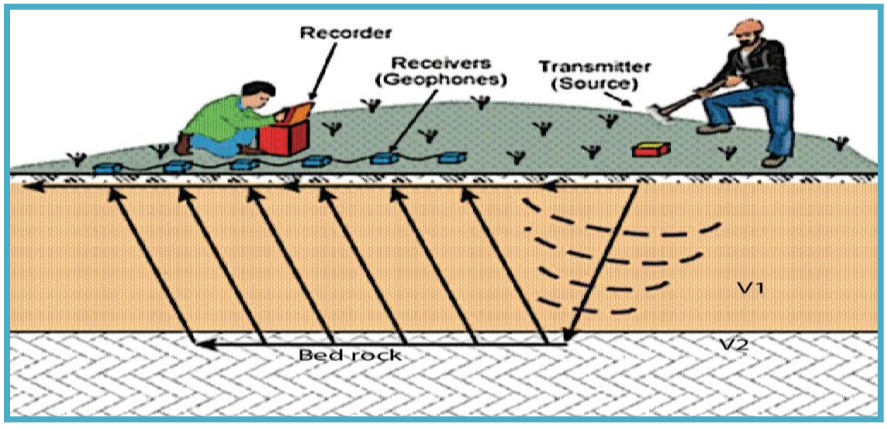

Figure 3.7: Seismic refraction surveying field layout

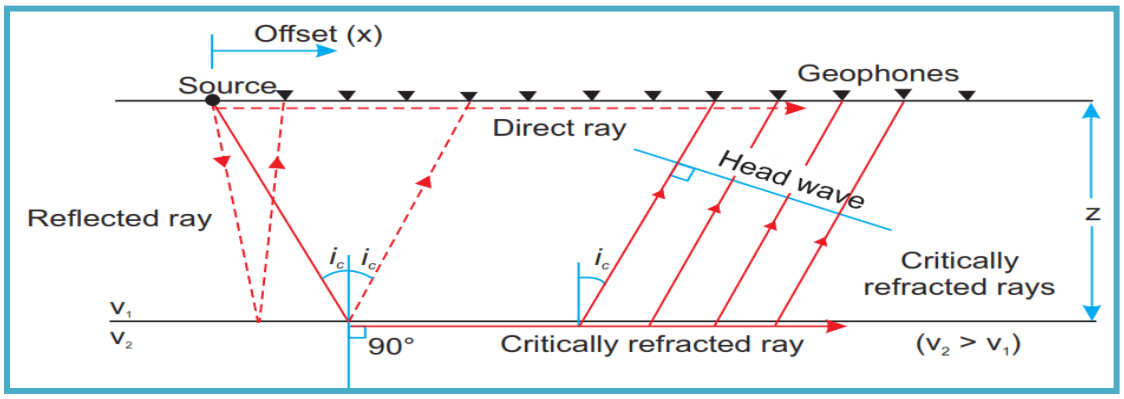

Figure 3.8:Direct, reflected and refracted waves for two layer earth model (Reynolds, 2011)

3.3.2 Overview of seismic waves

Seismic waves are waves that propagate outwards from a seismic source such as an earthquake or other artificial sources through Earth's interior. Sources suitable for seismic surveying usually generate short-lived wave trains, known as pulses that typically contain a wide range of frequencies. Except in the immediate vicinity of the source, the strains associated with the passage of a seismic pulse are minute and may be assumed to be elastic. Two major categories of seismic waves are known: body waves and surface waves.

Body waves - these waves propagate through the Earth's interior. Especially in refraction surveying, the body waves are used as the source of information used to image the Earth's interior. Body waves propagate away from the source in all directions. If the speed at which body waves propagate through the Earth's interior is constant, then at any time, these waves form a sphere around the source. This wave can be further subdivided into two classes of waves: P and S waves.

P-waves are also called primary waves, because they propagate through the medium faster than other wave types. In such waves, the particles constituting the medium are displaced in the same direction that the wave propagates, in this case, the radial direction. Thus, material is being extended and compressed as these waves propagate through the medium.

The other type of body wave is S-wave it sometimes called secondary waves, because they propagate through the medium slower than P waves. In these waves, particles constituting the medium are displaced in a direction that is perpendicular to the direction that the wave is

propagating. In most exploration seismic surveys we use P waves as their primary source of information.

Surface waves are waves that propagate along the Earth's surface. Their amplitude at the surface of the Earth can be very large, but this amplitude decays exponentially with depth. Surface waves propagate at speeds that are slower than S waves, are less efficiently generated by buried sources, and have amplitudes that decay with distance from the source more slowly than is observed for body waves.

Like body waves, there are two classes of surface waves, *Love* and *Rayleigh* waves that are distinguished by the type of particle motion they impose on the medium.

For homogenous and isotropic medium P and S waves are calculated mathematically as follows:

$V_P = \sqrt{\frac{\frac{4}{3}\mu + k}{\rho}}$ & $V_S = \sqrt{\frac{\mu}{\rho}}$ where μ and k are collectively called elastic parameters of a material through the wave passes and ρ is density of a material. The p wave velocity of different geological materials is presented in Table 3.2.

3.3.3 Depth and velocity determination from travel time curve

Let us consider a two layer horizontal stratified Earth as shown in figure 3.9 where x is the offset distance from seismic source to the geophone (receiver). Assuming Z1 and v_1 are the thickness and the velocity of the top layer respectively and V_2 is the velocity of the second layer. The path of the seismic signal is defined as SABG (Figure 3.9 a). From figure 3.9 a, consider that the wave SA which strikes the layer contact at the critical angle (θ_c). The total travel time for the refraction signal to travel from the source 'S' to the geophone 'G' is expressed as

$$T_{SG} = T_{SA} + T_{AB} + T_{BG} \quad (3.4)$$

Similarly, one can find the total travel time as follows in equation 3.5

$$T_{SG} = T_{SA} + T_{AB} + T_{BG}$$

$$T_{SG} = \frac{SA}{V_1} + \frac{AB}{V_2} + \frac{BG}{V_1} \quad (3.5)$$

From Figure 3.8a, we can relate mathematically as SA= BG which is equals to $\frac{Z_1}{\cos\theta c}$ and AB=X-2Z_1 tan(θc)

Now, by inserting the above equations to equation 3.5, we get:

$$T_{SG} = \frac{\frac{Z_1}{\cos\theta c}}{V_1} + \frac{X - 2Z1\tan(\theta c)}{V_2} + \frac{\frac{Z_1}{\cos\theta c}}{V_1} \quad (3.6)$$

After rearrangement

$$T_{SG} = \frac{x}{V_2} + \frac{2Z1}{\cos(\theta c)V_1} + \frac{2Z1\sin(\theta c)}{V_2\cos(\theta c)} \quad (3.7)$$

By applying Snell's law $\sin(\theta c) = \frac{V_1}{V_2}$ and using trigonometric identity ($\sin^2\theta c + \cos^2\theta c = 1$)

After a certain simplification the total travel time from the source to the geophone (T_{SG}) becomes

$$T_{SG} = \frac{x}{V_2} + \frac{2Z1\cos(\theta c)}{V_1} \quad (3.8)$$

Equation 3.8 represents the total travel time for two layer earth. The travel time curve illustrated in figure 3.9 b show the slope, crossover distance and intercept time of two layer media. The slope of the two layers is shown in the as the first layer ($\frac{1}{v_1}$) and layer two ($\frac{1}{v_2}$). The inverse of the slope is velocity of the individual layers. The critical distance (x_c) is the point on the surface at which the direct wave and the head wave arrived simultaneously. Before the critical distance, the direct

Waves arrive first while beyond the critical distance, the head wave arrives first. According to Figure 3.9 b), t_1 is the intercept of the second segment of the straight line graph. From figure 3.9 b) the depth of the first layers is obtained in Equation (3.9)

$$Z = \frac{t_1 v_1 v_2}{2\sqrt{v_2^2 - v_1^2}}$$

$$Z = \frac{X_C}{2}\sqrt{\frac{V_2 - V_1}{V_2 + V_1}}$$

For the general depth calculation for any number of layers using intercept time as

$$\frac{t_i v_i v_i}{2\sqrt{v_{i+1}^2 - v_i^2}}$$

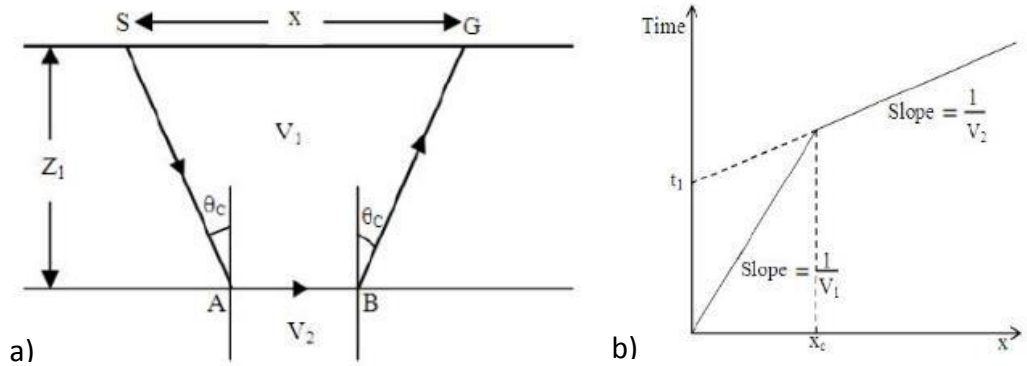

Figure 3.9: Two layer horizontal stratified earth (a) and Travel time curve for two layers earth (b) (Anomohanran, O., 2013)

Table 3.2: Seismic velocity for common Earth material (Keary *et al*., 2002)

Earth materials	V_P (km/s)
Sand (dry)	0.2–1.0
Sand (water-saturated)	1.5–2.0
Clay	1.0-2.5
Glacial till (water saturated)	1.5-2.5
Permafrost	3.5-4.0
Sandstone	2.0-6.0
Quartzite	5.5-6.0
Limestone	2.0-6.0
Chalk	2.0-2.5
Dolomite	2.5-6.5
Salt	4.5-5.0
Anhydrite	4.5-6.5
Gypsum	2.0-3.5
Granite	5.5-6.0
Gabbro	6.5-7.0
Ultramafic rocks	7.5-8.5
Serpentinite	5.5-6.5
Pure water	1.4-1.5
Petroleum	1.3-1.4
Ice	3.4

3.3.4 Inversion techniques

Inversion is a common mathematical tool to find a model analogous to the measured geophysical data. Now days, most geophysical software packages are designed with the consideration of mathematical and geometric models that will represent the actual earths. Especially in this study, modeling of the velocity of near surface layers was made by using *Seis Imager/2D* seismic refraction inversion software. Within this software package three different inversion techniques are designed. These inversion techniques are discussed in next subsections.

a) Time term method

This technique is a linear Least-Squares approach to determining the best discrete layer solution to the data. The math behind this technique is comparatively simple.

b) Reciprocal method

This method is a much more "hands on" approach than the time-term method. Fewer assumptions are made, and the interpreter interacts with the software to a much greater degree, providing much more input. The reciprocal method should be used when the desired result needs to be as detailed as possible. It needs more data because of its use of "delay times", which require a refracted arrival from each direction. Ideally, data is acquired such that a delay time can be computed beneath each geophone. The depth is then computed from the delay time and the velocity.

c) Tomographic analysis

This method, involves the creation of an initial velocity model, and then iteratively tracing rays through the model, comparing the calculated travel times to the measured travel times, modifying the model, and repeating the process until the difference between calculated and measured times is minimized. The math is quite complex; it needs better understanding of upper-level calculus and linear algebra. Finding the minimum travel time between source and receiver for each pair is the main goal of this technique. This is accomplished by solving for l (ray path) and s (inverse velocity or slowness). Since we know neither, the problem is under-constrained, and we must us an iterative, least-squares approach.

CHAPTER FOUR

4 FIELD DATA ACQUISITION, PROCESSING AND PRESENTATION

4.1 Survey layout and traverse selection

To effectively carry out, the primary electrical resistivity and seismic refraction data acquisition a systematic survey lines were selected within the study area. The selection of the traverse and profile lines is basically made with the consideration of site accessibility, local geological situation and investigation interest (objective of the particular study). As shown in Figure 4.1, nine sounding data points distributed along five profile lines, 2D imaging data along two profile lines and seismic refraction data along three spreads have been collected to address the research objectives stated in section 1.4. The primary collected data sets acquired from the field were further processed using various geophysical modeling software packages and presented in the form of sections and maps. The detail of each of the geophysical data acquisition, processing and presentation is outlined in the next sections.

4.2 Electrical resistivity

4.2.1 Data acquisition and instrumentation

To know both the lateral and vertical resistivity distribution of the near surface geological features underling the studied building foundation site, vertical electrical sounding and 2D imaging survey were applied. The data acquisition mechanism and instrumentation for both surveys are discussed in the following sub sections.

4.2.1.1 Vertical Electrical Sounding (VES)

In order to understand the near surface vertical resistivity distribution of buried earth treasures a Schlumberger configuration was used. The working procedure for this surveying is made by expanding both the current and potential electrodes symmetrically with respect to the sounding point. Nine sounding points distributed along five different profile lines were carried out in the study site. The distance between the successive sounding stations vary from 80 to 210 m. Three profiles were made parallel to one another and oriented SE to NW along the survey area. On the contrary, two profile lines (1 and 5) were made nearly perpendicular to the former three (2, 3,

and 4) profile lines (Figure 4.1). A Schlumberger configuration with a maximum half current electrode spacing of 220m (AB/2=220m) was utilized to infer the ground in depth. Most of the sounding profiles were made with the consideration of the 2D imaging and seismic refraction survey profiles.

4.2.1.2 Electrical Resistivity Imaging (ERI)

This survey was conducted to know both the vertical and lateral heterogeneity of near surface features underlying the study area. 2D imaging data were collected along two profile lines with 360 m and 270 m in length (Figure 4.1).The data acquisition was adopted by using axial dipole-dipole configuration with maximum unit electrode spacing of 30 m interval and data level up 4. A total of 44 and 33 for profile line one and profile line two data points were acquired within the target site respectively. The orientations of the both profile lines are nearly parallel except the readings were taken in the reverse direction (i.e. profile one (SE to NW) and profile two (NW to SE).

To collect both the sounding and imaging data two different resistivity system, namely the French made ELREC pro and the Canadian SARIS tetrameter, were utilized (Figure 4.2). The ELREC Pro Resistivity Imaging System uses a VIP5000 model transmitter capable of generating up to 2500 output Voltage. This system uses 6.5kVA generator as a power source, while SARIS uses rechargeable battery; and it is more portable and simple for operation. Both systems utilize common accessories, such as stainless steel and copper wire cables and electrodes.

The locations of study area boundary, electrical resistivity sounding points, dipole- dipole profiles lines, geophone position, relative distance between surveyed points , shot points and bore hole stations interims of Easting, Northing and elevations were recorded using the Garmin *GPS map 62* receiver, which provides readings with an accuracy of ±3m.

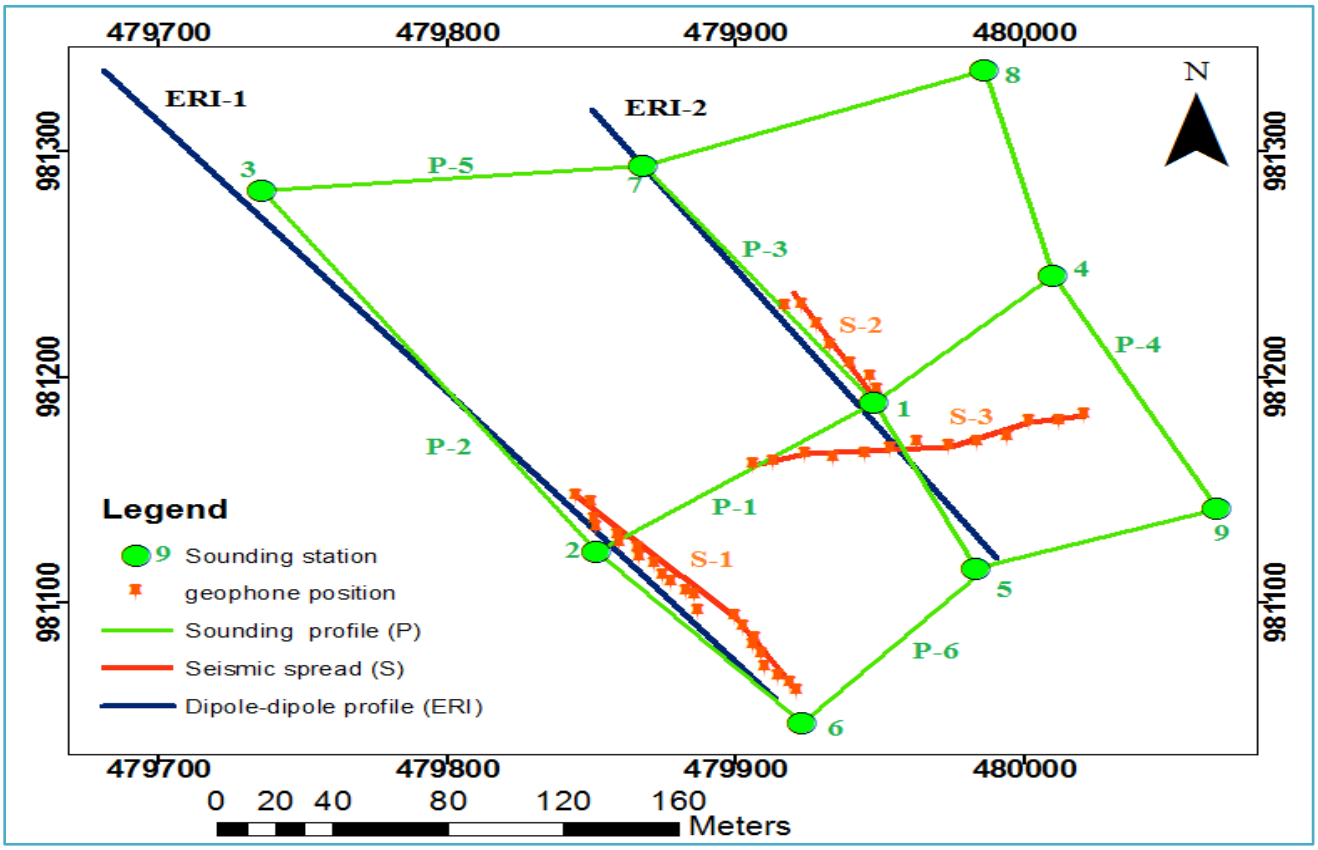

Figure 4.1: Geophysical data distribution and survey layout along the study area

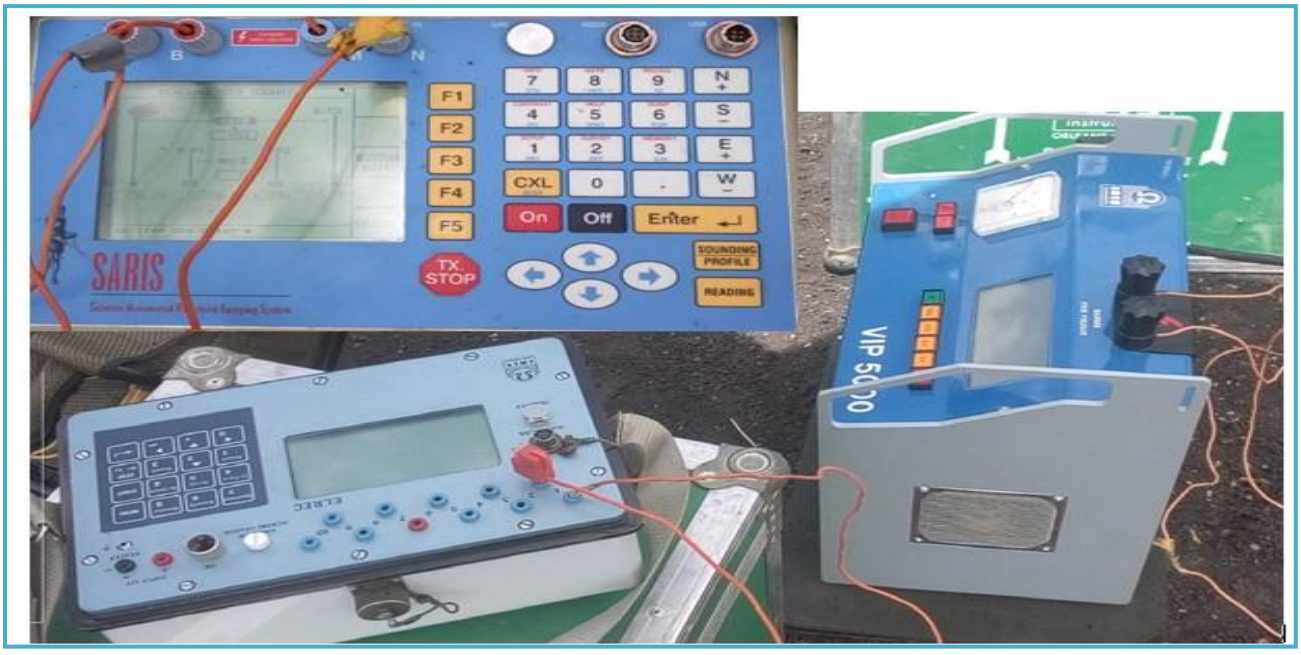

Figure 4.2: Electrical resistivity surveying instruments utilized in this study

4.2.2 Processing and presentation

4.2.2.1 Vertical Electrical Sounding

The primary VES data acquired from each sounding stations along five profile lines with Schlumberger array were processed by using *IPI2WIN* software to obtain the initial model of the layer parameters (thickness and true resistivity). Next, the obtained initial model parameters were used to process the data in *WinResist* software (Figure 4.3). Finally the individual interpreted curves provide for the preparation for geo-electric sections. On the other hand the raw apparent resistivity data in *Z*, distance in *X* and pseudo depth in Y axis are plotted by using *surfer* software package which results pseudo depth section map of the entire area along the same profile lines.

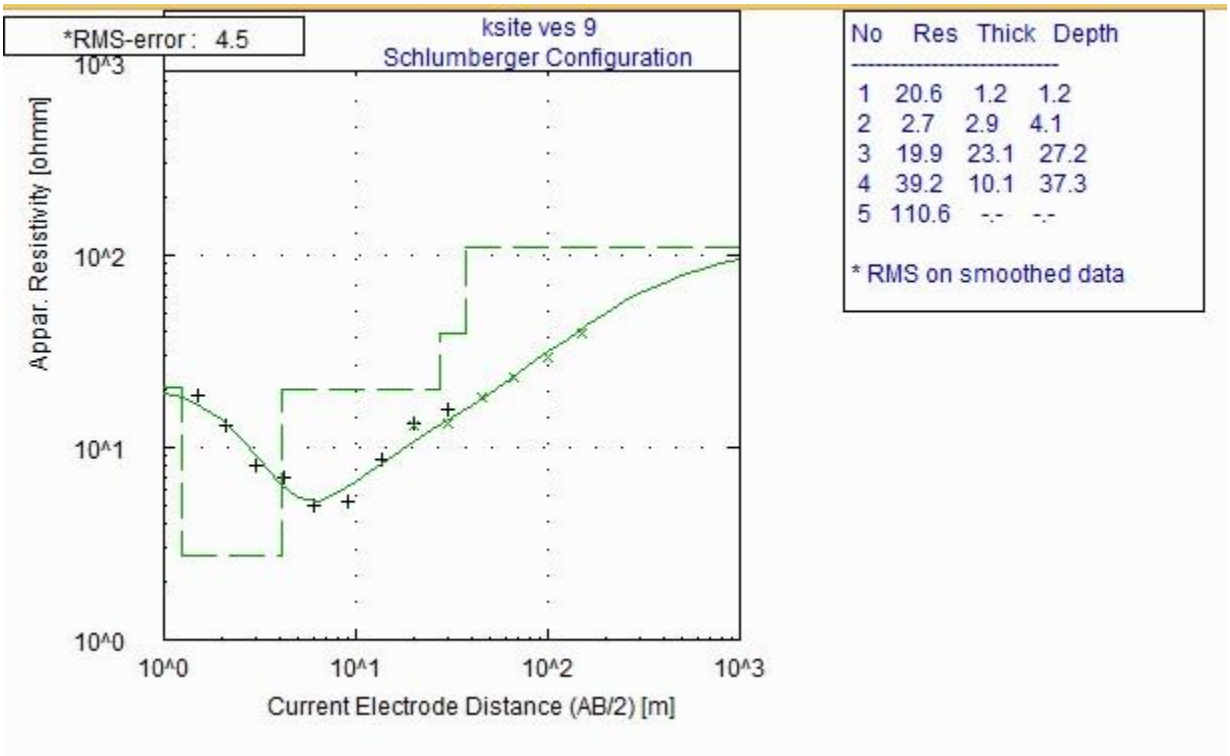

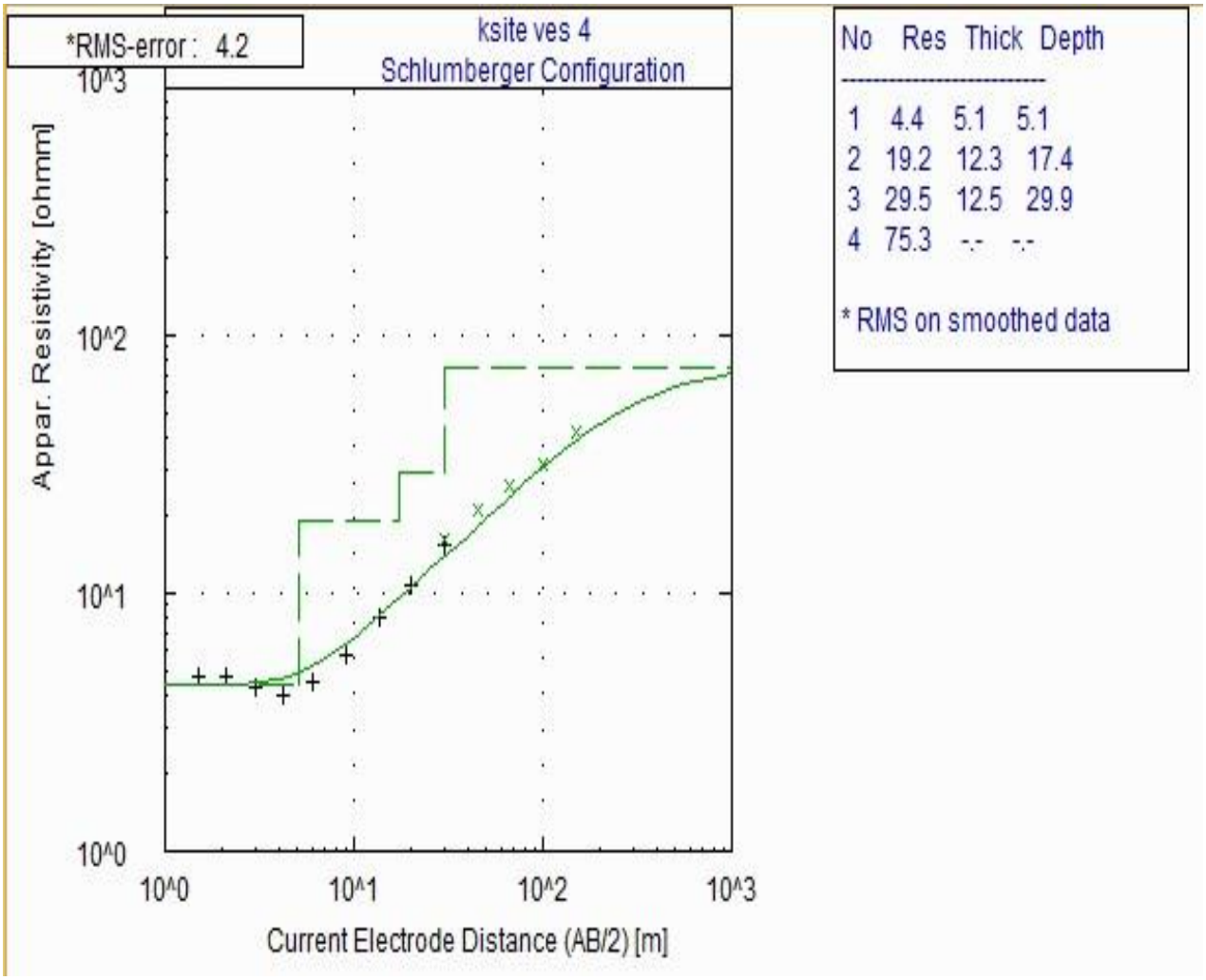

Figure 4.3: Individual VES interpreted curves

4.2.2.2 Electrical Resistivity Imaging survey

First, the primary 2D electrical resistivity raw data acquired in the field was downloaded from IRIS instrument with the help of Prosys–II software package. Next, removal of noise data was done. The rest of the valid data points are saved in the form of *.dat which is the file ready for processing in Res2Dinversion software. A total of 44 and 33 valid data points for profile 1 and profile 2 were processed separately for the inversion result. As a sample profile one which is made 360 m length, the measured apparent resistivity, the calculated, inversion resistivity section is shown in Figure 4.4. With the help of 2D inversion software program iterations have been applied three times to yield valid inversion result with RMS error of 6.6 and 8.1% respectively.

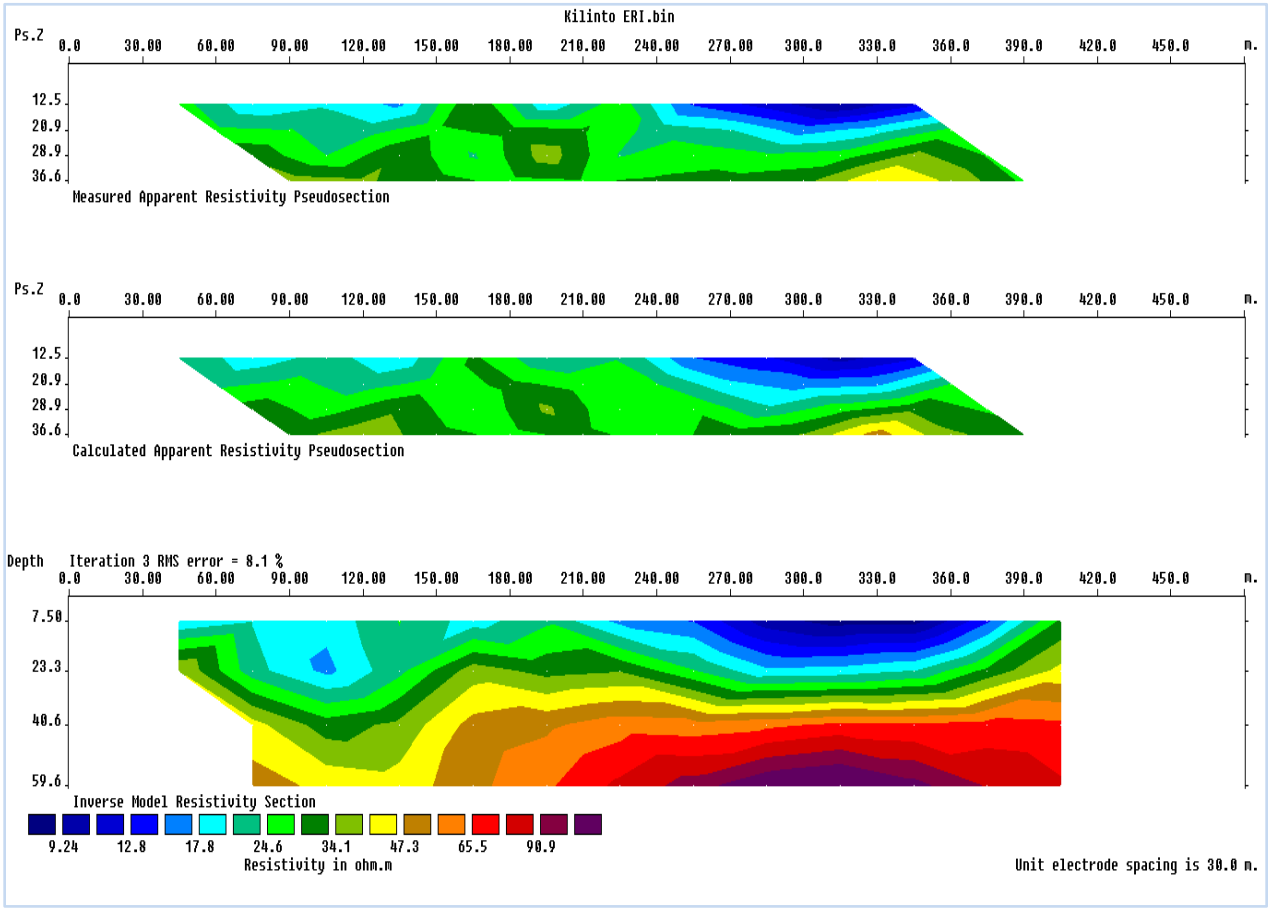

Figure 4.4: Measured, calculated and inverse 2D resistivity model

4.3 Seismic refraction survey

4.3.1 Data acquisition and instrumentation

In this study, seismic refraction surveys were conducted by using both 12 and 24 channel Dolang Seismograph along three profile lines with 55m and 115m in length. For both profile lines, a geophone spacing of 5m was applied. In order to generate elastic waves an artificial seismic source (10kg sledge hammer as an impact source and streak plate) was utilized. The strike plate was shouted by the sledge hammer repeatedly to enhance the elastic energy in a systematic way. The strike plate, sledge hammer, Dolang seismograph, lap top computer and geophones are connected by a means of seismic and trigger cables. Location of each successive geophones and shot points interims of easting, northing and elevation were taken with help of Garmin GPSmap 62.

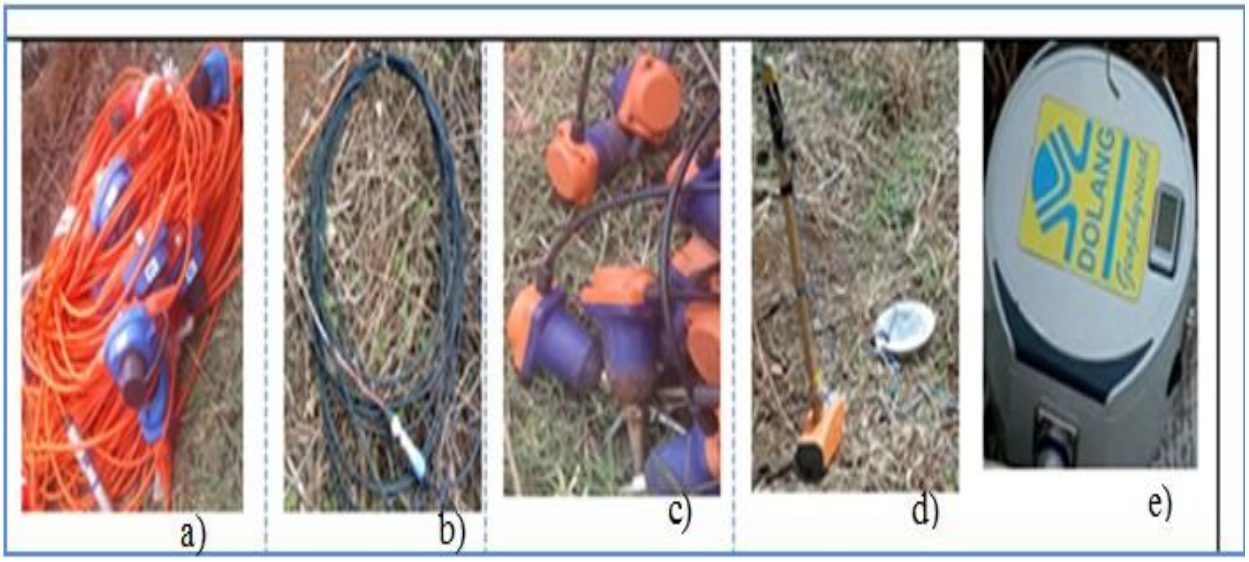

Figure 4.5: Seismic cables (a), trigger cable (b), geophones (c), hammer with plate (d) and DOLANG data logger (e) used in refraction survey

4.3.2 Processing and presentation

The wave form data recorded by personal computer are processed by using the help of seisImager/2D software package. The first break (arrival time) of the wave form data recorded in the field was picked with the help of pickwin95 software (Figure 4. 7(a)).Then, the picked arrival time was saved to generate the travel time curve (distance- time plot) and further processed with the help of plotrefa software to invert the travel time curve into the velocity model of the subsurface. To generate the seismic velocity model for all spreads a time- term inversion method were applied with the help of Plotrefa software. Figure 4.7 (b) show the final time term velocity model of spread two. The overall processing steps in seismic refraction data processing are presented in the form of flow chart as shown in Figure 4.6.

Table 4.1: Seismic refraction data acquisition and processing summary

Seismic refraction data acquisition and processing summary	
Instrument	*Dolang* (both 12 and 24 channel seismograph)
Source	Sledge hammer (10 kg)
Geophone	Vertical
Recorded parameter	Arrival time of the refracted waves in millisecond
Shooting interval	25 m
Geophone spacing	5 m
Initial shot point	2.5 m
No of spreads	3
Data format	SEG 2 format
Software	SeisImager/2D

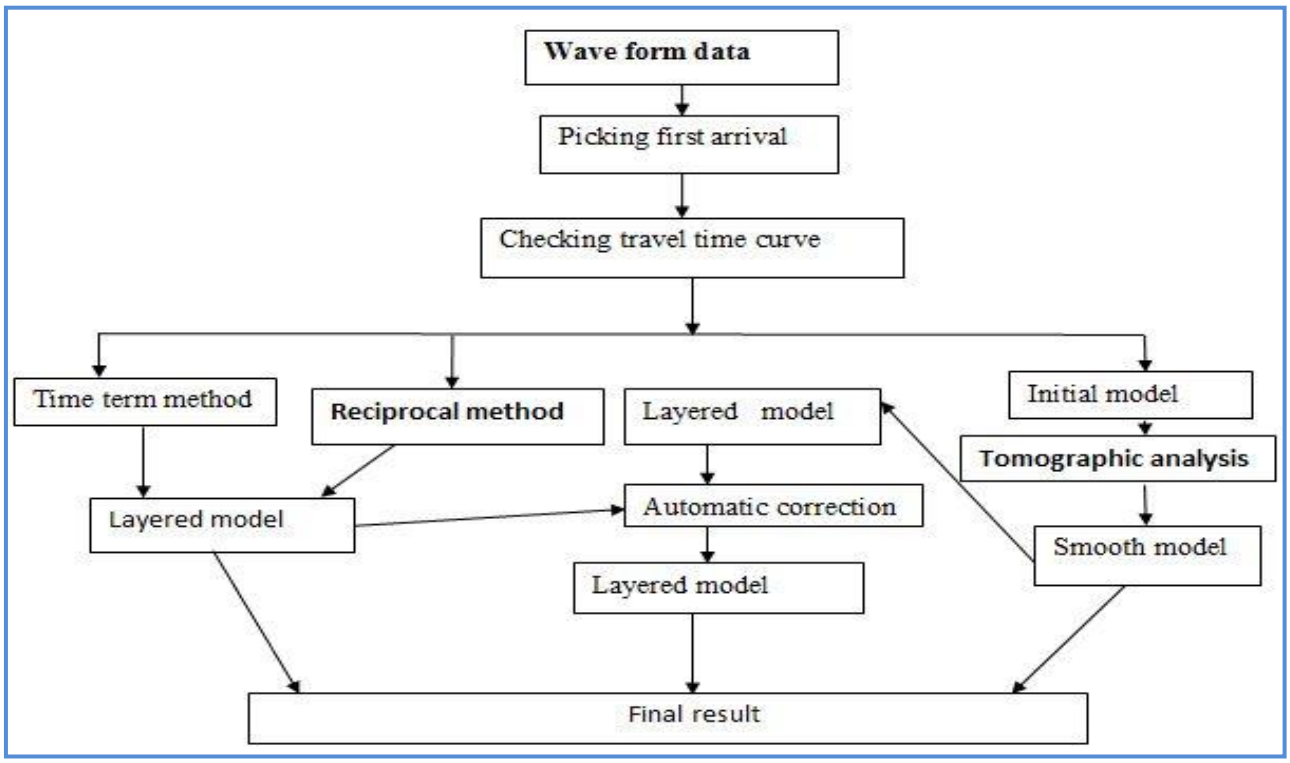

Figure 4.6: General Flow chart for seismic refraction data processing and analysis in SeisImager/2D software

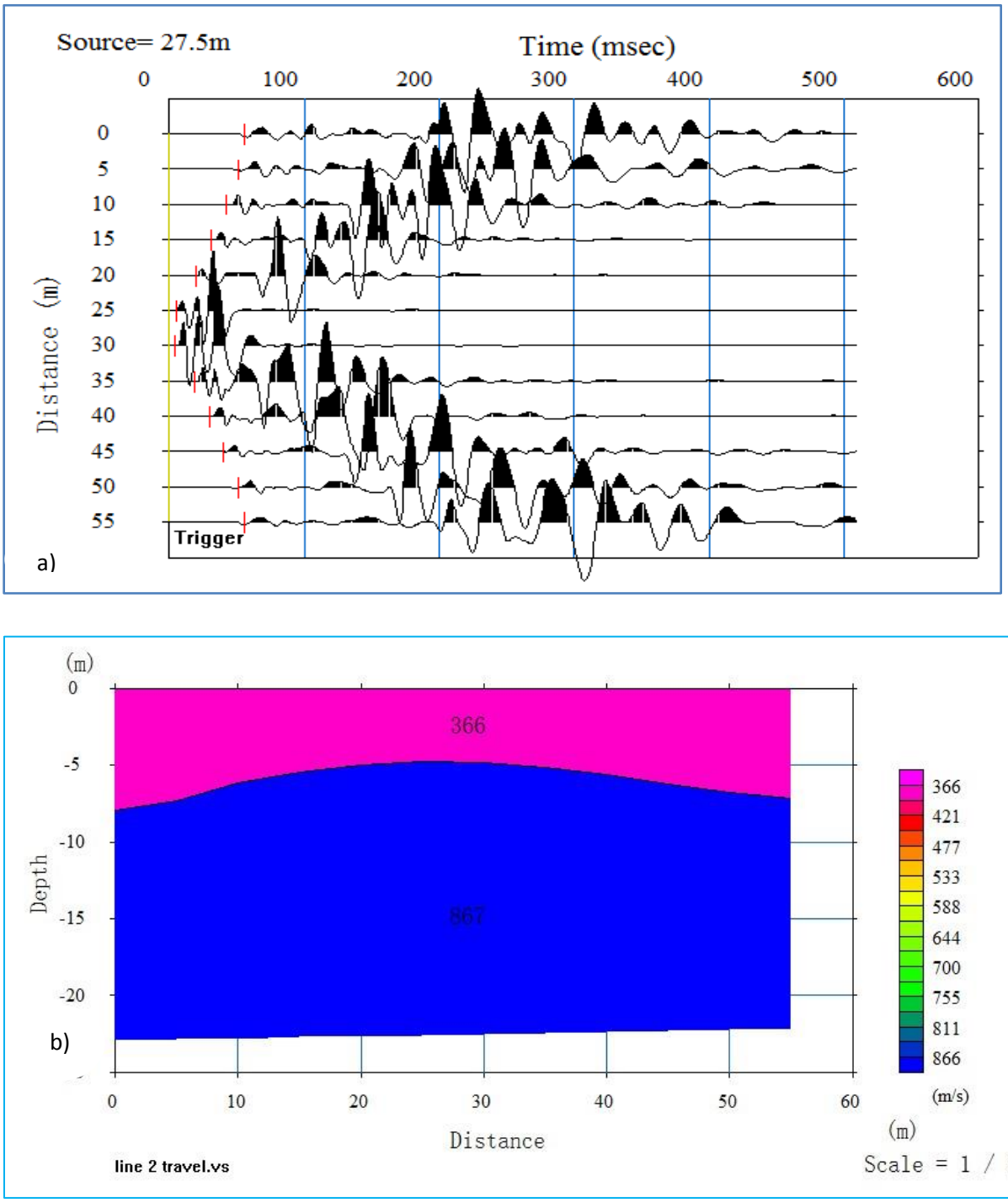

Figure 4.7: Wave form data and picked first break (red vertical lines) at the middle shot (a), and time –term velocity model for spread two (b)

CHAPTER FIVE

5 RESULT, DISCUSSION AND INTERPRETATION

5.1 Introduction

Geophysical survey data collected from the site and secondary geological information from nearby boreholes are integrated to conduct reliable interpretation and obtain clear picture about the foundation conditions of this specific site. The interpretation of individual Vertical Electrical Sounding data points, 2D electrical imaging and seismic refraction survey results are presented in the form sections, plan maps and individual sounding curves. Interpretation and analyses of the geo-electric sections and compressional wave velocity models are made integrating with the available lithological borehole log data from nearby areas, and thereby attempt has been made to minimize possible data interpretation ambiguities.

For this study information from borehole drilled to a maximum depth of 15m are used (boreholes logs are annexed in Appendix 2). This provides to reveal the vertical as well as lateral geological section of the study site well. The results of each survey data are presented and discussions in the sections below.

5.2 Electrical resistivity survey

To understand both the lateral and vertical variations within the underlying formations that serve as foundation materials for engineering structures a combination of VES and 2D imaging surveys were applied and their results are explained below.

5.2.1 Vertical Electrical Sounding

VES data was collected from nine stations distributed over the entire area roughly aligned in five traverse lines. Each profile includes three sounding station, where the maximum current electrode spacing is AB/2 equals 220m. The interpretation of each profile data displayed in the form of pseudo-depth, geo-electric sections and stacked pseudo depth map are discussed below.

5.2.1.1 Profile-1

This profile included sounding stations VES-2, VES-1 and VES-4. The spacing between them varies from 80 to 100m depending on site conditions. The result and interpretation of this profile is presented in the form of individual curves (Appendix 1), Pseudo depth and geoelectric sections.

Figure 5.1 is the pseudo-depth section plot which displays the resistivity distribution vertical and laterally. It has relatively a simple feature that reflects three distinct sections (zones) with contrasting responses and gradually increasing with depth. Accordingly, the uppermost section is characterized by very low apparent resistivity values ranging from about 2 to 16 Ω-m, which is associated with the response of top soil, composed of black cotton and siltyclay soil. Its thickness seems greater at the center (VES-1) and minimum around VES-2.

Underlying the upper low resistivity section there is a slight increment of valves to 16-28 Ω-m that correspond to a formation with more degree of soil compaction. The lower (third) section is relatively resistive than the overlying two zones and it value ranges from 28 to 50Ωm and attributed to highly to moderately weathered and fractured basalt.

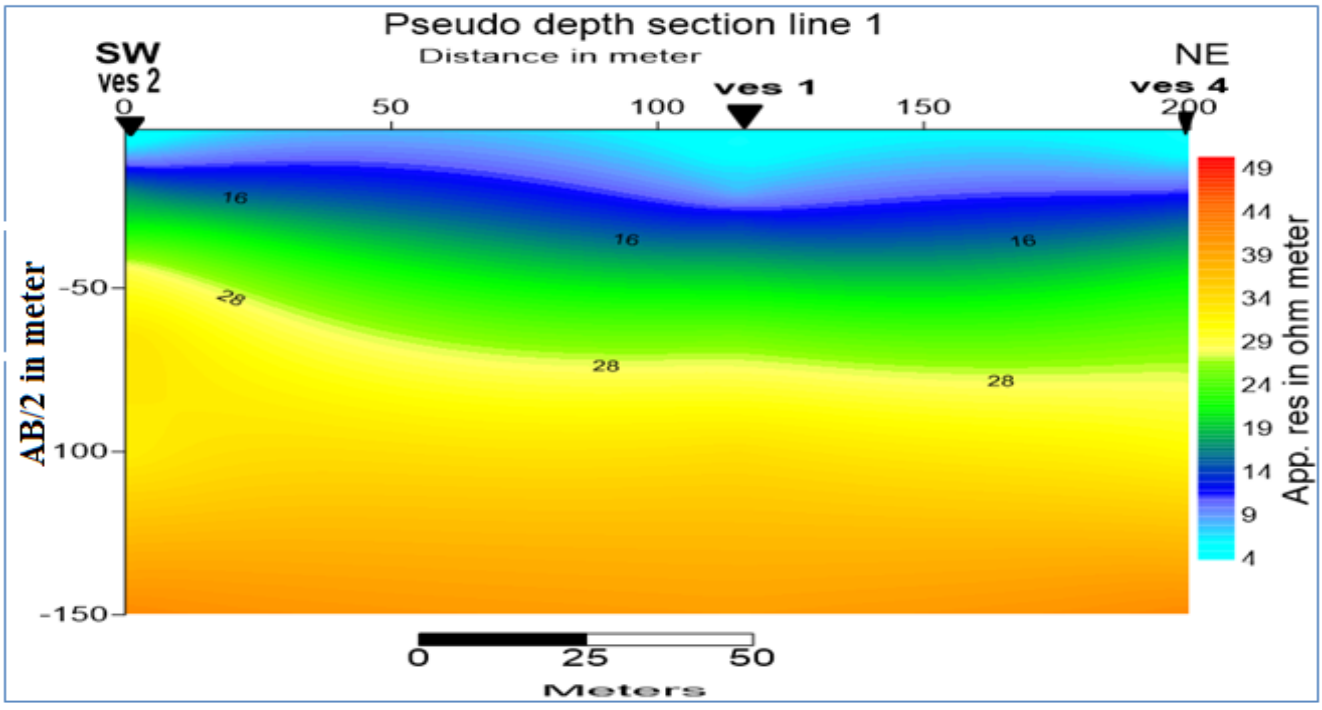

Figure 5.1: Pseudo-depth section along profile-1

Like the pseudo-section, the geo-electric section representing Profile-1 is produced using the quantitative interpretation of data from the same three VES stations curves, namely VES-2, VES-1 and VES-4, which are aligned in SW-NE direction (Figure 5.2) From this section four geological layers with contrasting resistivity are identified. The top layer, with thickness ranges of 4-6 m, shows a small resistivity contrast that varies from 4 to 5 Ω-m and reflecting the response of the top black cotton and siltyclay soil which a high expansive nature. As seen from the section this layer reaches its maximum thickness (~6 m) beneath VES 1 and minimum of 4 m more or less equally under VES-2 and VES-4.

The intermediate layer is a relatively thick horizon with resistivity values ranging from 17 to 24 Ω -m and has a thickness changing from 4 m under VES-2 and 18 m under VES-1. This layer is interpreted as a response of decomposed volcanic rock with considerable moisture content.
Compared to the overlying two layers, the third and fourth layer is relatively resistive (29-88 Ω-m) and has undulated morphology. It is attributed to be due to highly and moderately weathered basalt having a wide range of resistivity valve ranging from 29 to 88 Ω-m. From the engineering point of view, this layer is assumed to be relatively competent to bear loads multistory building structures.

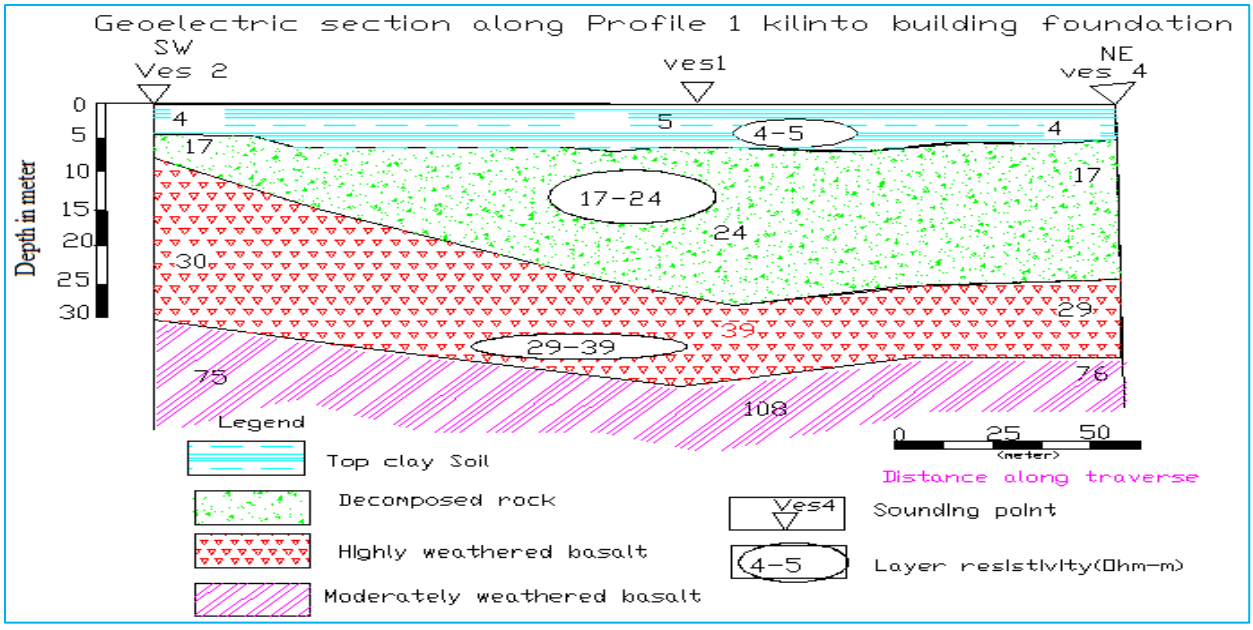

Figure 5.2: Geo-electric section of Profile-1

5.2.1.2 Profile-2

This SE-NW oriented profile is consisted of stations VES-6, VES- 2, and VES -3, which are placed with 100m average spacing in between.

The pseudo-section plot shown in Figure 5.3 displays the presence of three different geo-electric layers, which reflect a gradual increment of resistivity. The first very low resistivity layer shows values ranging from 4 to 18 Ωm and it is related to the response of black cotton and siltyclay soils. Meanwhile, under this conductive layer there is a moderately resistive bed with 18 to 33 Ω-m range. This response is likely due to a completely decomposed volcanic rock and its maximum thickness reaches at the NW part of the profile beneath VES-3. The bottom part of this profile is characterized by relatively resistive layer with values ranging from 33 to 60 Ω-m, are assumed to correspond with the effect of a highly to moderately weathered basalt. Generally, like on Profile-1, the resistivity values are increasing gradually.

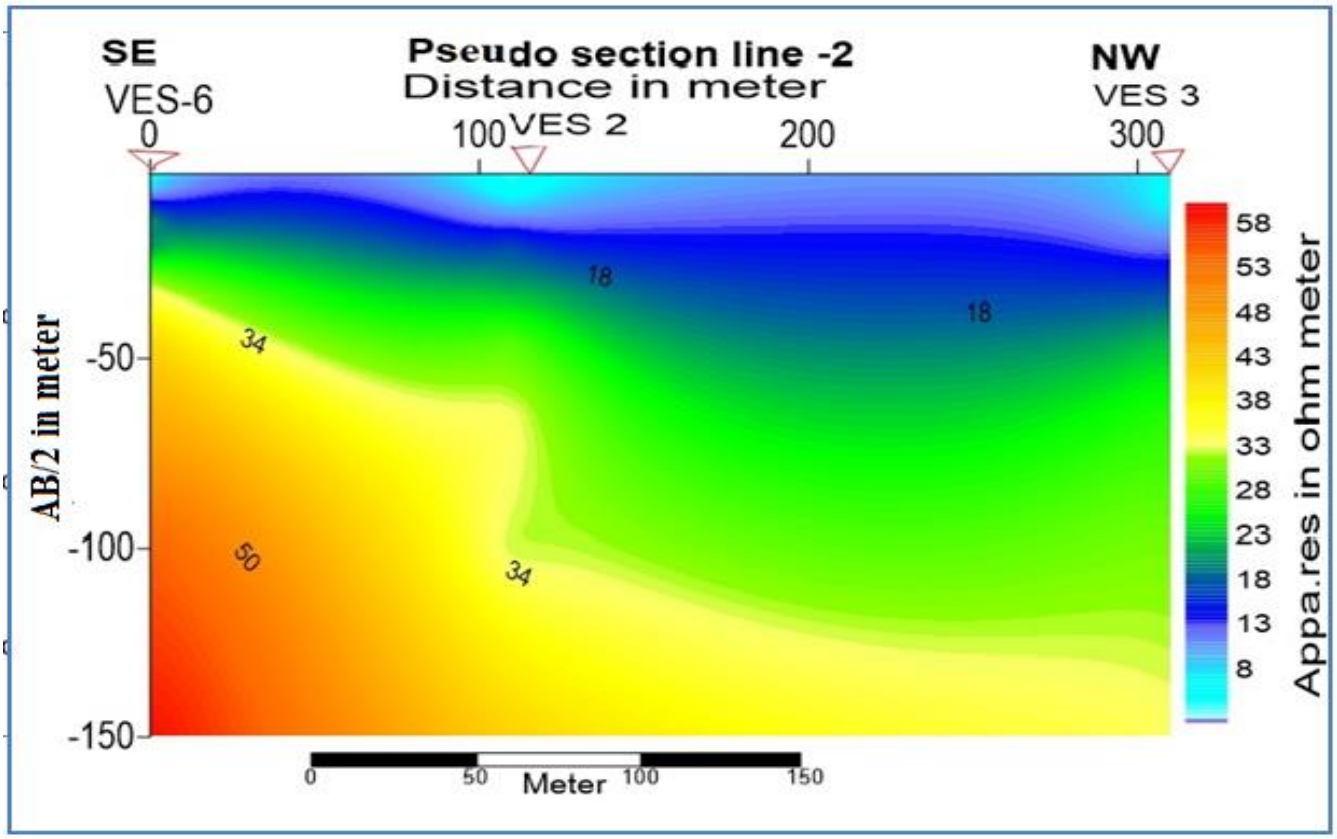

Figure 5.3: Pseudo depth section along Profile-2

On the other hand, the geo-electric section produced from Profile-2, oriented in SE-NW direction and providing quantitative subsurface information is shown in Figure 5.4. The first layer in the section revealed a resistivity range of 4-7 Ω-m, which is due to the top black cotton soil consists of expansive silty clay soil. As can be observed on the geo-electric section (Figure 5.4), very low resistivities are detected beneath all sounding stations and this is due to the highly moisturized nature of the clay soil that shows a uniform thickness of about to 5 m.

The second layer is mapped by relatively narrow resistivity range (17-20 Ω-m) and considerable thickness variation, thin at the southeastern part of the profile (VES -6) and thicker 13 m at NW part of the profile (beneath VES-3). This is also interpreted as decomposed rock response. At the bottom of the section two geoelectric layers are interpreted as highly and moderately weathered basalt distinguished by relatively high resistive values ranging from 29 to 88 Ω-m.

Generally, resistivity values along this profile increase gradually with depth from a minimum of to a maximum of 88 Ω-m. particularly, the third layer despite it occurs at greater depth it is competent enough to be used as structural foundation.

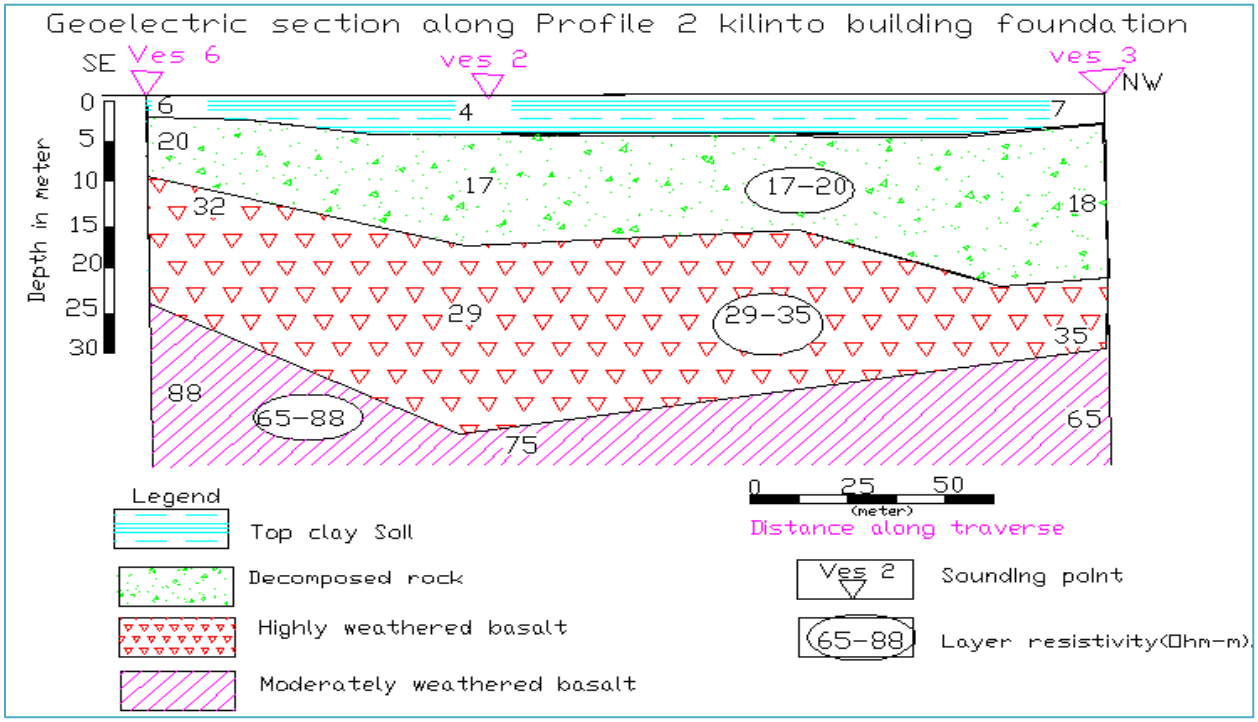

Figure 5.4:Geo-electric section along Profile-2

5.2.1.3 Profile-3

Profile-3 is orientated almost parallel to Profile-2 and it consists of sounding points VES-7, VES-1 and VES-5 that are located at 80-150m separations. The Pseudo-section plot displayed in Figure 5.5 shows the presence of three prominent resistivity anomalous features with gradual increment that could be associated with different lithologies. Similar to the previously discussed two profiles here also the upper black cotton (silty and clay soil) is marked by very low apparent resistivity up to 16 Ω-m. In the middle of the section the apparent resistivity values are slightly enhanced (16 to 26 Ω-m) indicating gradual improvement of formation's physical strength. This section is relatively thick at the NW side of the profile, i.e., beneath VES-7, but still less competent to serve as stable foundation material. Meanwhile, at the bottom of the section the resistivity increases to 26-44 Ω-m range.

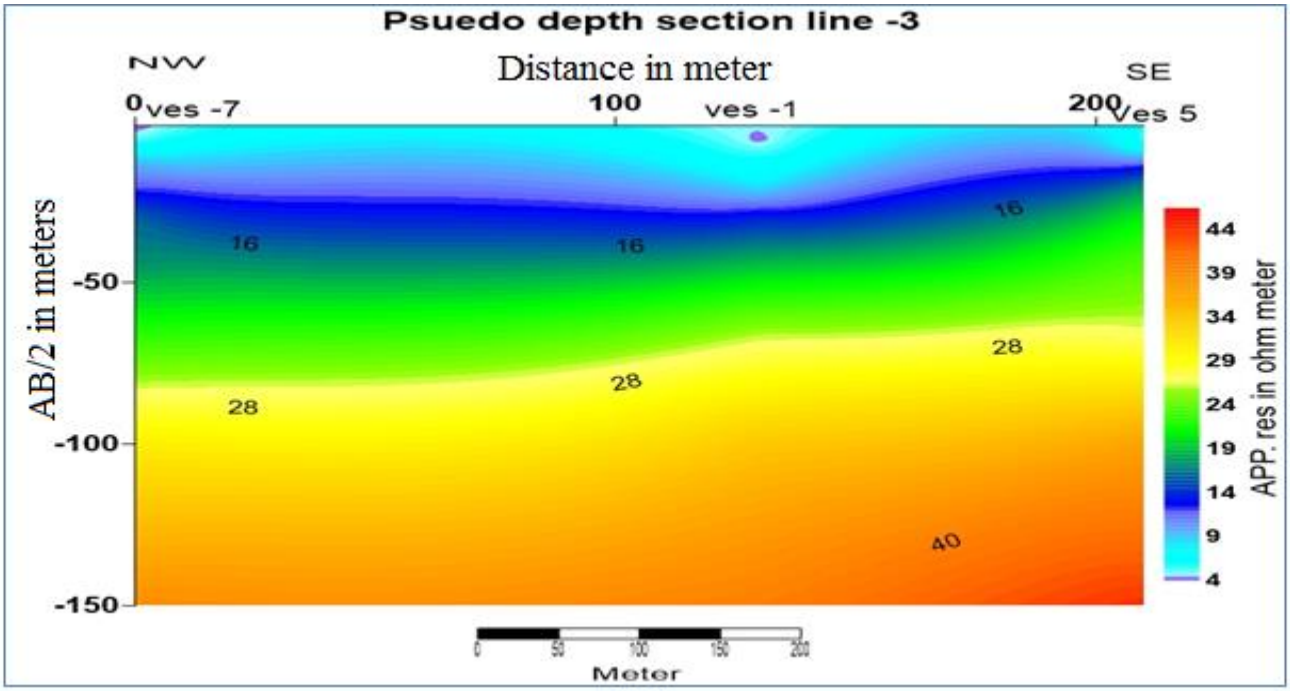

Figure 5.5: Pseudo-section plot along Profile-3

The geo-electric section constructed using data from three sounding stations, VES 7, VES-1 and VES-5 is displayed in Figure 5.6. The resistivity response has nearly uniform lateral distribution, but with gradually growth vertically. The first geo-electric layer revealed a resistivity contrast from 3 to 11 Ω-m, and its average thickness is about 6m. This low response indicates that the black cotton soil contains enough moisture.

The second relatively thick layer (18 to 27 m) is characterized by narrow range of resistivity responses, 19-24 Ω-m, that are associated with completely decomposed volcanic rock. This layer is thin (~18 m) at the central part of the profile, i.e., under VES-1 and relatively thick (~27 m) at the NW part of the profile beneath VES-7.

The third and fourth layer, interpreted as highly-moderately weathered basalt, is delineated by 26-108 Ω-m resistivity and compared to the overlying two layers this one represents a more competent horizon for civil engineering purposes.

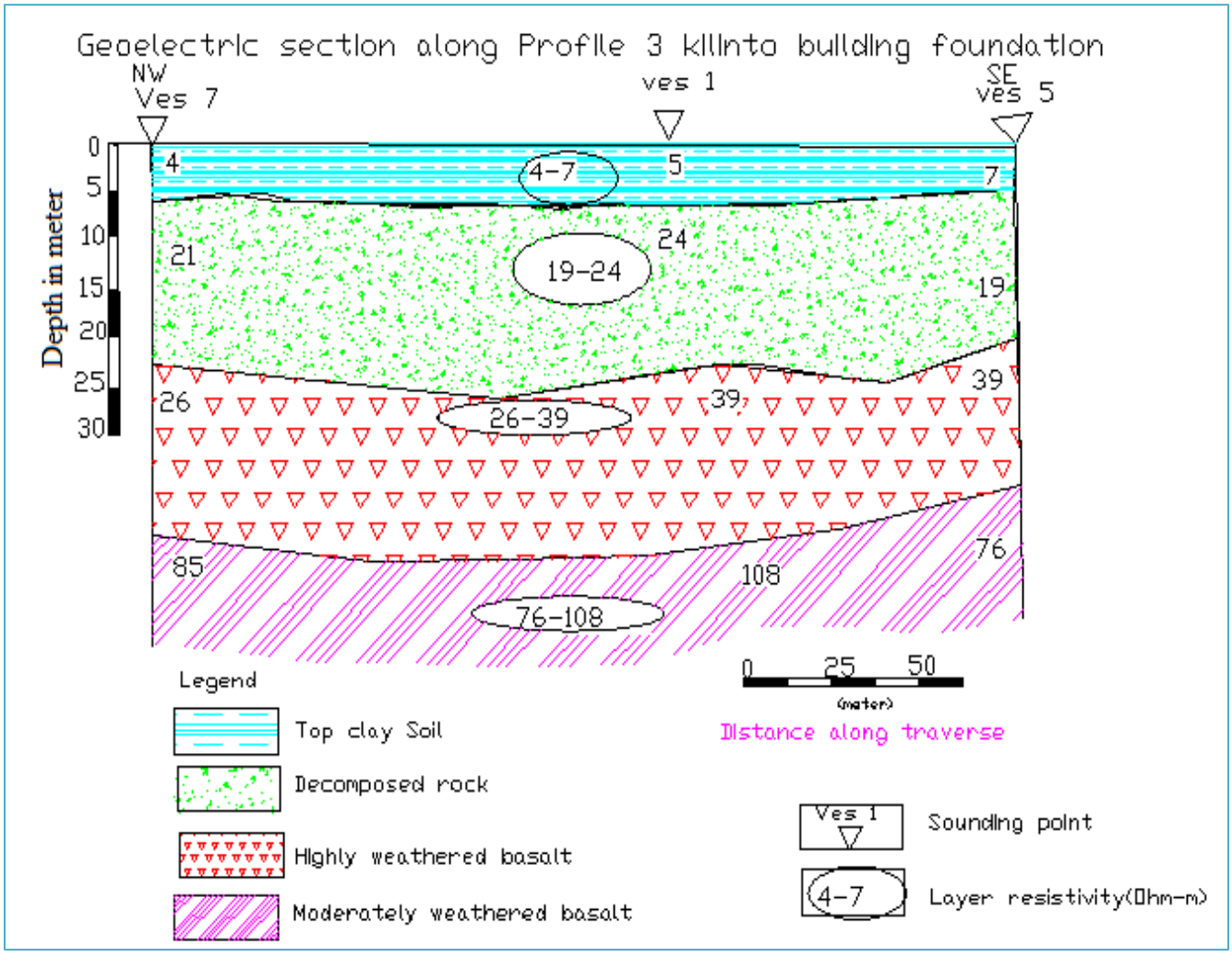

Figure 5.6: Geo-electric section along Profile-3

5.2.1.4 Profile-4

This profile line is parallel to the other two VES profile lines oriented almost SE-NW and it composed of stations VES- 9, VES- 4 and VES-8. The spacing between the consecutive sounding stations varies from 100 to 120 m depending on site conditions and its length is 210 m. Figure 5.7 show the pseudo-depth section along Profile-4 which is prepared by using data from VES-9, VES-4 and VES-8 and like other profiles this section is constructed to perform qualitative interpretation. From top to bottom the resistivity increases gradually with depth and three major horizons with contrasting apparent resistivity values are recognized. The first layer has very low apparent resistivities with values ranging from 4 to 16 Ω-m that reflect the response of the top layer represented by black cotton soil having a thickness almost similar along the profile.

The intermediate part, like the upper section show low resistivity values, but with slight increment that ranges from 16 to 26 Ω-m is due to the effect of decomposed volcanics. The bottom part is relatively resistive than the overlying ones (26 to 42 Ω-m) and attributed to a highly weathered and fractured basalt.

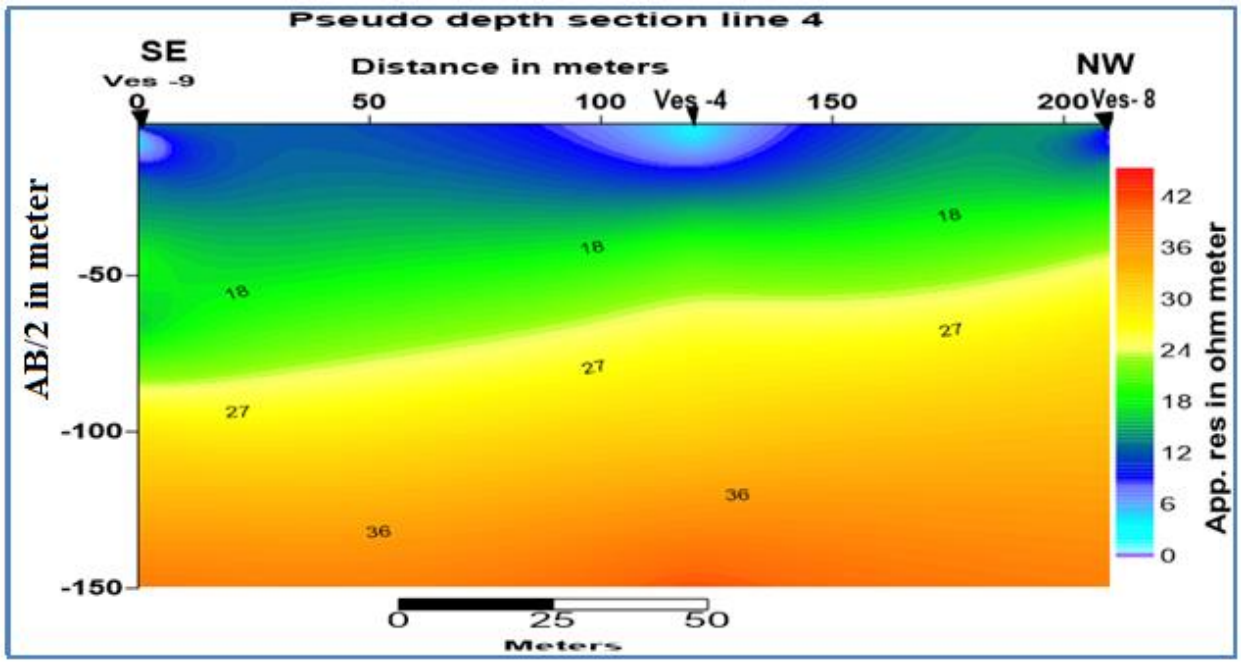

Figure 5.7: Apparent resistivity pseudo section along Profile-4

The geo-electric section displayed in Figure 5.8 is constructed using the interpreted layer parameters from three stations, VES-9, VES-4 and VES-8, oriented in SE-NW direction. This section reveals three nearly horizontal stratified units that probably represent three different geological features.

The upper most part of this section shows relatively wide range of resistivity contrast with a range of 2 to 40 Ω -m and it is attributed to the top expansive black cotton soil consists of (silty clay soil). At the NW part of the profile high resistivity (40 Ω-m) is measured below VES-8, which is due to human-made drainage and other buried utilities whose presence was partially noted during the field survey. On the other hand, 2 Ω-m resistivity was observed under VES-4 which most likely is due to the high moisture content within the upper clay bed having about 5 m thickness.

The top layer is underlain by a relatively thick layer with narrow resistivity range (21-24 Ω-m) that is interpreted to be due to a completely decomposed rock with thickness varying from 15m to 34m. As can be observed in Figure 5.8, this layer is thin at the center of the line directly under VES-4 and thick beneath VES-9. A thick section top soil and decomposed rock is detected below VES-9, which implies that here the depth to the relative competent bed is assumed to be maximum (40 m). Therefore, due attention must be given during construction of multistory building to avoid impacts of any geo-hazard events.

The bottom layer in the section is characterized by relatively high resistivity values ranging from 29 to 110 Ω-m. Here the shallowest competent layer represented by weathered and fractured basalt is delineated at the center of the profile, where the depth reached about 20bvm beneath VES-4.

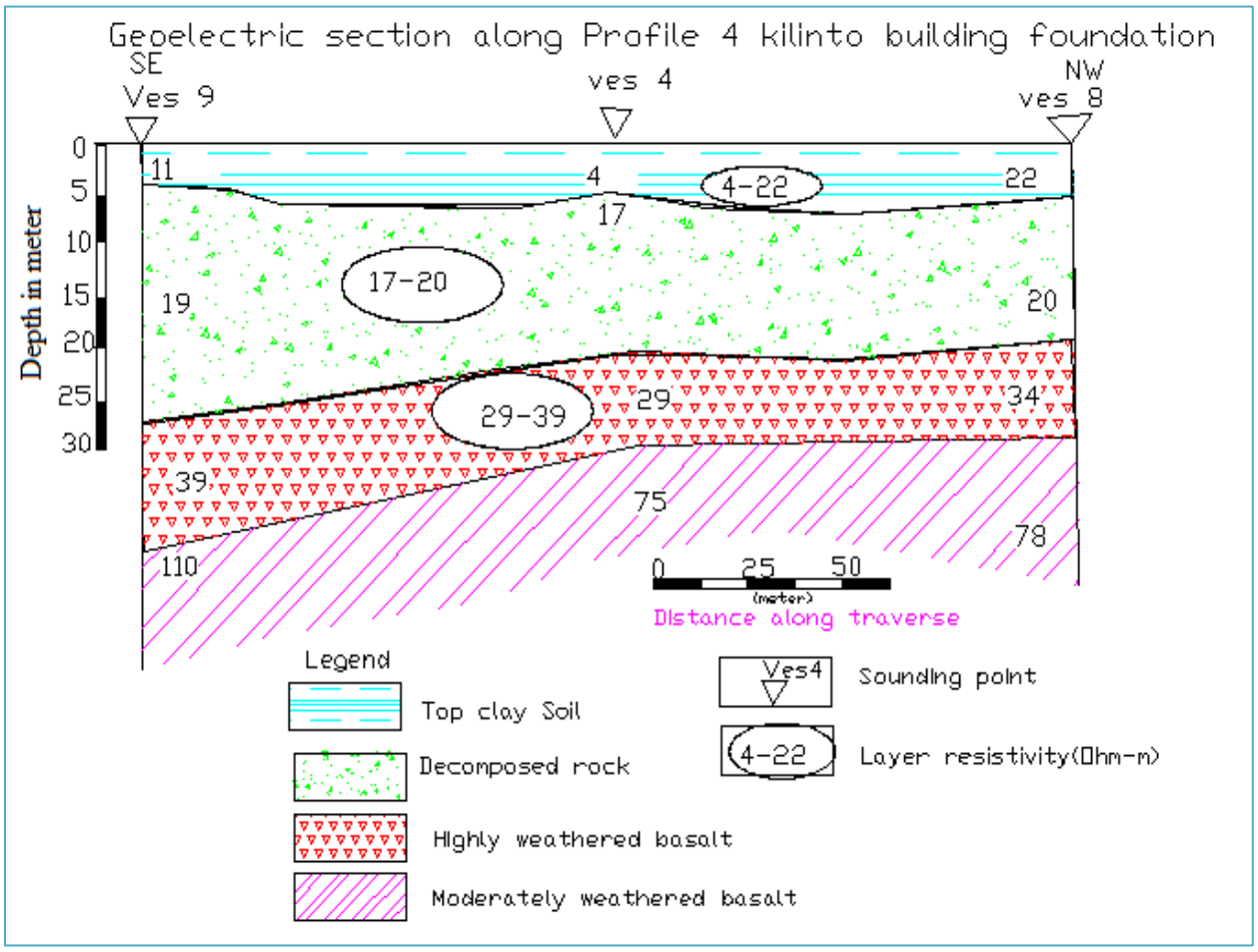

Figure 5.8: Geo-electric section along Profile-4

5.2.1.5 Profile-5

As shown in Figure 5.9, this profile line was constructed with 3 VES stations (VES- 3, VES- 7 and VES-8). It is oriented nearly E-W direction and almost parallel to Profile-1.The spacing between each successive sounding station varies from 120 to 130 m, whereas its length is 250 m.

The pseudo-section along Profile-4 is displayed in Figure 5.9 and on this map three anomalous features with distinct apparent resistivity values are recognized. The top part of this pseudo section is marked by very low apparent resistivity values (4-16 Ω-m) than the underlying horizons. Similar to other profiles the top very low resistivity is due to the presence of black cotton soil whose thickness is relatively thick at the center (below VES 7), whereas in the rest part of the profile it's thickness is nearly similar.

Beneath the first layer, relatively intermediate resistivities detected (16-24 Ω-m) that possibly correlate with completely decomposed volcanic rock.

The bottom part of the section is relatively resistive than the overlying layers and its value range from 24 to 39 Ωm that are associated with a highly to moderately weathered basalt. In this layer the resistivity increases with depth which is possibly interpreted.

Generally, analogous to other profile lines along this profile line nearly uniform trend of resistivity variation with depth was observed the increasing degrees of soil compactions and /or rock mass strength.

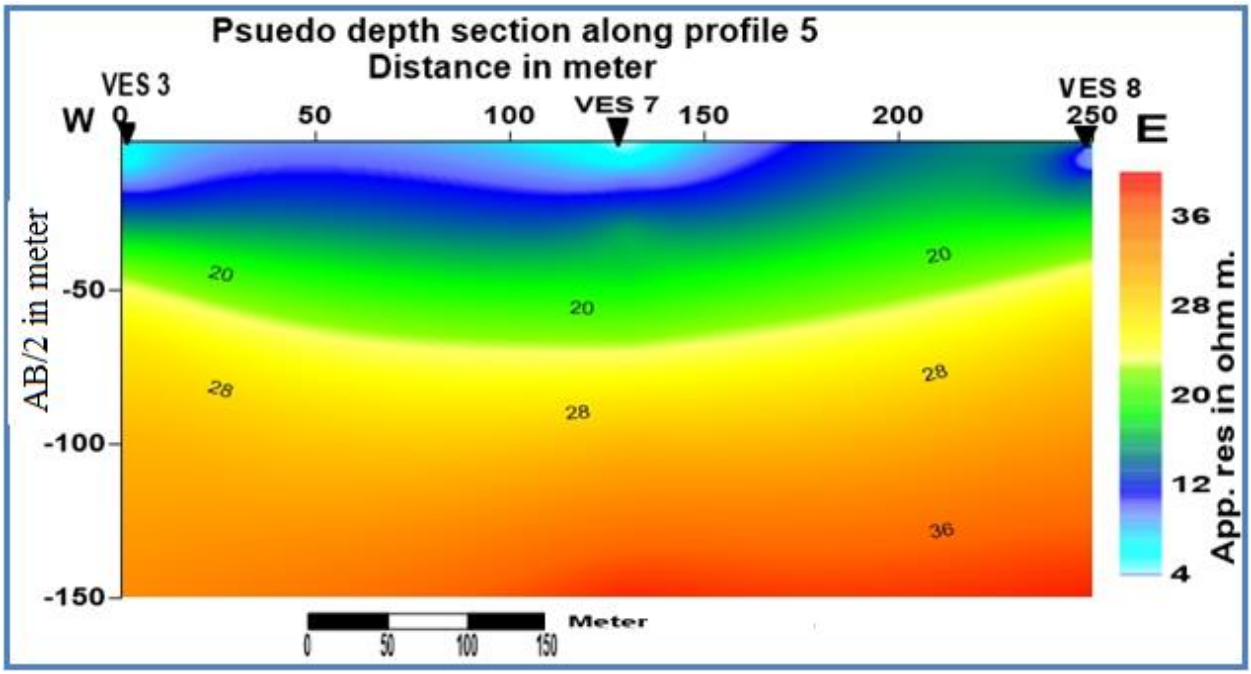

Figure 5.9: Apparent resistivity pseudo-section along Profile-5

Like other profile lines the geo-electric section of this profile is made by connecting three interpreted VES curve parameters (VES-3, VES-7 and VES-8) and its orientation is nearly E-W. Analogous to profile line four in this section nearly horizontal geoelectric horizons which reflecting four different major geological layers with contrasting resistivity are observed (Figure 5.10).

The first geo-electric layer in this section reveals relatively wide resistivity contrast ranging from 4 to 22 Ω-m and it is interpreted as top soil consisted of expansive black cotton soil (silty clay).

At the Eastern part of the section the resistivity is high (22 Ω-m) under VES-8, which is caused by the effect of human-made buried utilities. Meanwhile, very low resistivity (4 Ω-m) was observed beneath VES-7 which indicates the highly moisturized nature of clay layer. The thickness of this geo-electric layer is almost similar at all sounding stations except at the center of the profile (below VES-7), where it gets thicker and reaches 6 m.

Underlying the clay bed there is a relatively thick layer with narrow range of resistivity values (18-21 Ω-m). The thickness of this horizon varies from 15 m to 19 m. This geo-electric layer is interpreted as decomposed rock. As shown in Figure 5.10, the thickness of this layer is thinner at the western side of the profile directly below VES-3 and thicker at the center of the profile beneath VES-7. Significantly, in this profile section the thickness of the completely decomposed rock formation is increasing from W-E direction.

Relatively resistive geoelectric layers beneath the completely decomposed volcanic rock are mapped. It shows the resistivity valve ranging from 26 to 85 Ω-m. The gradual increment of resistivity with depth in this layer as well as the overlying geoelectric layers reflects the competency of the formation with depth. Hence, the depth relative to the competent formation is shallower beneath VES-3 and 8.

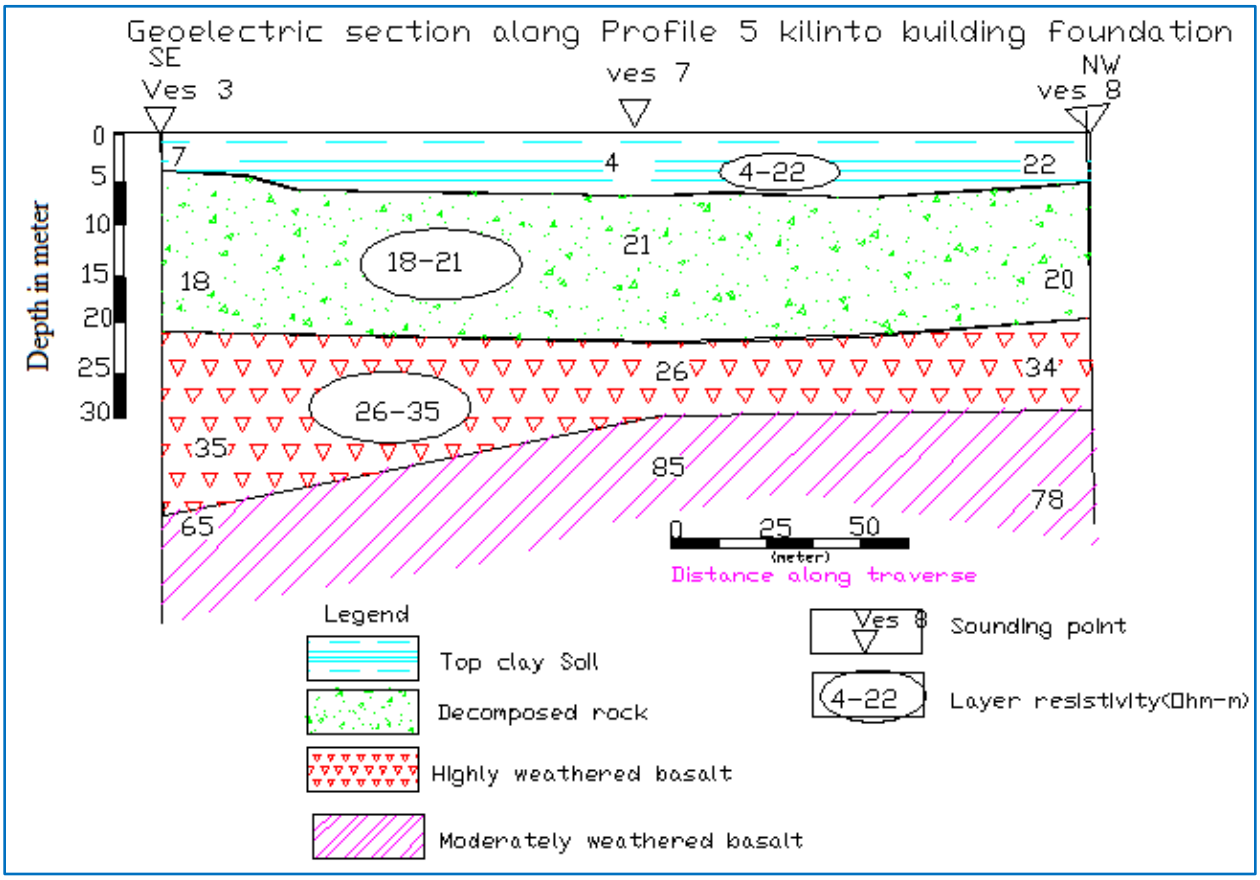

Figure 5.10: Geo-electric section of Profile-5

5.2.1.6 Profile -6

This is SW-NE oriented profile, consisted of stations VES-6, VES- 5, and VES -9, which are placed with 100m average spacing in between.

The pseudo-section plot shown in Figure 5.11 displays the presence of three different geoelectric layers, which reflect a gradual increment of resistivity. The first very low resistivity layer shows values ranging from 4 to 20 Ω-m and it is related to the response of black cotton and siltyclay soils. Meanwhile, under this conductive layer there is a moderately resistive bed with 20 to 34 Ω-m range. This response is likely due to a decomposed volcanic rock and its maximum thickness reaches at the NE part of the profile beneath VES-9. The bottom part of this profile is characterized by relatively resistive layer with values ranging from 33 to 60 Ω-m, are assumed to correspond with the effect of highly and moderately weathered basalt. Generally, like other profiles, the resistivity values are increasing gradually.

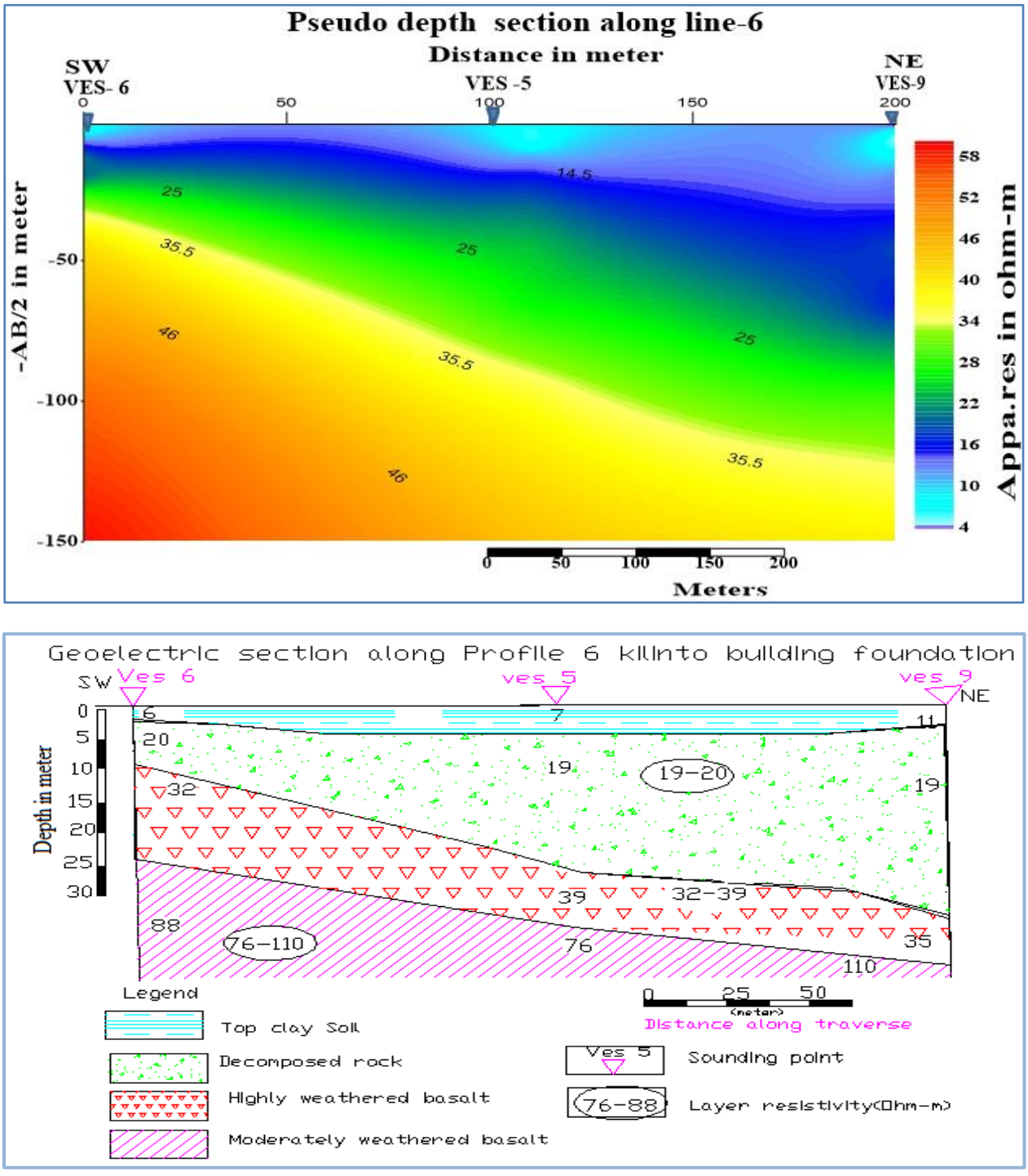

Figure 5.11: Pseudo depth section along profile -6 (a) and geoelectric section (b)

On the other hand, the geo-electric section produced from Profile-6, oriented in SW-NE direction and providing quantitative subsurface information is shown in Figure 5.11 (b). The first layer in the section revealed a resistivity range of 4-11 Ω-m, which is due to the top black cotton soil

consists of expansive silty clay soil. As can be observed on the geo-electric section (Figure 5.11(b)), very low resistivities are detected beneath all sounding stations and this is due to the highly moisturized nature of the clay soil that shows almost uniform thickness of about to 4 m.

The second layer is mapped by relatively narrow resistivity range (19-20 Ω-m) and considerable thickness variation, between 6 m the southeastern part of the profile (VES -6) at and 21 m at NW part of the profile (beneath VES-9). This layer is interpreted as decomposed rock response. At the bottom of the section is interpreted as highly and moderately weathered basalt distinguished by relatively high resistive values ranging from 32 to 110 Ω-m.

Generally, resistivity values along this profile increase gradually with depth from a minimum of to a maximum of 110 Ω-m. Particularly, the third and fourth layer despite it occurs at greater depth it is competent enough to be used as structural foundation.

5.2.2 Sliced stacked apparent resistivity pseudo section map

The measured apparent resistivity in all sounding stations range from 4 to 60 Ω-m. Figure 5.13 illustrates stacked apparent resistivity pseudo-section map of the study site. This map is extracted at all sounding stations with similar current electrode spacing at a particular depth. To understand the general trend of near surface anomalies five slices at (AB/2=1.5, 30, 66, 100 and 150 m) were selected and stacked. The selection of depends on the contrast between the measured apparent resistivity valve of the target site.

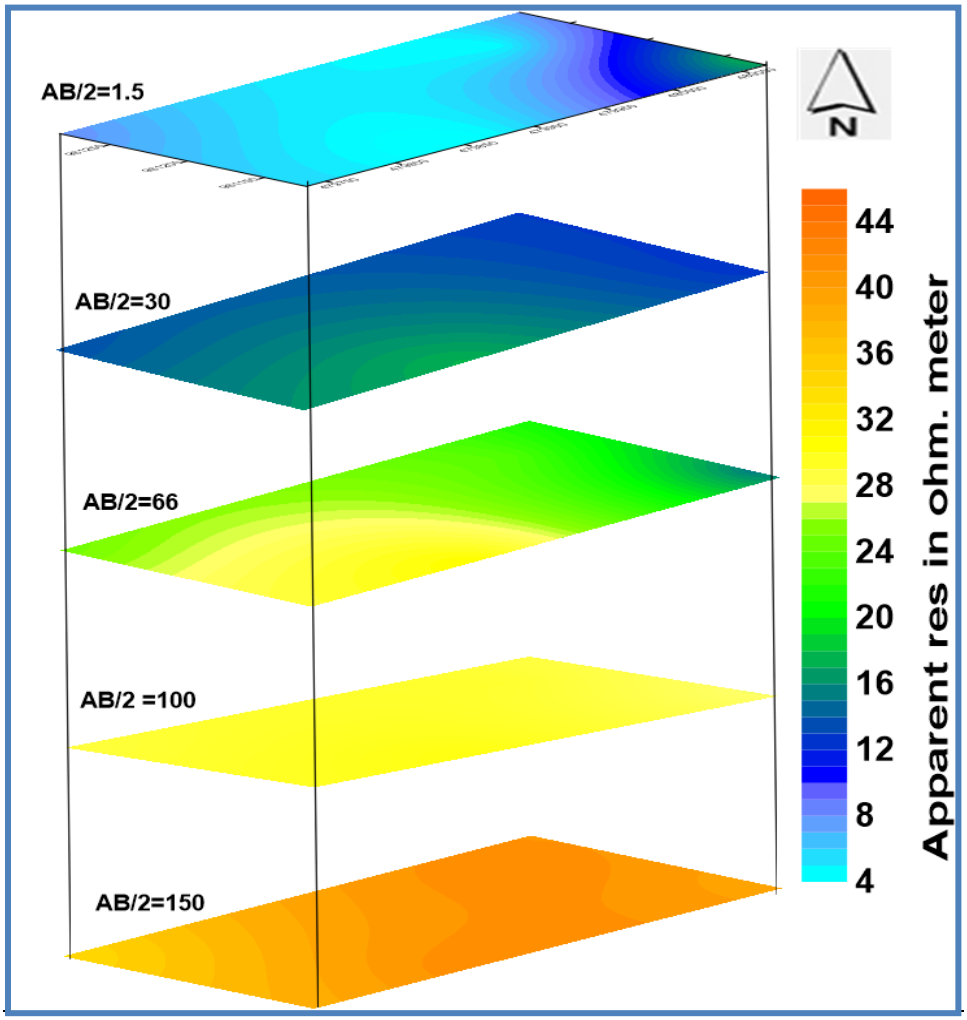

Figure 5.13: Sliced stacked apparent resistivity pseudo section map

From the sliced stacked pseudo-depth map presented in Figure 5.12, the following three major geo-electric layers are delineated:

a) *Layer-1:* it is relatively very low resistivity horizon with values ranging from 4 to 16 Ω-m. This very low resistivity layer is pronounced at the shallower section resulted due to the presence of expansive black cotton soil (clay and silt).

b) *Layer-2:* it has relatively intermediate resistivity range from 16 to 26 Ω-m and this slightly enhanced resistivity response detected at the intermediate depth section is associated with mixture of clay and silt bed with better degree of compaction and decomposed volcanic rock.

c) *Layer-3:* it underlies the deepest part of the lithological section and is characterized by relatively high resistivity values ranging from 26 to 50 Ω-m, which is attributed to highly weathered and fractured volcanic rock.

5.2.3 Electrical Resistivity Imaging (ERI)

In addition to the sounding survey, dipole-dipole profiling was conducted along two profiles to better understand and identify the subsurface geoelectric layers underlying the target area. To map subsurface features both laterally and vertically at the same time 2D resistivity imaging survey is a preferable and effective survey tool (Loke, 2001). Accordingly, the results of this survey are presented in form of 2D resistivity model sections and are discussed in the sections below.

5.2.3.1 ERI-1

The 2D resistivity data acquired employing the axial dipole-dipole configuration with a maximum electrode spacing of 30m and four (n=4) dipole levels were processed using the Res2Dinv software. The total length of this profile is 360 m and the result is shown in Figure 5.13.

From the presented 2D model, at least, three prominent sections can be identified that can be correlated with distinct lithological features observed from nearby borehole log data. Accordingly, the top expansive black cotton soil (clay) and partly the silty clay layers distributed up to about 7m is can't be fully reflected on this model as the minimum depth of investigation by this configuration is about 7m. Nevertheless, from about 7 m to a maximum of nearly 60m depth the resistivity of the underlying formations increases gradually from 4 to 110 Ω-m, which clearly indicate that the strength of the underlying formations considerably improve vertically. Correlating the dipole- dipole 2D model with the nearby lithological log data, it is became evident that the top low resistivity zone (4-20 Ω-m) approximately extending to about 27 m represents the cumulative effect of the top black cotton soil composed of, clay and silty and completely decomposed volcanic rock.

The thickness of this section shows a significant increment towards SE direction, but at the center of the profile, i.e., between stations around 75 and 165 this conductive layer seems bulged upward and its thickness decreases to less than 7.5 m, whereas on both ends it reaches its maximum thickness.

The intermediate parts of the section is characterized by relatively enhanced resistivity values ranging from 20 to 40 Ω-m and are attributed to the highly weathered and volcanic bed, whose thickness is larger at the central part of the profile and shows undulation with the station interval 0-240m. The resistivity of the bottom part changes from 40 to 110 Ω-m is associated with the occurrence of relatively competent volcanic bedrock.

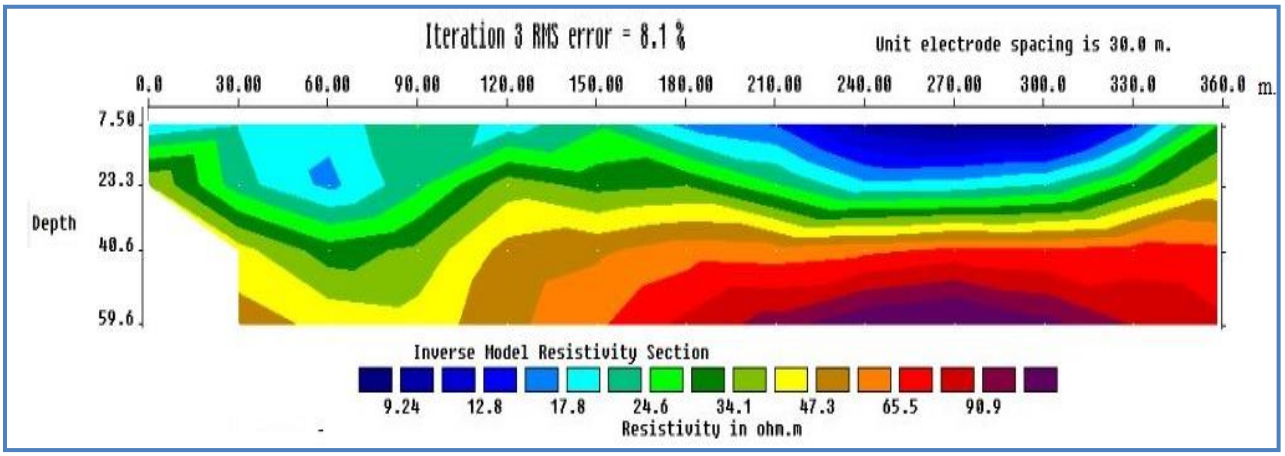

Figure 5.13: 2D resistivity model section along ERI-1

5.2.3.2 ERI-2

2D primary electrical resistivity raw data was acquired through employing axial dipole -dipole configuration with maximum unit electrode spacing of 30 m, and dipole level (n=4) and 33 data points were processed for the inversion result. The length of this profile is 270m.The produced inversion resistivity section is presented in Figure 5.14.

Analogous to the first in this profile three distinct geo electrical layers were identified and correlated with the available geological information and borehole data. The top layer indicates potentially low resistivity layer that varies from to 5 to 20 Ω- m and it corresponds to black

cotton soil (clay and siltyclay materials). The thickness of this layers show a significant increment from NW to SE direction along the profile. This layer is significantly thick in the NW part. The greater thickness of soil at this zone could be due to the high degree of weathering. Underlying the clay soil layer relatively intermediate resistivity variation varies from 20 to 40 Ω-m is delineated. This layer attributed to highly to moderately weathered basalt. Its morphology is almost uniform and horizontal throughout the profile.

The true resistivity of the third layer ranges from 40 to 115 Ω- m which is related to the occurrence of comparatively strong formation than the overlaying layers. Its thickness is almost unique along the profile.

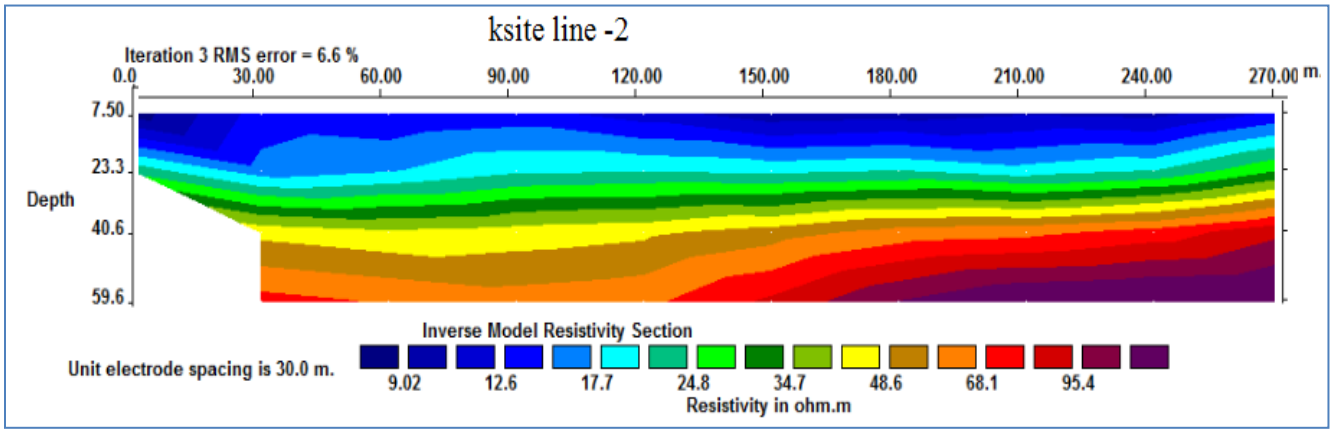

Figure 5.14: 2D resistivity model section along ERI-1

5.3 Seismic refraction survey

To map the subsurface underlying the study area (i.e., thickness of the overburden materials and depth to more competent hard formation) through determination of compressional wave velocity (Vp), three seismic refraction lines have been surveyed. After determining the first break arrival time of wave using the of *pickwin95* software, and further processing of the picked travel time curves with the help of *plotrefa* software, then later were inverted and velocity models are generated.

5.3.1 Velocity model for Line S1

This is a 24 channel seismic refraction spread with 5m geophone take out spacing, i.e., having a total length of 115m, and its velocity model is illustrated in Figure 5.15. This model shows three distinct horizons with P-wave velocity changing from 260 to 1070 m/s, of which the upper layer is characterized by low compressional wave velocities ranging from 260 to 340 m /s and its thickness, is approximately 4.5 m. This low velocity is due to the top dark clay and siltyclay soils. Meanwhile the second ,which are marked by comparatively intermediate P-wave velocity that varies from to 900 to 950 m/s is associated with the response of completely decomposed rock showing undulated morphology the thickness of this layer is maximum at the left periphery and at the center (12 m) and thinner in the right hand side of the profile. The bottom layer ,which is marked by comparatively high P-wave velocity that varies from to 960 to 1070 m/s is associated with the response of highly weathered basalt showing undulated morphology which seem deeper at the center of the profile (18 m) and shallower in the right hand side of the profile (9 m).

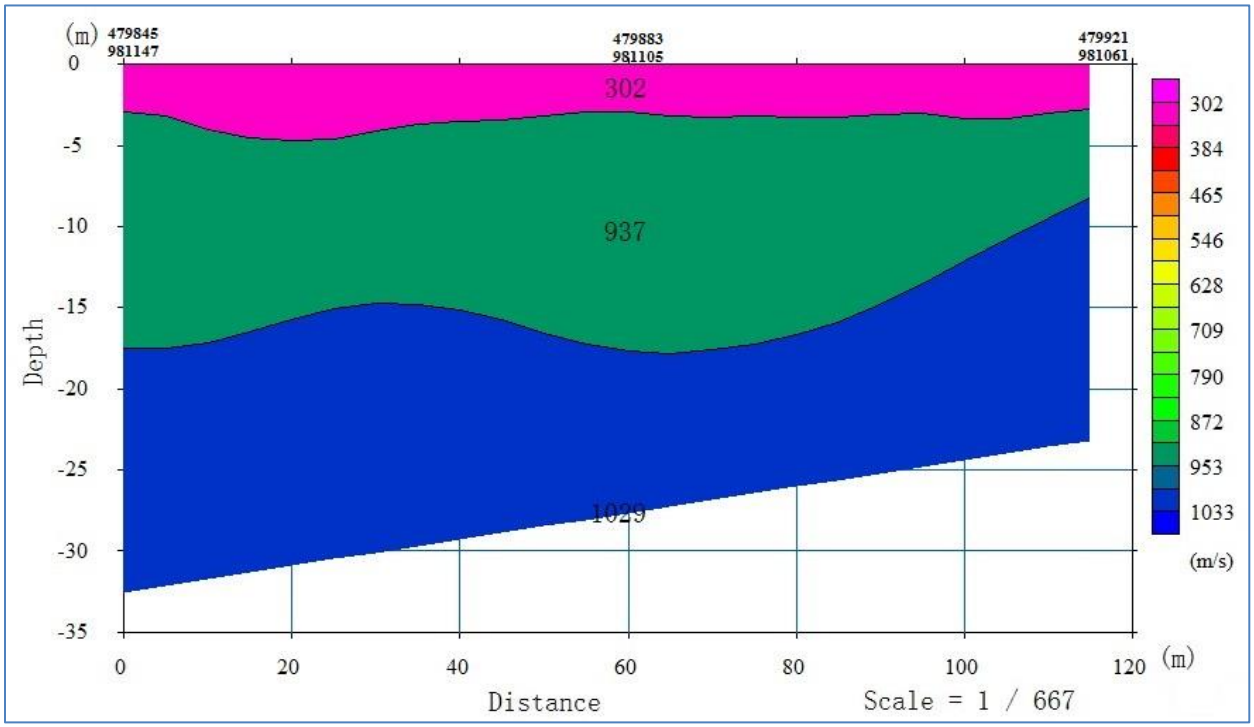

Figure 5.15: Velocity model along line S1

5.3.2 Velocity model for Line S2

This is a 12-channel spread and 55m long profile, whose velocity model is displayed in Figure 5.16. Similar to the previous case, here also two layers with contrasting P-wave velocities, ranging from 350 to 800 m/s, are differentiated. The first layer has indicated low compressional wave velocity varying from 350 to 400 m/s and 3- 6.5 m thickness, which is due to the upper dark clay-silty clay soil. Meanwhile, the underlying layer is mapped by relatively high P-wave velocity that varies from 740 to 800 m/s and it is associated with the response of decomposed volcanic rock.

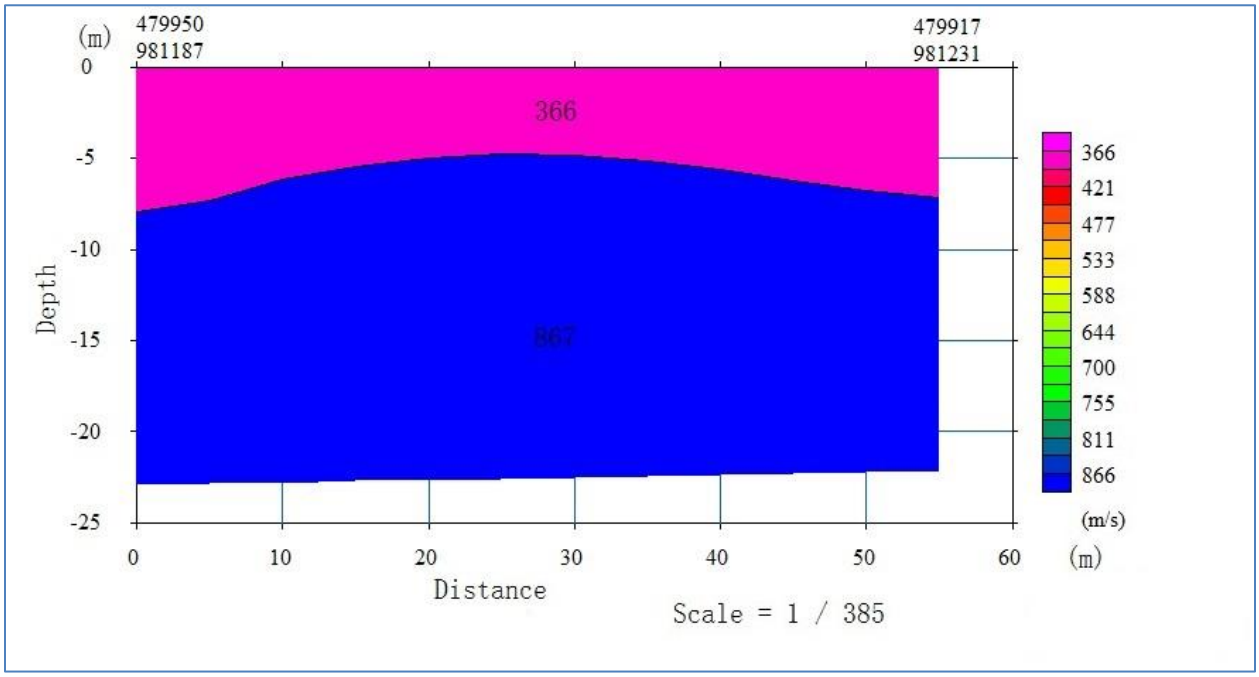

Figure 5.16: Seismic velocity model along line S2

5.3.3 Velocity model for Line S3

Profile S3 has 115 m length and surveying was executed using 24-channels with 5m geophone interval. The velocity model displayed in Figure 5.17 shows two contrasting lithologic features which are discussed in the above two sections, the top black cotton soil with 258-300 m/s velocity and 4-6 m thickness ranges, whereas the lower horizon is mapped by 910-1015 m/s velocity range associated with the response of completely decomposed rock.

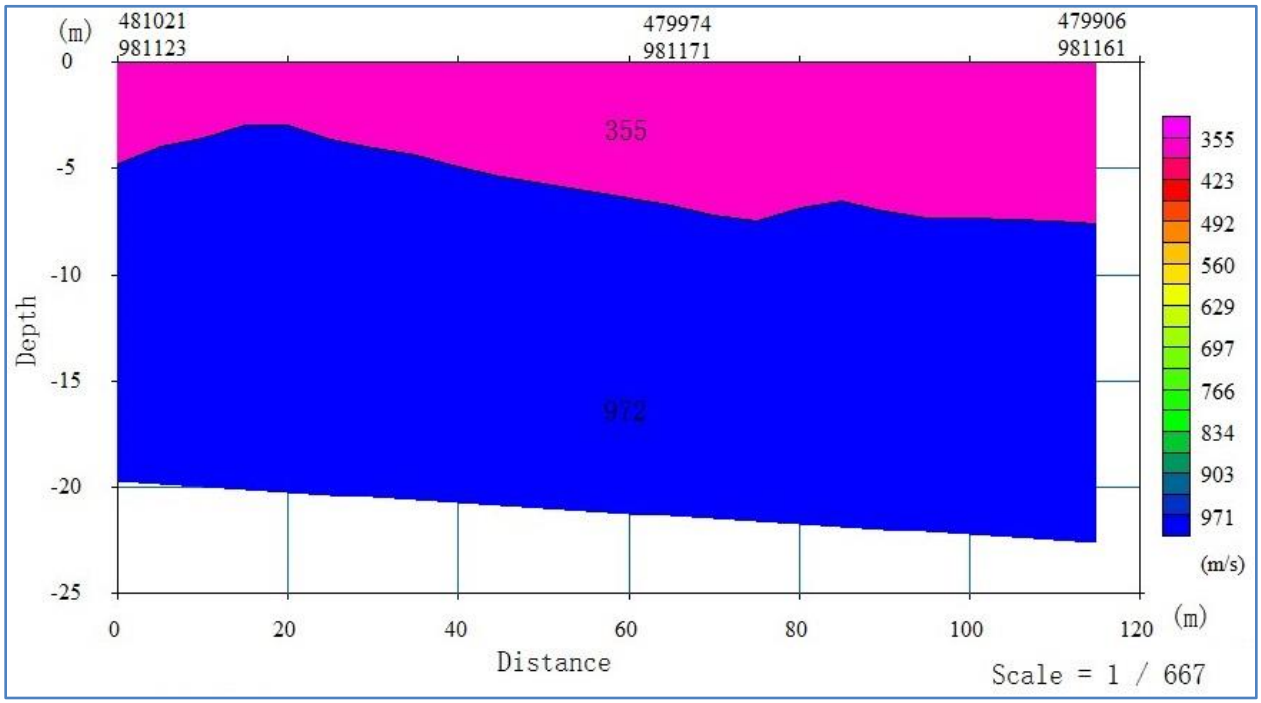

Figure 5.17: Seismic velocity model along Line S3

5.4 Integrated geophysical and geological data analysis

5.4.1 Analyses of 2D ERI models and VES geo-electrical sections

From examination and detail comparison of the vertical electrical sounding data the following points are forwarded. From general point of view, the dipole -dipole profiling is more reliable at delineating the subsurface morphologies clearly (both lateral and vertical resistivity contrast). However, the vertical electrical sounding shows the layer resistivity directly below the sounding point and general resistivity distribution of target site. It is simply an extrapolation and doesn't represent the subsurface morphologies laterally.

5.4.1.1 ERI-1 vs Profiles -2

Figure 5.18 demonstrates the correlation between the Vertical Electrical Sounding and the Dipole-Dipole profiling survey results, which revealed almost identical trends about the subsurface characteristics. Accordingly, both sections confirm that the resistivity is increasing with depth and they show the competency of the formation increases with depth. The only difference is that the 2D model has better outlined the subsurface undulations because of its

higher resolution in identified lateral variation unlike that of the sounding where information is obtained only at few specific points and the rest is simple interpolation.

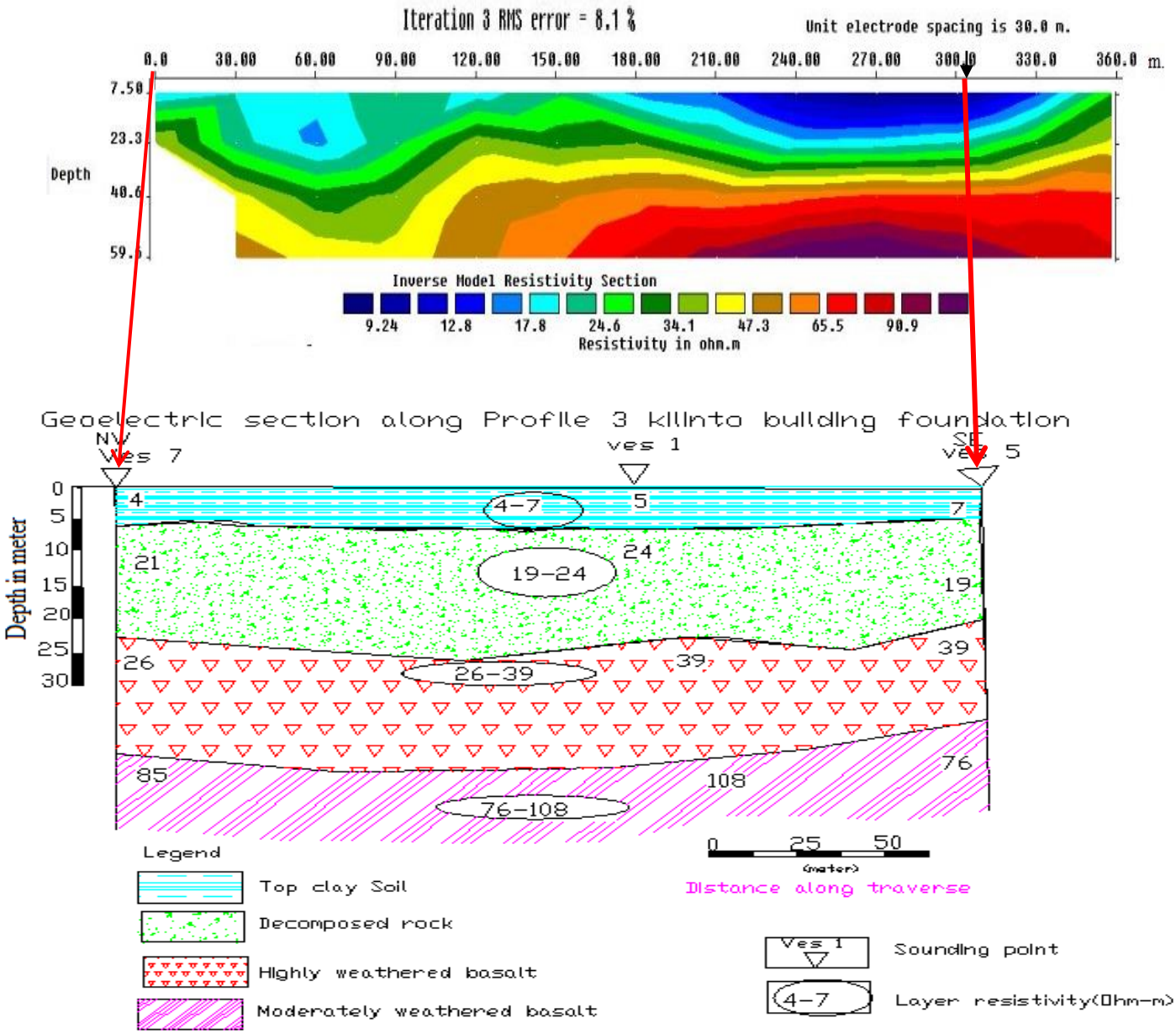

Figure 5.18: ERI-1 VS geo-electric section along Profile-2

5.4.1.2 ERI-2 and geo-electric section along Profile-3

Figure 5.19 shows the inverted 2D resistivity model and geo-electric section, where similar trend of resistivity variation is observed characterized by almost a horizontal layering of the

underlying earth materials can be clearly depicted whose intensities gradually increase with depth. Besides, both sections show that the thickness of the low resistivity layer increases northwest wards, whereas on the southeastern side the high resistive body significantly rises to the subsurface occurs at a relatively shallower depth.

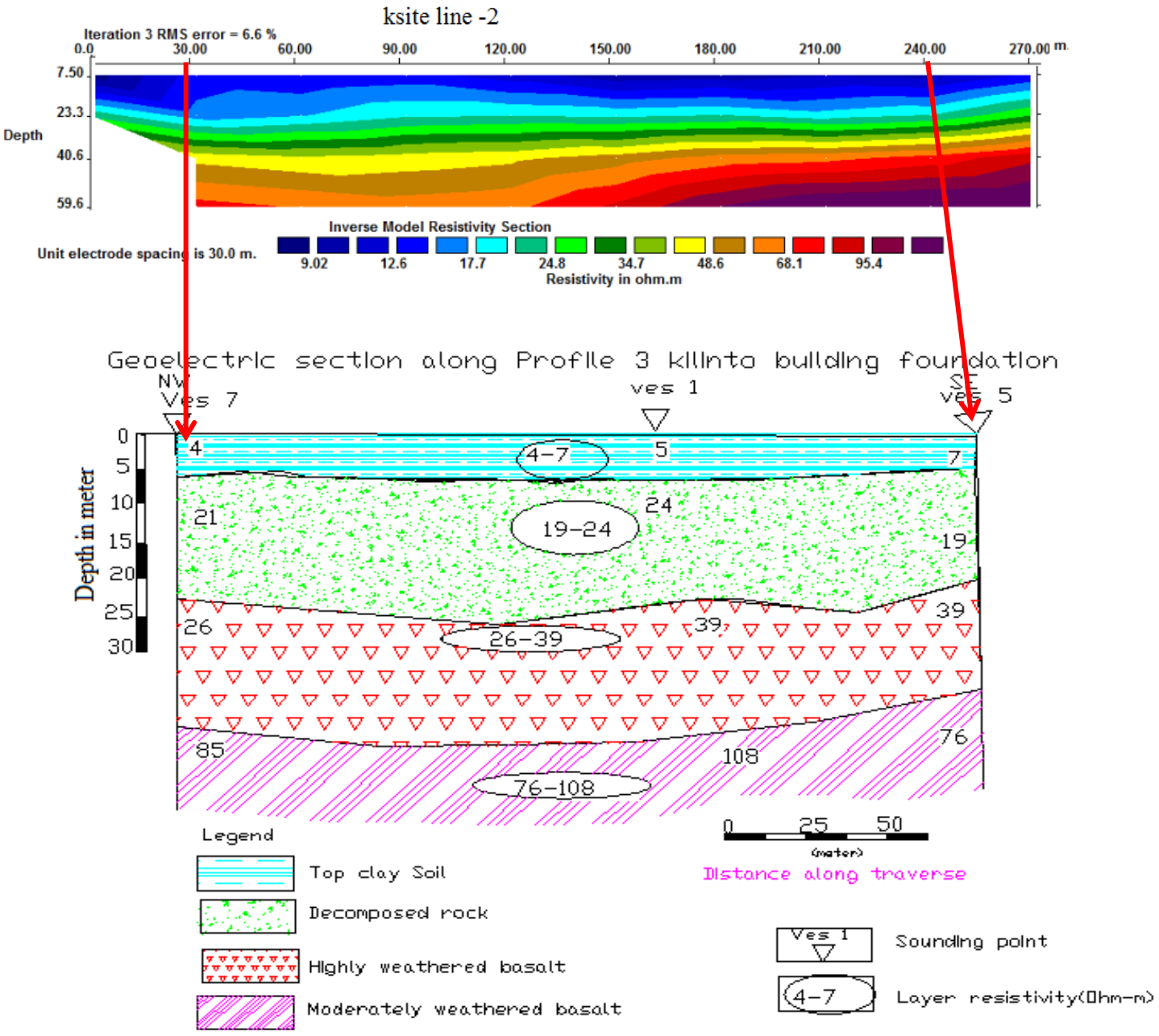

Figure 5.19: ERI-2 VS geo-electric section along Profile-3

CHAPTER SIX

6 CONCLUSIONS AND RECOMMENDATIONS

6.1 Introduction

Integrated electrical resistivity sounding (VES), dipole-dipole profiling and seismic refraction surveys were carried out at a site nearby the Addis Ababa Science and Technology University, just in front of the Tulu-Dimtu condominiums, located at eastern Addis Ababa City. Analyses of these data were conducted with the purpose of mapping the subsurface geology and elucidating its suitability for the construction of multistory residential and commercial complexes. Therefore, incorporating the available geological log data valuable conclusions and recommendations are drawn by, that are summarized in the sections below.

6.2 Conclusions

From the integration of the surveying results and available lithological log data the following conclusions are drawn:

a) From 2D resistivity models and geo-electric section and partially from seismic velocity models three to four distinct anomalous features are identified that are associated with different lithological units. Accordingly, the upper most layers, characterized by low resistivities (2-11Ω-m) and low P-wave velocities (< 350 m/s) are associated with the effect of the upper black cotton soil, composed of clay and silty clay materials. The thickness of this layer varies from 3.5 to 7 m. Underlying the top soil there is a relatively thick (6-21 m) layer with narrow resistivity range (17-22 Ω- m) and this response is due to a decomposed volcanic rock, which is thinner at the SE and thicker at the NW part of the study area. Meanwhile, the bottom part of the section is more resistive (25-115 Ω-m) than the overlying two layers and interpreted as the responses of a highly weathered and fractured basaltic rock. At places the depth to the surface of this competent hard formation reaches up to 40 m.
b) The gradual increasing of resistivity responses and elastic wave velocities with depth is a direct indication of continuous change of engineering properties of the subsurface

formations, and thereby provides a hint for the increasing competency of the foundation materials with depth.

c) The very low seismic wave velocities and low resistivities determined for shallow depths range suggest the physically weak nature of the top black cotton soil and decomposed volcanic rocks, which are not preferred foundation materials.

d) The resistivity responses show slight variations laterally possibly due to changes in the degrees of soil compactions, moisture content and composition.

e) From the geophysical signatures, no abrupt anomaly discrepancies that might be signs of tectonic discontinuities are not observed.

6.3 Recommendations

Based on the geophysical surveying results of the study the following recommendations are forwarded:

a) The upper section of the site mainly consisted of expansive clay soils (black cotton and silty clay soils) are not competent enough to bear loads from heavy engineering structures. Therefore, erecting multistory structures over such relatively weak formation require proper engineering measures during the design and construction stages. Hence, in addition to other precautionary measures, compaction, stabilization, removing and backfilling by another well graded material can be implemented as supplementary remedial steps.

b) To prevent percolation of surface runoff to soil and thereby protect the base of the structures from cracking and settlement, proper drainage should be constructed to maintain the moisture content in the underlying materials.

c) Analogous to the top section the second geo-electric layer (decomposed rock) also show low resistivity hence at places where this formation is thick it possibly affect the structure and due attention must be given.

d) As the study area is close to the Main Ethiopian Rift (MER) system and moreover the studied area is characterized by weak foundation materials which amplify and aggravate earthquake effects, the likely impacts of seismic activity should be considered carefully during designing and construction of multistory buildings.

e) Due to the existence of thick black cotton soil and less compacted formation at the upper most layers of study site (overburden material), the source used (Sledge hammer) is not enough for generation elastic energy as usual means. Therefore to better understand the subsurface condition, other recommendable elastic energy source is recommended.

f) Relatively the depth of the bed rock is shallow towards SW part of the study area; hence development of high rise buildings is preferable in that part of the site.

g) To better refine and confirm the geophysical result further drilling work is essential and recommended: especially the thickness at which the black cotton soil is maximum and minimum.

REFERNCES

Abebe, T., Mazzarini, F., Innocenti, F. and Manetti, P., (1998). The Yerer–TulluWellel volcanotectonic lineament: a transtentional structure in central Ethiopia and the associated magmatic activity. *J. Afr. Earth Sci*., **26**: 135–150.

Anomohanran, O. (2013). Seismic Refraction Method: A Technique for Determining the Thickness of Stratified Substratum. *American Journal of Applied Sciences.***10**:857-862.

Anteneh Girma (1994). Hydrogeology of Akaki area. Addis Ababa University, Addis Ababa, Ethiopia, Unpublished Master Thesis.

Assegid Getahun (2007). Geology of Addis Ababa City, Ethiopian. Unpublished technical report, Institute of Geological Survey, Addis Ababa, Ethiopia, 31 pp.

Bell, F.G. (2007). *Engineering Geology*, 2nd ed., Butterworth-Heinemann, Burlington.

Best consulting PLC (2014), subsurface geotechnical investigation and foundation recommendation for G+7 and G+4 buildings at Koye and Feche Condominium sites, unpublished technical report, Addis Ababa, Ethiopia, 42pp.

Construction Design Share Company (2011). Geotechnical investigation report of Addis Ababa Science and Technology University. Unpublished Report, Addis Ababa, Ethiopia.

EBCS-8 (Ethiopian Building Code Standard) (1995). Design of Structures for Earthquake Resistance, Unpublished technical report, Ministry of Works and Urban Development, Addis Ababa, Ethiopia, 109 pp.

Emmanuel Addai, Van-Dycke Sarpong Asare and Akwasi Acheampong Aning (2016). Application of Shallow Seismic Refraction and 2D Electrical Resistivity Imaging to Site Investigations.

Ethiopian Construction Design and Supervision Works Corporation (2014). Subsurface geotechnical investigation and foundation recommendation for G+7 and G+4 buildings at Koye and Feche Condominium sites. Unpublished technical report, Addis Ababa, Ethiopia, 100pp.

Haile Selassie Girmay and Getaneh Assefa (1989). The Addis Ababa-Nazareth Volcanism: A Miocene-Pleistocene Volcanic Succession in Ethiopian Rift. *SINET*: *Ethiopian Journal of Science,* **12**(1).

Hilemariam Syuim. (2011). Integrated Geophysical and Direct Geotechnical Investigation for Addis Ababa Science and Technology University Building Foundation site, Akaki, Addis Ababa, Ethiopia. Unpublished Master's Thesis, Addis Ababa University, Ethiopia, 100 pp.

Kearney, P. Brooks, M. and Hill, I. (2002). *An Introduction to Geophysical Exploration*, 3rd ed., Blackwell Science Ltd. UK, 160 pp.

KebedeTsehayu and Tadesse Hailemariam (1990*).* Engineering Geological Mapping of Addis Ababa, Unpublished technical report, Ethiopian Geological Survey, Addis Ababa, Ethiopia, 84 pp.

Laikemariam Asfaw(1985), Seismicity and Seismic risk in Addis Ababa region Bull, Geophysical Observatory, Addis Ababa, Ethiopia.

Lateef T.A and Adegoke J.A (2011). Geophysical Investigation of Foundation of a Site in Ikere-Ekiti, Ekiti State, Southwestern Nigeria. *Australian Journal of Applied and Basic sciences.*

Loke, M.H. (1999). *Electrical Imaging Survey for Environmental and Engineering Studies: A practical guide to 2-D and 3-D surveys*, Penang, Malaysia, 57 pp.

Loke, M.H. (2000). *Electrical Imaging Survey for Environmental and Engineering Studies: A practical guide to 2D and 3D surveys*, Penang, Malaysia.

Loke, M.H. (2001*). Electrical Imaging Survey for Environmental and Engineering Studies: A practical guide to 2D and 3D surveys.*

Messele Haile (2004). Seismic Microzonation for the City of Addis Ababa by Using Microtremors. **IN**: *Proceedings of the 13th World Cong. on Earthquake Engineering, August* 1-6, Paper No. 2092, Vancouver, B.C., Canada.

Morton, W.H. (1979). Riftward Younging of Volcanic Rocks in the Addis Ababa Region. Rift Valley Ethiopian. *Nature*, **280**: 284-288.

Solomon Gerra (2000). A short introduction to the geology of Ethiopia.

Soupois, P., Georgakopoulos, P., Papadopoulos, N., Saltas, V., Andreadakis, A., Vallianatos, F., Sarris, A. and Makris, J.P. (2007). Use of engineering geophysics to investigate a site for a building foundation. *Journal of Geophysics and Engineering* **4**(1): 94–103.

Redpath, B.B. (1973). Seismic Refraction Exploration for Engineering Site Investigations. Technical Report, U.S. Army Engineer Waterways Experiment Station, Vicksburg, MS.

Reynolds, J. M. (2011). *An introduction to applied and environmental geophysics*. John Wiley & Sons.

Water Works Design and Supervision Enterprise (WWDSE) (2008). Evaluation of water resources of the Ada'a and Becho groundwater basin for irrigation development project, unpublished technical report, WWDSE, Addis Ababa, Ethiopia, 147 pp.

World Bank Group (2015). Global Practice on Social, Rural, Urban and Resilience: Enhancing Urban Resilient: a case of Addis Ababa City. Unpublished report, Washgton, DC, USA, 46pp.

https://en.climate-data.org/location/532/) accessed on March 2018.

Appendix -1

Interpreted VES curves

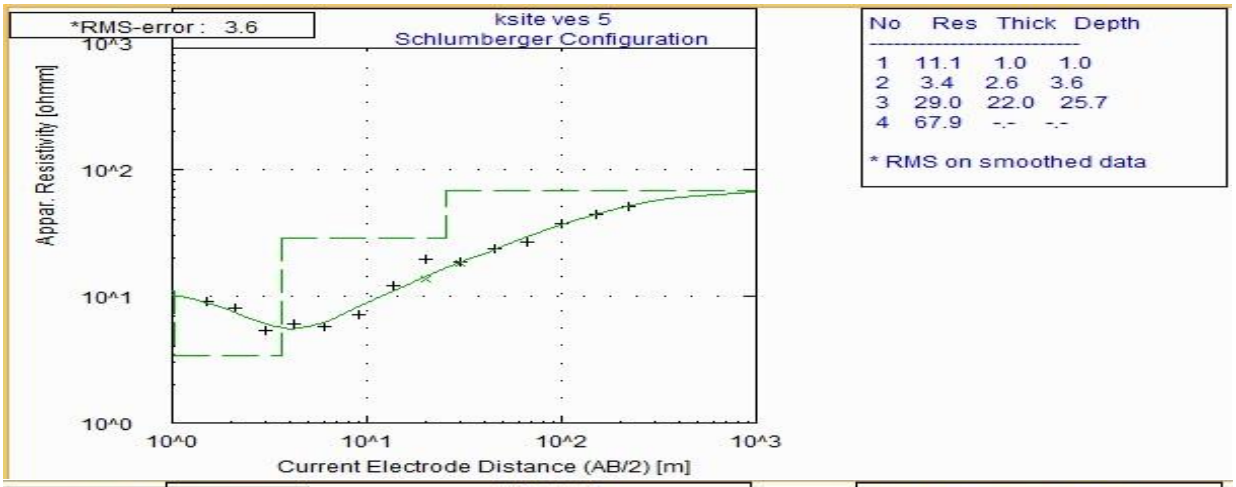

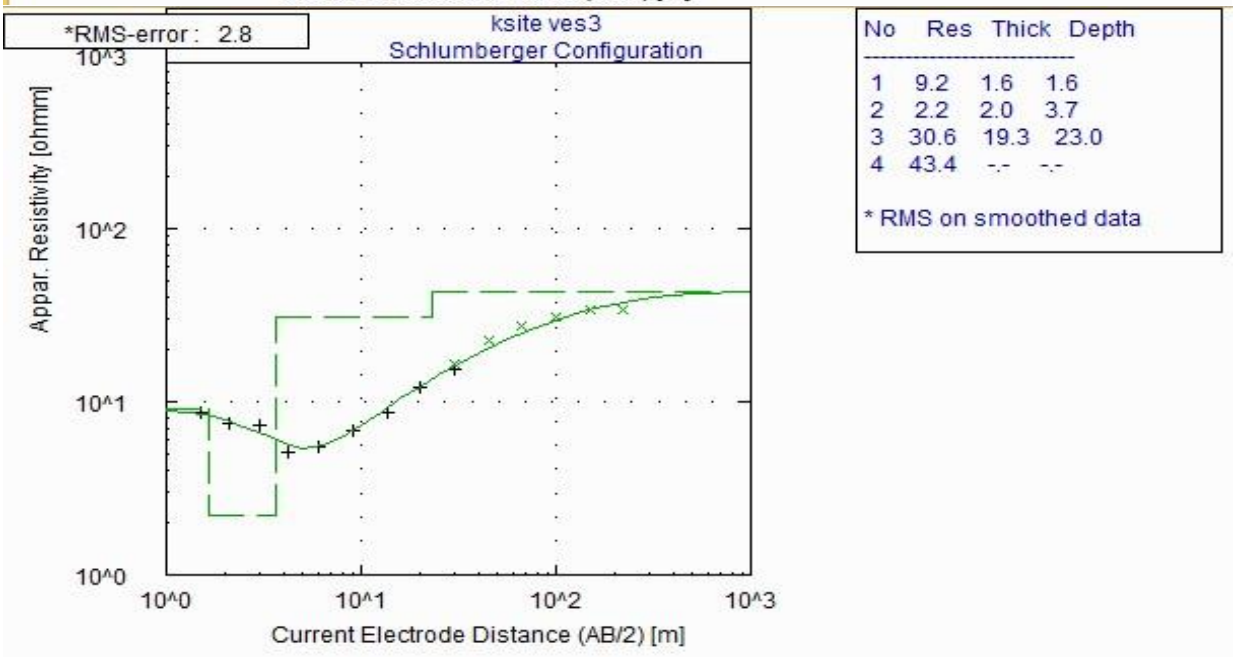

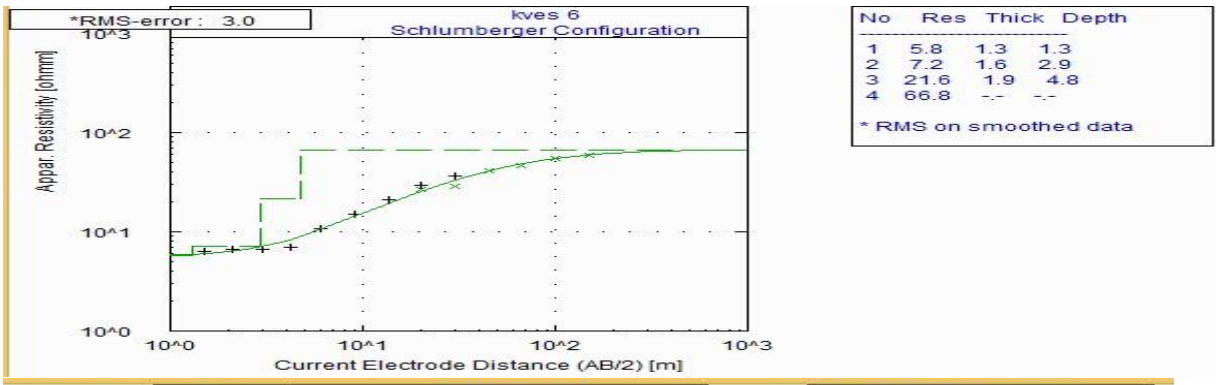

No	Res	Thick	Depth
1	5.8	1.3	1.3
2	7.2	1.6	2.9
3	21.6	1.9	4.8
4	66.8	-.-	-.-

* RMS on smoothed data

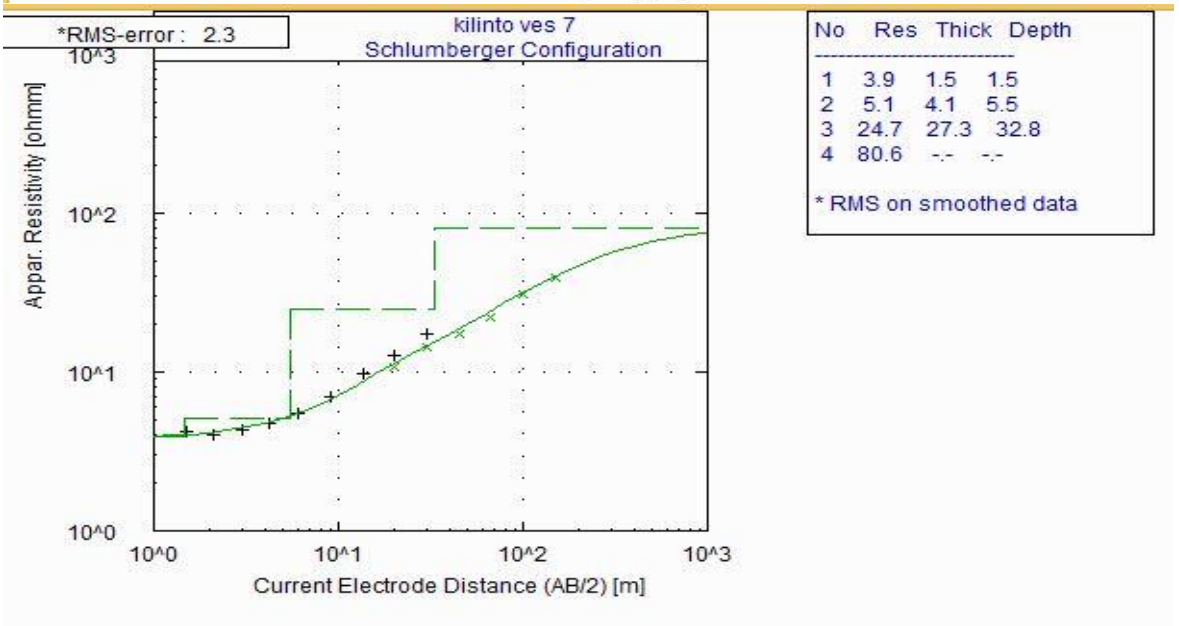

No	Res	Thick	Depth
1	3.9	1.5	1.5
2	5.1	4.1	5.5
3	24.7	27.3	32.8
4	80.6	-.-	-.-

* RMS on smoothed data

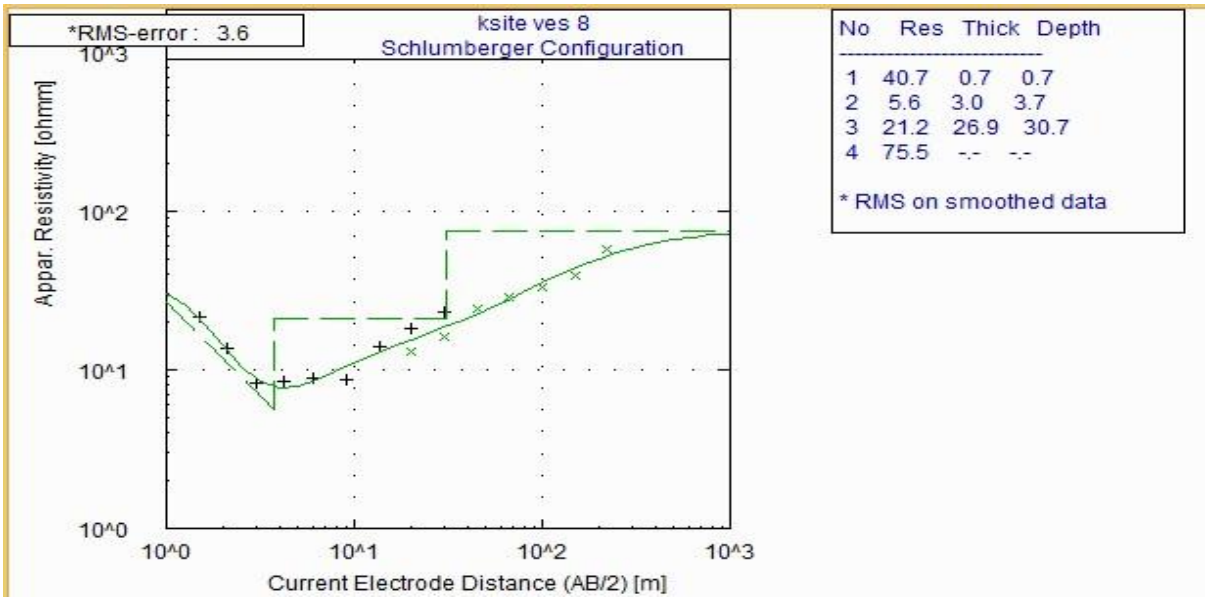

No	Res	Thick	Depth
1	40.7	0.7	0.7
2	5.6	3.0	3.7
3	21.2	26.9	30.7
4	75.5	-.-	-.-

* RMS on smoothed data

Appendix -2

Sample borehole logs (after CDSC, 2011 and ECDSWC, 2014)

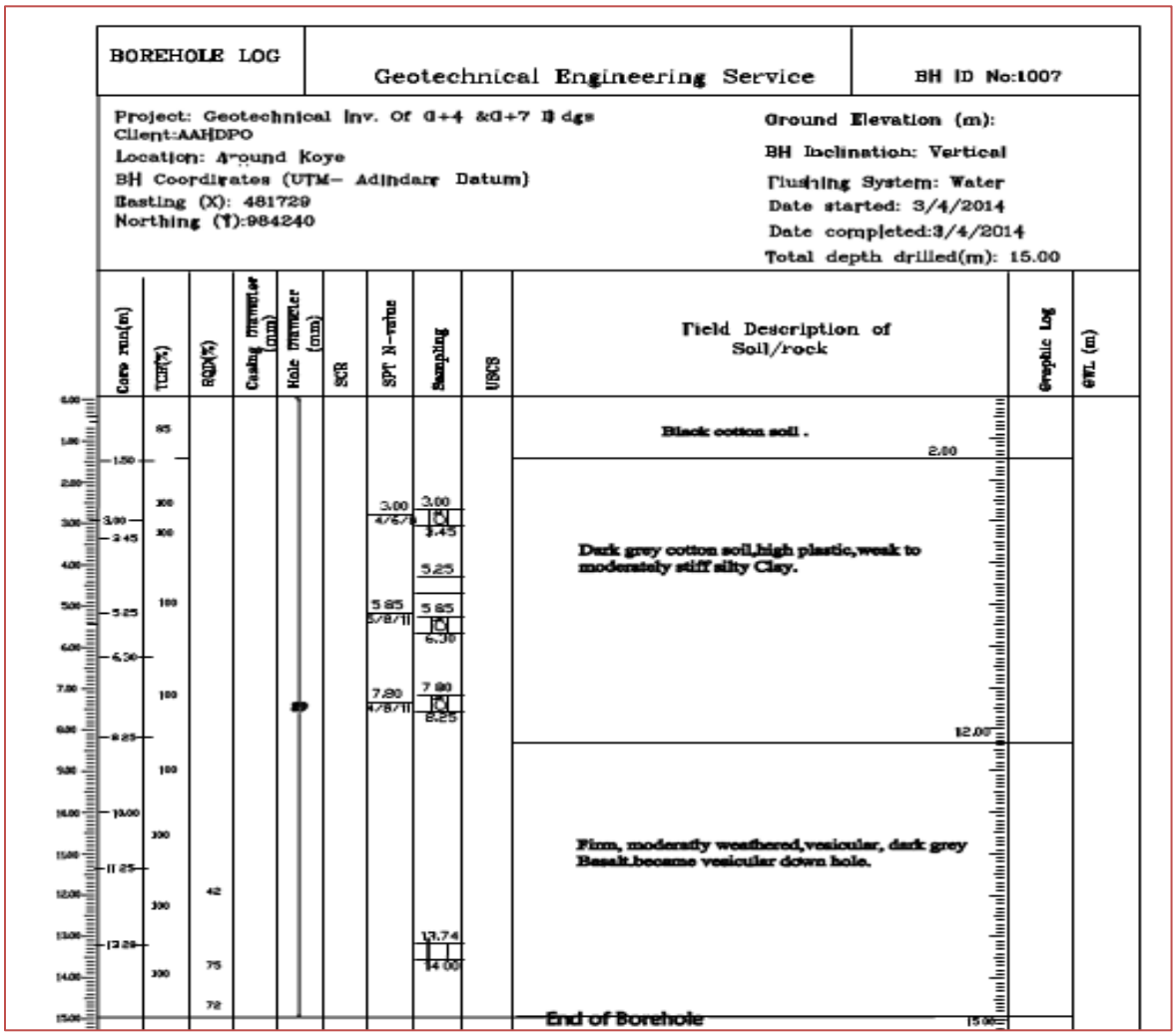

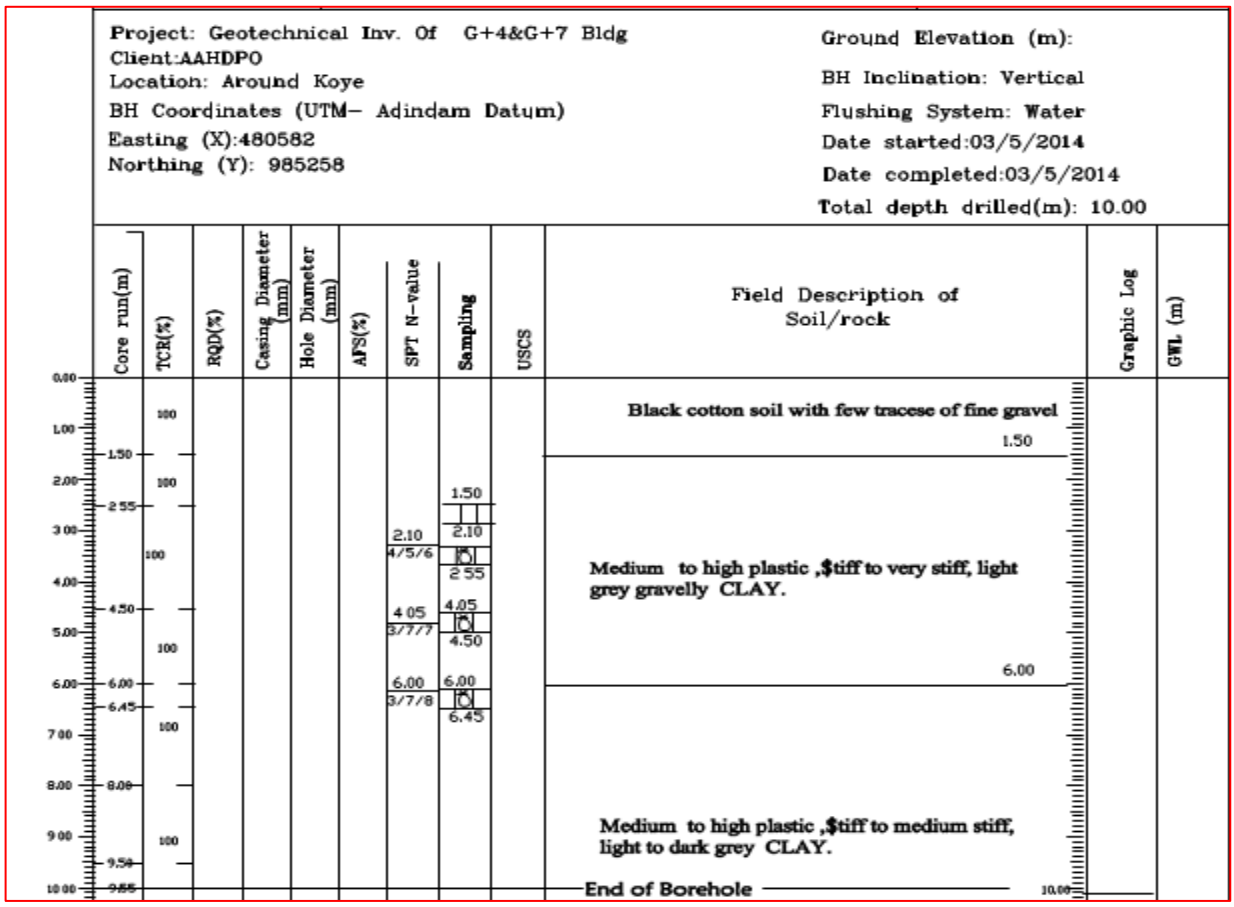
Project: Geotechnical Inv. Of G+4&G+7 Bldg
Client:AAHDPO
Location: Around Koye
BH Coordinates (UTM– Adindam Datum)
Easting (X):480582
Northing (Y): 985258
Ground Elevation (m):
BH Inclination: Vertical
Flushing System: Water
Date started:03/5/2014
Date completed:03/5/2014
Total depth drilled(m): 10.00
Core run(m)
TCR(%)
RQD(%)
Casing Diameter (mm)
Hole Diameter (mm)
AFS(%)
SPT N-value
Sampling
USCS
Field Description of Soil/rock
Graphic Log
GWL (m)
Black cotton soil with few tracese of fine gravel
1.50
Medium to high plastic ,$tiff to very stiff, light grey gravelly CLAY.
6.00
Medium to high plastic ,$tiff to medium stiff, light to dark grey CLAY.
End of Borehole
10.00
2.10
4/5/6
4.05
3/7/7
6.00
3/7/8
6.45

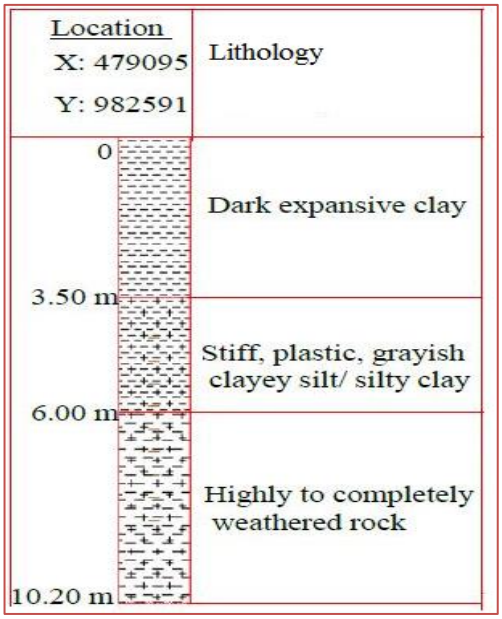
Location
X: 479095
Y: 982591
Lithology
0
Dark expansive clay
3.50 m
Stiff, plastic, grayish clayey silt/ silty clay
6.00 m
Highly to completely weathered rock
10.20 m

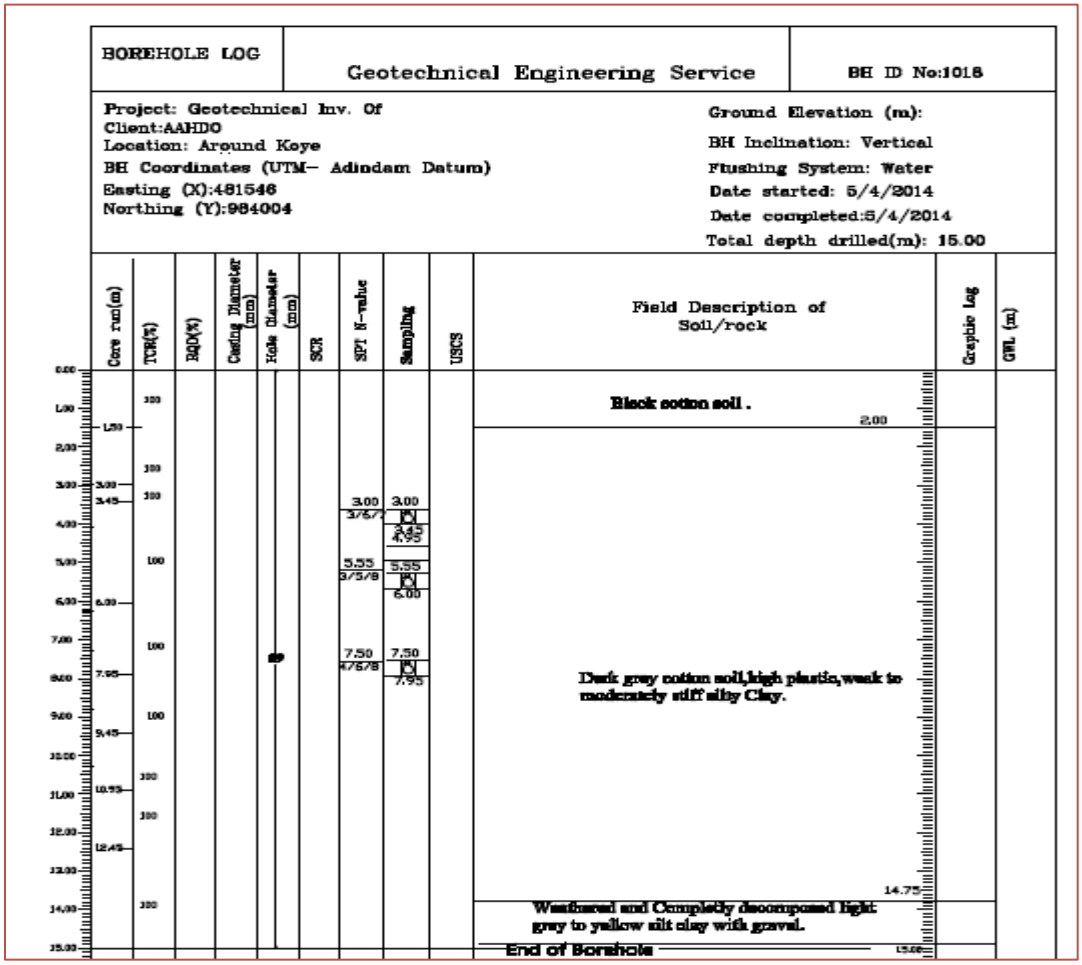
BOREHOLE LOG
Geotechnical Engineering Service
BH ID No:1018
Project: Geotechnical Inv. Of
Client:AAHDO
Location: Around Koye
BH Coordinates (UTM– Adindam Datum)
Easting (X):481546
Northing (Y):984004
Ground Elevation (m):
BH Inclination: Vertical
Flushing System: Water
Date started: 5/4/2014
Date completed:5/4/2014
Total depth drilled(m): 15.00
Core run(m)
TCR(%)
RQD(%)
Casing Diameter (mm)
Hole Diameter (mm)
SCR
SPT N-value
Sampling
USCS
Field Description of Soil/rock
Graphic Log
GWL (m)
Black cotton soil .
2.00
Dark grey cotton soil,high plastic,weak to moderately stiff silty Clay.
14.75
Weathered and Completely decomposed light gray to yellow silt clay with gravel.
End of Borehole
15.00